ANALYSIS OF THE EFFECTS OF VANCOMYCIN CONTAINING BIOCERAMIC/POLYMER COMPOSITES ON BIOFILM PREVENTION, BIOCOMPATIBILITY AND OSTEOGENIC MODIFICATION OF MESENCHYMAL STEM CELLS

A THESIS SUBMITTED TO
THE GRADUATE SCHOOL OF NATURAL AND APPLIED SCIENCES
OF
MIDDLE EAST TECHNICAL UNIVERSITY

BY

BERNA KANKILIÇ

IN PARTIAL FULFILLMENT OF THE REQUIREMENTS
FOR
THE DEGREE OF DOCTOR OF PHILOSOPHY
IN
BIOTECHNOLOGY

SEPTEMBER 2015

Approval of the thesis:

ANALYSIS OF THE EFFECTS OF VANCOMYCIN CONTAINING BIOCERAMIC/POLYMER COMPOSITES ON BIOFILM PREVENTION, BIOCOMPATIBILITY AND OSTEOGENIC MODIFICATION OF MESENCHYMAL STEM CELLS

submitted by **BERNA KANKILIÇ** in partial fulfillment of the requirements for the degree of **Doctor of Philosophy in Biotechnology Department, Middle East Technical University** by,

Prof. Dr. Gülbin Dural Ünver
Dean, Graduate School of **Natural and Applied Sciences** _____

Prof. Dr. Filiz Bengü Dilek
Head of the Department, **Biotechnology** _____

Prof. Dr. Erdal Bayramlı
Supervisor, **Chemistry Dept., METU** _____

Prof. Dr. Feza Korkusuz
Co-supervisor, **Sports Medicine Dept., Hacettepe University** _____

Examining Committee Members:

Prof. Dr. Abdullah Öztürk
Metalurgical and Materials Engineering Dept., METU _____

Prof. Dr. Erdal Bayramlı
Chemistry Dept., METU _____

Assoc. Prof. Dr. Hakan Eroğlu
Pharmaceutical Technology Dept., Hacettepe University _____

Assoc. Prof. Dr. Dilek Keskin
Engineering Sciences Dept., METU _____

Prof. Dr. Necdet Sağlam
Nanotechnology and Nanomedicine Dept., Hacettepe University _____

Date: 07.09.2015

I hereby declare that all information in this document has been obtained and presented in accordance with academic rules and ethical conduct. I also declare that, as required by these rules and conduct, I have fully cited and referenced all material and results that are not original to this work.

Name, Last name: Berna Kankılıç
Signature:

ABSTRACT

ANALYSIS OF THE EFFECTS OF VANCOMYCIN CONTAINING BIOCERAMIC/POLYMER COMPOSITES ON BIOFILM PREVENTION, BIOCOMPATIBILITY AND OSTEOGENIC MODIFICATION OF MESENCHYMAL STEM CELLS

Kankılıç, Berna

Ph. D., Department of Biotechnology

Supervisor: Prof. Dr. Erdal Bayramlı

Co-Supervisor: Prof. Dr. Feza Korkusuz

September 2015, 90 pages

Osteomyelitis is a difficult to treat bone infection. In clinic, osteomyelitis is treated with surgical debridement followed by the antibiotic therapy. But, due to the low blood circulation in the infection area and the production of an exopolysaccharide, biofilm, by the pathogen violence the treatment. Therefore local drug delivery systems are generated. These systems transmit the effective dose to the infection area without any toxic effects.

In this study, vancomycin containing PDLLA/β-TCP and PLGA/β-TCP composites were developed and characterized. Vancomycin containing PDLLA/β-TCP and vancomycin containing PLGA/β-TCP composites released 3.1 ± 0.2 mg and 3.4 ± 0.4 mg vancomycin for six weeks, respectively and the released vancomycin was sufficient for MRSA susceptibility. Also, the released vancomycin inhibited the biofilm formation of Methicillin Resistant S. aureus. Vancomycin containing PDLLA/β-TCP and vancomycin containing PLGA/β-TCP composites were biocompatible with Mesenchymal Stem Cells and SaOS-2 osteosarcoma cells.

The composites showed alkaline phosphatase activity at day 21. But for the RT-PCR studies conducted with the extraction medium of the composites, the vancomycin

containing PDLLA/β-TCP and vancomycin containing PLGA/β-TCP composites were not induced the differentiation of mesenchymal stem cells by not expressing some of the osteogenesis related signalling molecules.

Keywords: Antibiotic, osteomyelitis, PDLLA, PLGA, vancomycin, bone, polymer, MRSA, drug delivery systems, controlled release, biodegradable polymer, biofilm

ÖZ

VANKOMİSİN İÇEREN BİYOSERAMİK/POLİMER KOMPOZİTLERİN BİYOFİLİM ENGELLEMESİ, BİYOUYUMLULUĞU VE MEZENKİMAL KÖK HÜCRELERİN OSTEOJENİK DEĞİŞİMLERİ ÜZERİNE ETKİLERİNİN ANALİZİ

Kankılıç, Berna
Doktora, Biyoteknoloji Bölümü
Tez Yöneticisi: Prof. Dr. Erdal Bayramlı
Ortak Tez Yöneticisi: Prof. Dr. Feza Korkusuz

Eylül 2015, 90 sayfa

Osteomiyelit tedavisi oldukça zor bir kemik enfeksiyonudur. Klinikte osteomiyelit tedavisi cerrahi debridman sonrası sistemik olarak verilen antibiyotikler ile sağlanmaktadır. Ancak enfeksiyon bölgesinde yeterli kan akışının olmaması ve enfeksiyon yaratan patojenin biyofilim adı verilen ekzopolisakkarit yapının içinde antibiyotiklere karşı dirençli olması nedeniyle enfeksiyon tam anlamıyla yok edilememektedir. Bu nedenle enfeksiyon bölgesine ilaç taşıyıcı sistem yerleştirme fikri doğmuştur. Bu sistemler vücutta herhangi bir toksik etki yaratmadan direkt olarak enfeksiyon bölgesine etkin dozu ulaştırmaktadır.

Gerçekleştirilen çalışmada vankomisin içeren PDLLA/β-TCP ve PLGA/β-TCP kompozitler geliştirilmiş ve karakterize edilmiştir. Vankomisin içeren PDLLA/β-TCP ve PLGA/β-TCP kompozitler altı hafta boyunca 3.1 ± 0.2 mg ve 3.4 ± 0.4 mg vankomisin salmıştır ve salınan miktar MRSA duyarlılığı için yeterlidir. Ayrıca salım ortamlarından alınan örneklerle gerçekleştirilen biyofilm oluşumu engelleme çalışmasında, geliştirilen kompozitlerin MRSA biyofilm oluşumunu engellediği gösterilmiştir. Geliştirilen kompozitler mezenkimal kök hücreler ve SaOS-2

osteosarkoma hücreleri ile biyouyumludur. Ayrıca, kompozitlerin hücrelerle 21 günlük kültürü sonunda hücreler alkalin fosfataz aktivitesi göstermiştir. Ancak, kompozitlerden salınan maddelerin bulunduğu besiyerlerlerinin kullanıldığı RT-PCR çalışmasında kompozit grupları bazı osteogenez ilintili sinyal moleküllerini ifade etmeyerek mezenkimal kök hücrelerin farklanmasını tetiklememiştir.

Anahtar Kelimeler: Antibiyotik, osteomiyelit, PDLLA, PLGA, vankomisin, kemik, polimer, MRSA, biyouyumluluk, ilaç taşıyıcı sistemler, kontrollü salım, biyobozunur polimer, biyofilim

To Poyraz Arslan Kankılıç

ACKNOWLEDGEMENTS

First of all, I would like to express my gratitudes to my supervisor Prof. Dr. Erdal Bayramlı for his support and help. I would like to thank my co supervisor Prof. Dr. Feza Korkusuz for his support and guidance through the study.

I would like to thank Prof. Dr Duygu Uçkan Çetinkaya, Assoc. Prof. Dr. Ayşen Günel Özcan, Assist. Prof Dr. Fatima Aerts Kaya, Dr. Betül Çelebi Saltık and all the members of Hacettepe University Stem Cell Research and Application Center for their helps during my study.

I want to express my thanks to Prof Dr Petek Korkusuz for her support. I also would like to thank Prof Dr. Burçin Şener for her guidance during the microbiological studies and for providing the bacterial strains. I would like to thank Dr Pelin Mutlu for PCR studies.

I would like to express my gratitudes to my dear friend Sevil Köse for her support.

At the end, I would like to thank my beloved friends Ilgın Çağnan and Dr. Çağla Köprü for their helps and supports through the study.

Lastly, I would like to thank my dear husband Coşkun Serhat Kankılıç and my family for their helps and supports during this long way.

TABLE OF CONTENTS

LIST OF TABLES

TABLES

LIST OF FIGURES

FIGURES

ABBREVIATIONS

%	Percent
°C	Degrees Celsius
ACTB	Beta Actin
AHSG	Alpha-2-HS-glycoprotein
ALP	Alkaline Phosphatase
ALPL	Alkaline Phosphatase, liver/bone/kidney
ANOVA	Analysis of Variance
ANXA5	Annexin A5
BGLAP	Bone Gamma Carboxyglutamate (gla) Protein
BMPs	Bone Morphogenetic Proteins
CALCR	Calcitonin Receptor
CDH11	Cadherin 11, type 2, OB-cadherin (osteoblast)
cDNA	Complementary DNA
CLSI	Clinical and Laboratory Standards Institute
cm	Centimeter
COL1A1	Alpha-1 Type I Collagen
COL1A2	Alpha-2 Type I Collagen
COMP	Cartilage Oligomeric Matrix Protein
Cp	Crossing Point
CTSK	Cathepsin K
DMEM	Dulbecco's Modified Eagle Medium
DMP1	Dentin Matrix Protein 1
ECM	Extracellular Matrix
EDS	Energy-Dispersive Spectrometry
EGF	Epidermal Growth Factor
EGFR	Epidermal Growth Factor Receptor
FGF	Fibroblast Growth Factor
FGFR1	Fibroblast Growth Factor Receptor 1
FGFR2	Fibroblast Growth Factor Receptor 2
FTIR-ATR	Fourier Transformed Electron Microscopy

g	G Force
g/l	Gram per Liter
G6PD	Glucose-6-phosphate dehydrogenase
GAPDH	Glyceraldehyde-3-phosphate dehydrogenase
GDF10	Growth Differentiation Factor 10
GDFs	Growth Differentiation Factors
h	hours
IGFs	Insulin Like Growth Factors
ITGB1	Integrin, beta 1
$kmol/dm^3$	Kilomol per Decimetercube
min	Minutes
MMP10	Matrix Metallopeptidase 10
MMP2	Matrix Metallopeptidase 2
MMP8	Matrix Metallopeptidase 8
MMP9	Matrix Metallopeptidase 9
MRSA	Methicillin Resistant *Staphylococcus Aureus*
MSC	Mesenchymal Stem Cells
nm	Nanometer
OD	Optical Density
PBS	Phosphate Buffered Saline
PDGF	Platelet Derived Growth Factor
PDLA	Poly (D-lactide)
PDLLA	Poly (D, L-lactide)
PGA	Polyglycolic Acid
pH	Power of Hydrogen
PHEX	Phosphate Regulating Endopeptidase Homolog, X-linked
PLA	Polylactic Acid
PLGA	Poly (D, L-lactide-co-glycolide)
PMMA	Polymetylmethacrylate
pNPP	*p*-nitrophenylphosphate
rpm	Rounds per Minute
RT-qPCR	Real Time Quantitative Polymerase Chain Reaction

RUNX2	Runt Related Transcription Factor
SBF	Simulated Body Fluid
s	Seconds
SMAD1	SMAD family member 1
SMAD2	SMAD family member 2
SMAD3	SMAD family member 3
SMAD4	SMAD family member 4
SOX9	SRY (sex determining region Y)-box 9
TGF-β	Transforming Growth Factor Beta
TNF	Tumor necrosis factor Precursor (TNF-alpha)
TWIST1	Twist Homolog 1 (Drosophila)
VDR	Vitamin D (1,25- dihydroxyvitamin D3) receptor
VEGFs	Vascular Endothelial Growth Factors
wt,%	Weight Percent
β	Beta
β-TCP	Beta-tricalcium Phosphate
µg/ml	Microgram per Milliliter
µl	Microliter

CHAPTER 1

INTRODUCTION

Osteomyelitis is a difficult to treat orthopedic infection, which arose as a result of the colonization of pathogens, especially the most causative organism methicillin resistant *Staphylococcus aureus* (MRSA) (1). The treatment of osteomyelitis is generally done with surgical debridement and parenteral antibiotic administration up to six weeks (2).

In parenteral antibiotic administration, the antibiotic reached to the infection area cannot eradicate the pathogen, since only lower amounts of antibiotic can reach to infection area due to low blood circulation and the circulated amount is lower than the minimum inhibitory concentration. Also, the pathogen can capable of forming a biofilm in the infection area. Biofilms protect the pathogen from immune defenses and they are resistant to antibiotics, so the parenteral antibiotic cannot eradicate the pathogen (3).

Drug delivery systems are developed in order to control and treat bone infections. In drug release systems, biodegradable and biocompatible polymers or bioceramics carries drugs. In some cases, both kinds of materials are used to minimize each material's disadvantages and composites are developed. These drug delivery systems should be active against the pathogen involved in the infection, release antibiotic at least ten times higher than the minimum inhibitory concentration of the pathogen, not evoke any immune response (4).

Poly (D, L-lactide) (PDLLA) and poly (D, L-lactide-co-glycolide) (PLGA) are biodegradable and biocompatible polymers generally used as carrier in drug delivery systems (5). The disadvantages of these polymers are their acidic products after the biodegradation. The acidic products decrease the pH of the environment and fasten the further degradation. Also, these polymers have low cell adhesion potential (6).

Beta-tricalcium phosphate (β-TCP) is a biodegradable bioceramic used in local drug delivery systems. The bioceramic has high solubility rate, and degrades faster (2), (7). It also shows osteointegration and osteoconduction properties (8).

From this point of view, we developed two different drug release systems; vancomycin containing PDLLA/β-TCP composites and vancomycin containing PLGA/β-TCP composites and searched for their biofilm inhibition potential and biocompatibility with mesenchymal stem cells.

CHAPTER 2

BACKGROUND INFORMATION

2.1 Bone

Bone is a tissue that supports and protects the organs, provides motility, stores minerals and produces red and white blood cells. Bone is made up of organic compartment type 1 collagen, inorganic compartment carbonate hydroxyapatite (Ca, Mg, Na)$_{10}$ (PO4 , CO3)$_6$ (OH)$_2$) and water (9). The organic compartment, type I collagen, gives rigidity while inorganic compartment, hydroxyapatite, gives the elasticity to the tissue.

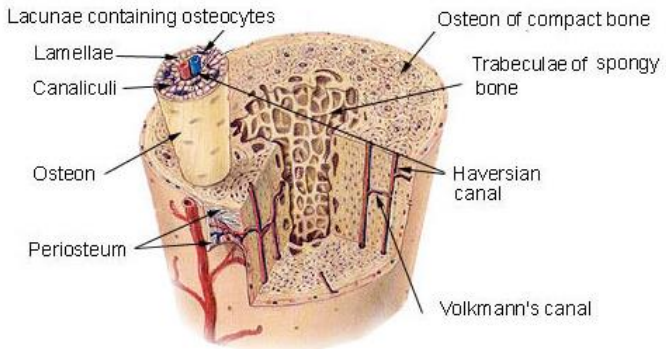

Figure 1. The structure of bone (10).

The outer layer of the bone is called cortical or compact bone. The primary functional unit of cortical bone is called osteon. Osteons are connected to each other and the periosteum, the membrane covering the bone, by Volkmann's canals. Volkmann's canal provides energy and nourishing elements for osteon (Figure 1). Each osteon also surrounds Haversian canal, which protects blood vessels and nerve cells of the bone and enables the communication between osteocytes by canaliculi (Figure 2) (11).

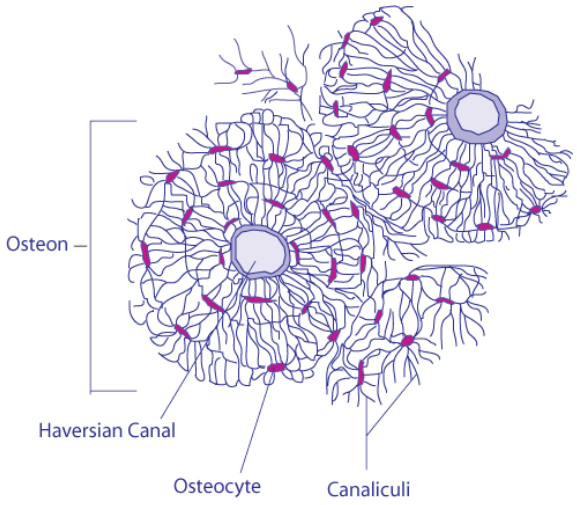

Figure 2. The structure of an osteon (12).

Osteocyte is a star shaped bone cell derived from osteoprogenitor cells and embedded in bone matrix. They can differentiate into osteoblasts and osteoids. Osteocytes regulate mineral homeostasis by resorbing the bone with their osteocytic osteolysis function and have mechanosensory mechanisms (13). Osteoblast is another type of bone cell responsible from bone formation. Mesenchymal stem cells (MSC) or osteoprogenitor cells differentiate into preosteoblasts and then to mature osteoblasts. The unmineralized organic portion of bone matrix forms prior to bone tissue formation is known as osteoid or bone extracellular matrix (ECM) is secreted by these osteoblasts and as the osteoid becomes mineralized, osteoblasts are trapped in lacunae and osteocyte become bone lining cells (14). Osteoclasts are another bone cell type that degrade the mineralized bone and bone ECM by secreting proteolytic enzymes and acids and derived from hematopoietic cells (11, 15). The ECM of bone consists of collagens, proteoglycans, glycosaminoglycans and glycoproteins like alkaline phosphatase osteonectin, osteocalcin, bone sialoprotein and osteopontin. Bone ECM upregulates or downregulates the signaling pathways and regulates bone cells while providing the mechanical property of bone (14).

Spongy bone, also known as trabecular or cancellous bone, is another type of osseous tissue found at the ends of long bones. This tissue has higher vascularity and responsible from production of blood cells (11).

2.1.1 Bone Formation

The bone is formed by two mechanisms: intramembranous ossification and endochondral ossification. In intramembranous ossification, MSC differentiate into osteoblasts and form an ossification center. Osteoblasts secrete osteoid and it begins to calcify. The osteoblasts trapped in calcified osteoid become osteocytes and by the entrapment of osteocytes on mesenchymal surface, periosteum forms. Later, the mineral deposition continues leads to creation of trabeculae and forms the spongy bone. Finally, the trabeculae under the periosteum thicken and replaced with lamellar bone and form compact bone plates. Spongy bone stays internally and its vascular tissue becomes red marrow. Flat bones of skull, mandible and maxilla are formed by intramembranous ossification (16). In endochondral ossification, a hyaline cartilage model grows by cell division of chondrocytes. As the chondrocytes become mature, hyaline cartilage model begins to calcify. The perichondrium around the hyaline cartilage vascularizes and becomes periosteum. The osteoprogenitor cells in the periosteum use calcified matrix and becomes osteoblasts. The osteoblasts secrete osteoid and form trabeculae. The ossification of long bones and bone fracture healing is followed by endochondral ossification (17).

In bone formation and regeneration, many signaling molecules are essential. Some of these signaling molecules like transforming growth factor beta (TGF-β), bone morphogenetic proteins (BMPs), and growth differentiation factors (GDFs) belong to TGF-β superfamily. TGF-β induces MSC, chondrocyte, preosteoblast and osteoblast proliferation and collagen, proteoglycan, osteopontin, osteonectin and alkaline phosphatase production (8). It triggers the BMP synthesis and induces the inhibition of osteoclast activity (13). BMPs are responsible from osteogenesis, mesenchymal and osteoprogenitor cell proliferation, differentiation and bone extracellular matrix synthesis. BMPs are divided into four groups: BMP-2 and BMP-4 form group 1, BMP-5, BMP-6 and BMP-7 form group 2, BMP-12, BMP-13 and BMP-14 form group 3 and BMP-3 and BMP-3b form group 4. BMP-3 is an antagonist to other BMPs and it down regulates the bone density. Unlike the other BMPs, BMP-1 induces the development of bone and cartilage but it does not belong to TGF-β

superfamily (18). BMPs bind to serine/threonine kinase receptors and initiate Smad signaling. Smad family has eight members and divided into three groups. The receptor regulated Smads (SMAD 1, 2, 3, 5 and 8), common mediator Smad (SMAD 4) and the inhibitory Smads (SMAD 6 and 7). Once the Smads are activated, they regulate the transcription of target genes (19). BMPs also induce the secretion of other growth factors like insulin like growth factors (IGFs) and vascular endothelial growth factors (VEGFs) (20). IGFs are secreted from osteoblasts, chondrocytes, bone matrix and endothelial cells. IGF-1 induces the formation of bone matrix while IGF-2 stimulates cellular proliferation and type 1 collagen production (21). Nearly at the end of endochondral ossification, cartilage and bone are degraded to induce the angiogenesis by VEGF dependent pathway. VEGF expressed by osteoblasts and osteoblast like cells is stimulated by BMPs (22). Platelet derived growth factor (PDGF) is another growth factor expressed by macrophages, osteoblasts and platelets for the proliferation of MSCs and osteoblasts (19). Fibroblast growth factor (FGF) is also expressed by macrophages, osteoblasts and MSCs and it triggers the cell division of MSCs and osteoblasts (23).

Besides the growth factors, matrix metalloproteinases secreted by macrophages degrade the bone ECM and they are essential for bone formation (23, 24). There are also many transcription factors that regulate bone formation according to osteoblast differentiation and they control the expression of many ECM protein genes or osteogenic genes during the differentiation. Runt related transcription factor (RUNX2) is a transcription factor responsible from the differentiation of osteoblasts. It also regulates the expression of alpha-1 type I collagen (COL1A1), alpha-2 type I collagen (COL1A2) and bone gamma carboxyglutamate (gla) protein (BGLAP). During the differentiation of mature osteoblasts into osteocytes, mature osteoblasts express BGLAP while osteocytes express dentin matrix protein 1. Runx2 is a leading gene expressed during bone formation; since this gene is expressed by osteoblasts and without osteoblasts there will not be any bone formation (25).

2.1.2 Mesenchymal Stem Cells (MSCs)

Mesenchymal stem cells found in bone marrow have self-renewal ability and they

can differentiate into many cell types like bone, fat, cartilage, muscle (26, 27). They can be easily isolated and expanded in vitro, therefore they are frequently used in regenerative medicine and tissue engineering (28). After the signaling of major molecules interleukin 1 and 6 (IL-1 and IL-6) in the inflammation of bone, fracture repairment is followed by the signaling of TGF-β, IGF, FGF, PDGF, BMPs and VEGF. All these signaling molecules induced the proliferation and differentiation of MSCs (17, 22, 29, 30). In the regeneration or formation of the bone, mesenchymal stem cells are activated and they can differentiate into osteoblasts and chondrocytes. Once MSCs differentiate into chondrocytes, they can form the bone by endochondral ossification. MSCs can be isolated from various sources in the body like, bone marrow, mineralized bone and adipose tissue. BMP and FGF signaling pathways influence the differentiation of MSCs (31). MSCs can be induced to differentiate into osteoblasts *in vitro* by using dexamethasone, L-ascorbic acid and beta glycerophosphate during cell culturing (23, 32).

2.2 Osteomyelitis

Osteomyelitis is an inflammatory difficult to treat bone infection caused by pyogenic bacteria which are capable to form pus (33). The infection is generally arisen secondary from a contigous focus of infection such as trauma, surgery or vascular insufficiency and hematogenous spread (34). Osteomyelitis can be classified as acute or chronic osteomyelitis; acute osteomyelitis lasts for days and weeks while chronic osteomyelitis lasts for months or years (35).

In the mechanism of infection, microorganisms adhere to host bone tissue with their adhesins specific for host proteins like collagen, fibronectin and bone sialoprotein (36). Macrophages attack to the pathogen, release proteolytic enzymes and leads to tissue lysate. In the manner of adaptive immunity, pus spreads to vascular channels in the bone and deteriorate blood flow (37). As the infection progresses to chronic state, necrotic bone is fragmented and sequestrum is formed (Figure 3) (34). Chronic osteomyelitis is generally treated with surgical debridement and four to six week lasting parenteral antibiotic therapy (38).

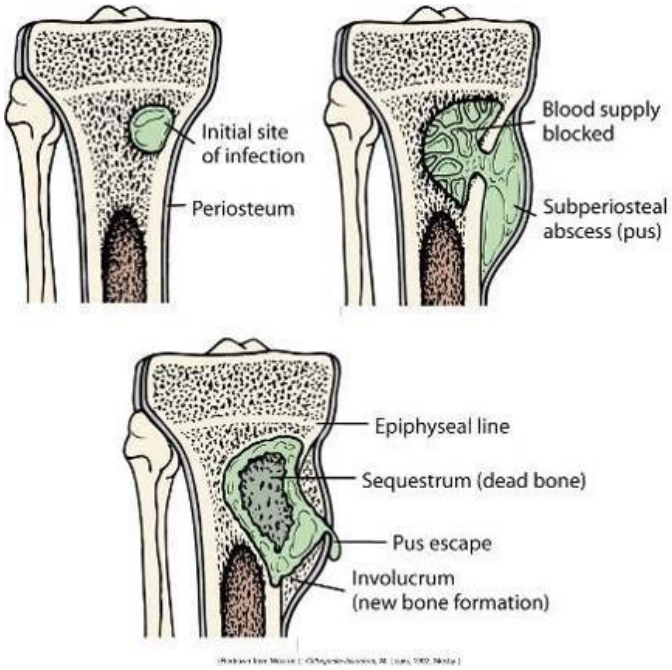

Figure 3. Illustration of osteomyelitis (39)

Methicillin resistant *Staphylococcus aureus* (MRSA) is the most common pathogen isolated from the infection site but other pathogens like *Staphylococcus epidermidis*, coagulase-negative staphylococci, *Enterobacter* species, *Pseudomonas aeruginosa* and *Mycobacterium* species are also responsible for osteomyelitis. *Staphylococcus aureus* is a gram positive, facultative anaerobe. It has a spherical shape with 0.5 to 1.5 μm diameter and forms bead like clusters when colonized. *Staphylococcus aureus* is naturally found in human skin and nostrils. It attaches to the surface with its adhesins and exotoxins and many of its strains are capable of forming biofilm. Biofilm protects the pathogen from environmental conditions like antibiotics and phagocytosis (40).

2.2.1 Biofilm

Biofilm is a three dimensional extracellular polymeric matrix formed by the irreversible attachment of the *Staphylococcus aureus* to a surface (41). Once *Staphylococcus aureus* attach to a surface, it begins to produce multi-layered

biofilms under glycocalyx, or slime layer (35). Gross et al. found that teichoic acids found in the pathogen are the leading cause for biofilm formation (42). Besides, polysaccharide intercellular adhesin (PIA) is also responsible for biofilm formation (43). In a biofilm environment, bacteria can communicate with chemotaxis, known as quorum sensing when they reach to a threshold cell density (44). Biofilm protects the bacteria from outer environmental conditions like antibiotic agents, phagocytosis, oxygen radical and protease defenses. As biofilm decreases the permeability of antimicrobial agents by acting as a diffusion barrier, in order to eradicate the bacteria within the biofilm, higher concentrations of antimicrobial agents are needed (45). Also under the protection of a biofilm, mature bacteria colonies can detach from the biofilm and they can migrate and form new biofilms in uninfected areas (46) (Figure 4).

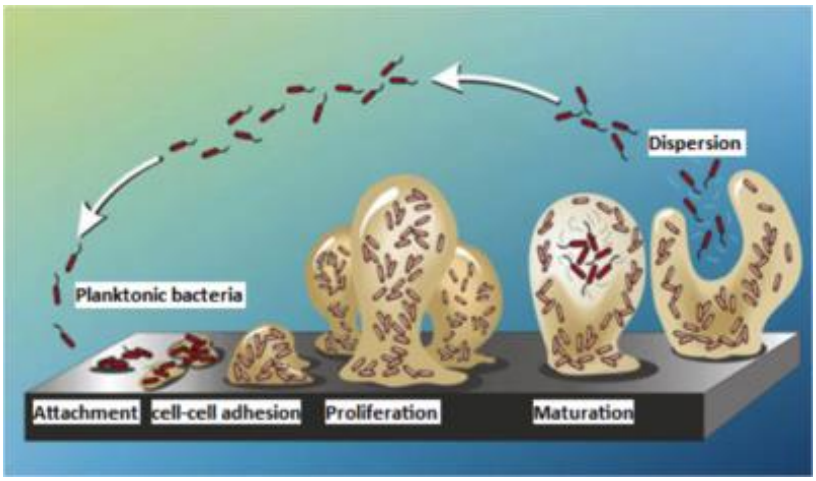

Figure 4. The stages of biofilm formation (47).

Biofilms can be detected by various techniques like tissue culture plate, tube method, Congo Red Agar method, bioluminescent assay, and fluorescent microscopy. In tissue culture plate method, which is the major biofilm detection technique, biofilm forming bacteria are inoculated into 1% glucose containing trypticase soy broth. Bacteria culture is placed in 96 well tissue culture plate as 200 µl per well. The plate is incubated at 37°C for 24-48 hours. After, planktonic bacteria are poured out and wells are washed. The wells are filled with 0.1% crystal violet stain and then washed with water to get rid of the excess stain. Remaining crystal violet stain is solubilized

with 95% ethanol and optical density (OD) is measured in ELISA reader at 620 nm (48). In another technique; tube method, bacteria are again inoculated in 1% glucose containing trypticase soy broth but this time test tubes are used instead of a tissue culture plate. Same procedures are carried out like in tissue culture method but at the end this time biofilm formation is detected qualitatively according to control strains. Biofilm formation is scored as weak/none, moderate or strong. In Congo Red Agar method, Congo Red indicator is added to sucrose containing brain heart infusion agar. Microorganisms are inoculated into Congo Red Agar plates and incubated at 37° for 24 hours. Dry crystals containing black colonies give qualitative biofilm formation (45). Xiong et al. monitored the biofilm formation in a mouse infection model with bioluminescent bacteria (49). Lux operon inserted S.aureus and P. aeruginosa are monitored real time with the help of an imaging system. Also a multi photon laser scanning microscopy can be used for the detection of biofilm formation in fluorescent bacteria (50).

2.2.3 Vancomycin

Vancomycin is a tricyclic glycopeptide antibiotic isolated from *Streptomyces orientalis*, effective against Gram-positive bacteria, especially MRSA (51-53). The drug shows its bactericidal effect by inhibiting the cell wall biosynthesis with binding to the cell wall precursors (54). Vancomycin has side effects such as nephrotoxicity, ototoxicity, poor venous tolerance thus systemic administration of this drug has some limitations (55). Vancomycin has four to six hours *in vivo* half-life and it is extracted from the body by renal extraction. On the other hand, *in vitro* half-life of the drug at 37°C is nine hours (56). The minimum inhibitory concentration (MIC) of vancomycin for MRSA is ≤ 2 μg/ml (57).

2.3 Controlled Drug Delivery Systems

Controlled drug delivery systems gain attention, since the infection in the body cannot be eradicated by systemic or parenteral drug delivery. As the infection deteriorates the blood circulation, systemically delivered drugs cannot reach to infection area. Beside the delivery of the drug to the infection area, these systems also have advantages like improving the efficacy of the drug and diminishing its

toxic effects (58). In controlled drug release, the drug concentration is in therapeutic level for the desired time of action (Figure 5) (59).

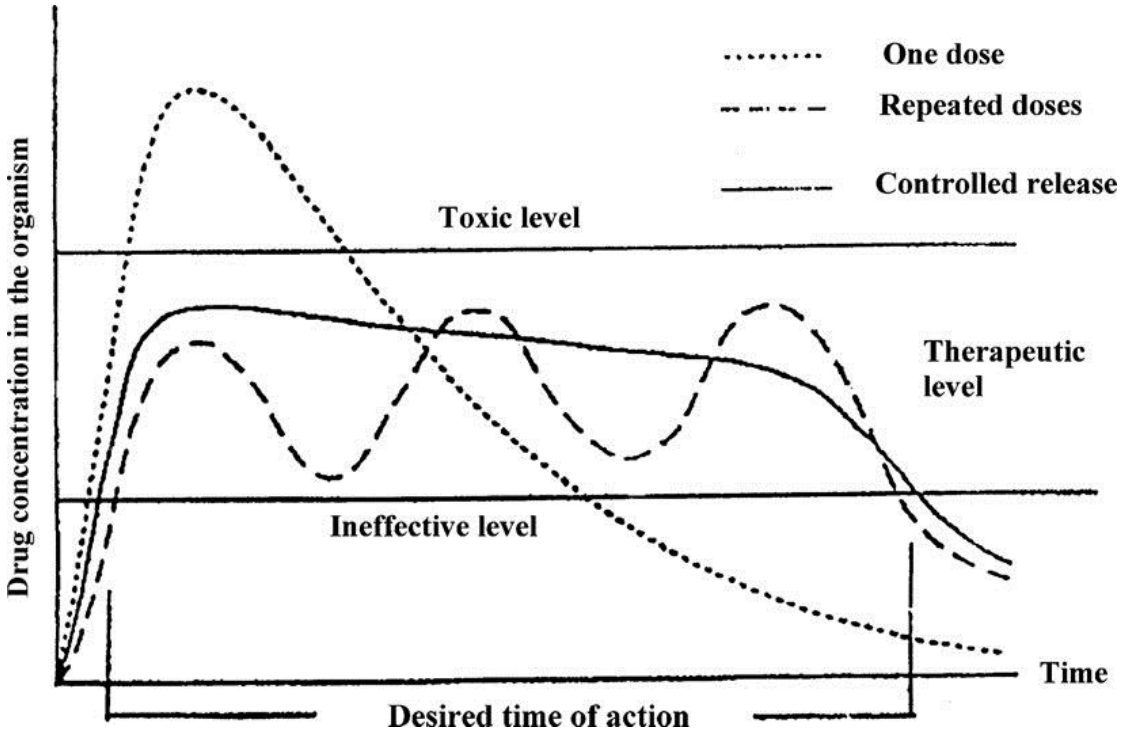

Figure 5. The illustration of controlled release (59).

For controlled drug delivery, there must be a carrier for the drug and drug is released either by diffusion, chemical reaction or solvent activation and transport. In diffusion systems, there is either a matrix (monolithic systems) or a reservoir (membrane systems) and drugs are diffused through these systems. In a matrix; drug is uniformly dissolved or dispersed (60) whereas in reservoir systems, drugs are surrounded by the carrier (61).

In chemically controlled drug delivery systems, drug is released by degradation of the carrier material by water or a chemical reaction. Also, the drug can be linked to the carrier material with unstable bonds that can be degrading by water or a chemical reaction and release the drug. In solvent activated mechanism, the drug can be released either by swelling of the carrier material or by osmotic effect in which external water enters the system and gives out the drug (Figure 6) (59).

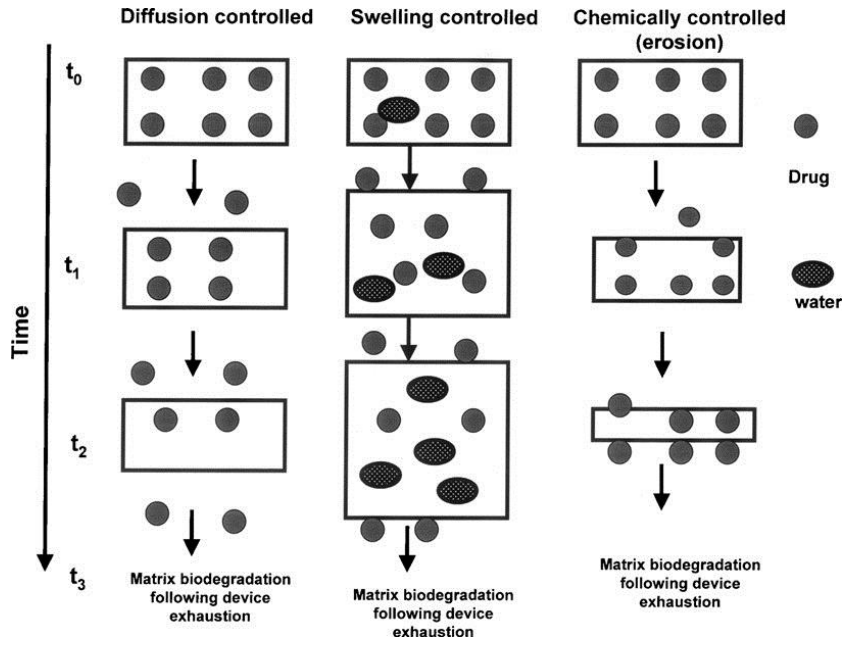

Figure 6. The illustration of three mechanisms for controlled drug delivery (59).

Drug release systems can be classified as nonbiodegradable and biodegradable systems and many different types of carrier materials like polymers, ceramics and polymer/ceramic composites can be used in their fabrication.

2.4 Polymers

Polymers are the macromolecules that are made up of the repeating units of monomers. Polymers are classified as natural and synthetic polymers, and they are widely used as surgical sutures, implants, and drug delivery systems and as scaffolds in tissue engineering. The natural polymers are found and extracted from the nature while synthetic polymers are industrially synthesized (55). Agarose (62), alginate (63), hyaluronic acid (64), chitosan (65), methylcellulose (66), fibrin (67) and collagen (68) are all natural polymers used for these purposes. On the other hand, poly alpha-hydroxy acids, polyhydroxyalkanoate (69), polyacrylate, polycaprolactone (70), polyanhydrides (71), polyorthoester (72), polyvinyl alcohol (73) and polymethylmethacrylate (74) are all synthetic polymers used to manufacture drug release systems, scaffolds and implants.

Polymetylmethacrylate (PMMA) is used as an antibiotic carrier for orthopedic infections since 1970s (75). Unfortunately, PMMA has several drawbacks: PMMA is a nonbiodegradable polymer, so a second surgery is needed for its removal from the body. The polymer shows an exothermic reaction during polymerization, thus only heat stable antibiotics can be carried and the material has a poor elution profile (76, 77). In order to alter these disadvantages, biodegradable biopolymers can be used. Poly alpha-hydroxy acids like polylactic acid (PLA) and polyglycolic acid (PGA) and their copolymers are biodegradable polymers generally used instead of PMMA as a drug carrier.

2.4.1 Poly (D, L-Lactic acid) (PDLLA)

PDLLA is a copolymer of PLA, which can be found in two different forms: L-lactide (PLLA) and D-lactide (PDLA). These two forms are in semi cystalline structure. When the racemic mixtures of L-lactide and D-lactide are polymerized, an amorphous poly (D,L-lactide) is formed (78). PDLLA is used as a controlled release system carrier and scaffold material due to its biocompatibility and biodegradability (79). During the biodegradation of PDLLA, the center is degraded more faster than the outer layer as a result of high levels of acidic degradation products (80).

2.4.2 Poly (D, L-Lactide-co-Glycolic acid) (PLGA)

Poly (D, L-lactide-co-glycolic acid) is a biodegradable and biocompatible polymer used for various medical purposes, and synthesized by ring opening co-polymerization of D,L-lactide and glycolide. Since the chain compositions determine the degradation rate of the polymer, the glycolic acid found its structure leads the faster degradation of the polymer (55). The degradation rate of PLGA can be adjusted by modifying the lactide:glycolide ratio of the polymer (81). If the lactide ratio is higher than the glycolide ratio, polymer degrades much slower. As an exception, PLGA with 50:50 lactide:glycolide ratio, degrades at a fastest rate (82).

2.4.3 Biodegradation of PDLLA and PLGA

Biodegradation is the biological breakdown of the polymers and changing their physicochemical properties as a result of their interactions with the surrounding environment. The biodegradation rate is based on the molecular weight, surface area, material phase (crystalline versus amorphous) and racemic ratio of the polymer, presence of additives, implantation site and degradation mechanism (83, 84).

Biodegradation can occur as surface erosion or bulk erosion. In surface erosion, only the surface is degraded while the inner structure is nondegraded. By contrast in bulk erosion, all material is degraded (85).

Polymers can be degraded by hydrolysis, oxidation and enzymatic mechanisms. In hydrolytic degradation, the chemical bonds found in the backbone of the polymer are sheared by the water attack and form monomers. In oxidative degradation, the polymers are generally exposed to body. Since this exposition evokes the immune response, the reactive oxygen species produced by macrophages and leukocytes will sheared the polymer chains and lead the biodegradation of the polymer. In enzymatic degradation, enzyme is diffused to the surface of the polymer and adsorbed by the substrate. After, hydrolytic mechanism is catalyzed and polymer degrades (84).

When a polymer degrades, it also releases some side products, which can induce the local inflammation (Figure 7) (86).

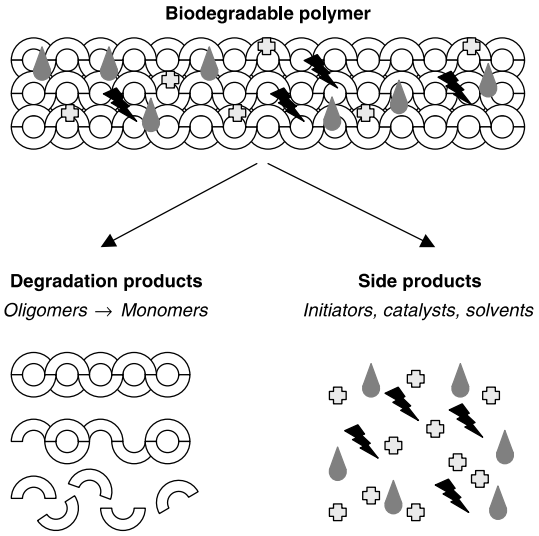

Figure 7. Biodegradation of a polymer (86).

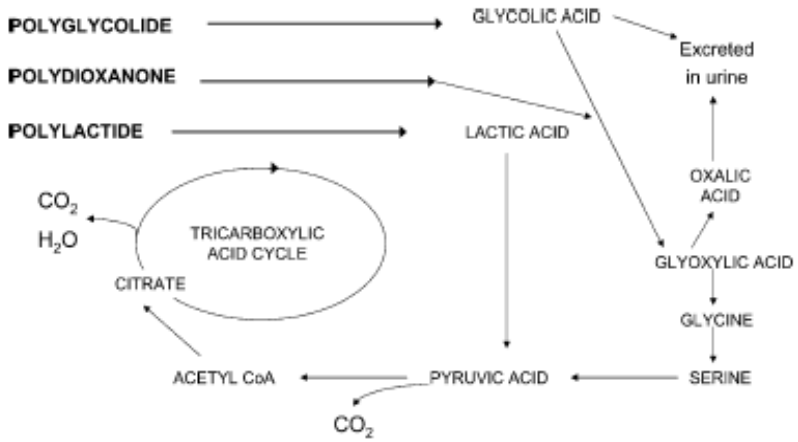

Figure 8. The metabolic biodegradation of PDLLA and PLGA (87).

In the biodegradation of PDLLA and PLGA polymers, their ester bonds are cleaved by hydrolysis. As a result of the degradation, lactic acid and glycolic acid monomers come off and in *in vivo* conditions, these monomers enter the tricarboxylic acid cycle and excreted from the respiratory system as water and carbon dioxide (Figure 8) (86, 87). The lactic acid and glycolic acid monomers also trigger the further degradation since the acidic products lower the pH of the solution (55).

2.5 Bioceramics

Bioceramics are widely used as implant materials and drug carriers especially in the orthopedics. As they can restore the functions of teeth and bone, they are also used as bone fillers since 1960s (88). There are various types of bioceramics used in medical field like calcium phosphates such as hydroxyapatite (89) , beta-tricalcium phosphate (90), biphasic calcium phosphate (91) ; (92) calcium sulphate; and bioactive glasses (93).

2.5.1 Beta-Tricalcium Phosphate (β-TCP)

Beta-tricalcium phosphate ($Ca_3 (PO_4)_2$) is the beta (β) polymorph of tricalcium phosphate known as a biodegradable ceramic (94). Besides biodegradability, β-TCP also has osseointegration, osseoconduction and bioactivity properties (95). β-TCP is more soluble than hydroxyapatite but its resorption rate is not high enough for complete osseointegration (52).

2.6 Research Questions

We asked whether;
Vancomycin containing PDLLA or PLGA/β-TCP composites can be developed and characterized.
These composites will release vancomycin for six weeks while showing antibacterial activity against MRSA and inhibit biofilm formation.
These composites will allow cell proliferation and differentiation and stimulate osteogenesis related signaling molecules.

2.7 Hypotheses

The hypotheses of the study were:
Vancomycin will be released from vancomycin containing PDLLA/β-TCP and vancomycin containing PLGA/β-TCP composites for six weeks and will have antibacterial activity against MRSA and inhibit biofilm formation.

The vancomycin containing PDLLA/β-TCP and vancomycin containing PLGA/β-TCP composites will proliferate and differentiate mesenchymal stem cells in *in vitro* conditions and stimulate osteogenesis related signalling molecules.

2.8 Aims of Study

The aims of the study are;

1) to develop and characterize vancomycin containing PDLLA/β-TCP and vancomycin containing PLGA/β-TCP composites
2) These composites will release vancomycin for six weeks, having antibacterial activity against MRSA and inhibit biofilm formation
3) These composites will be biocompatible with mesenchymal stem cells in *in vitro* conditions.

2.9 Study Design

This study was done to search (a) the biofilm inhibition potential of vancomycin containing PLGA/β-TCP and PLGA/β-TCP composites in *in vitro* conditions and (b) the biocompatibility of vancomycin containing PLGA/β-TCP and PLGA/β-TCP composites with mesenchymal stem cells. At the beginning, the composites were fabricated and characterized. Later, the *in vitro* degradation of the composites was analyzed. This was followed with the analysis of bone like apatite formation on the surface of the composites. Also, vancomycin releases from the composites were observed for six weeks. Further, microbiological studies were conducted for antibiotic susceptibility and biofilm formation. At the end, cell culture studies were done with respect to the biocompatibility of the composites.

CHAPTER 3

EXPERIMENTAL

3.1 Materials

PLGA (Resomer RG858S) and PDLLA (Resomer R202S) were purchased from Evonik Industries (Evonik Industries, Essen, Germany). These were both solid polymers with white to off white colour. PLGA composed of 85% D,L-lactide and 15% glycolide according to its molar ratio. PLGA and PDLLA had 1.4 dl/g and 0.22 dl/g inherent viscosity, respectively. Vancomycin hydrochloride was purchased from Zhejiang Medicine (Zhejiang Medicine Co.,Ltd, Xinchang Pharmaceutical Factory, Zhejiang, China). It was an almost white, hygroscopic powder, which was freely soluble in water and slightly soluble in 96% ethanol. Beta tricalcium phosphate (β-TCP) was purchased from BMT Calsis (BMT Calsis Health Technologies Co., Ankara, Turkey). It was a white powder with 75-200 μm particle size. Dichloromethane (CH_2Cl_2) (JT Baker, Avantor Performance Materials, Pennsylvania, United States of America) was used to dissolve the polymers.

3.2 Preparation of Vancomycin containing Polymer/Bioceramic Composites

In order to prepare vancomycin containing PLGA/β-TCP composites, a total of 8574 mg of PLGA was dissolved in 40 ml of dichloromethane. After, 5355 mg of vancomycin hydrochloride powder was added into the solution followed by the addition of 16071 mg β-TCP. The mixture was stirred on a magnetic stirrer with a closed lid and dried at room temperature for 24 hours. After the evaporation of dichloromethane, the rest powdery structure was grinded in a porcelain mortar. For vancomycin containing PDLLA/β-TCP composites, all the procedures mentioned

above were repeated but this time 8574 mg of PDLLA was used instead of PLGA. The powders were hand pressed in a tablet pressing machine and totally 149 vancomycin containing PLGA/β-TCP composite discs and 160 vancomycin containing PDLLA/β-TCP composite discs were obtained. The composite discs had 3 mm height with 6 mm diameter. The final content ratios of the composites were 53.57% β-TCP, 28.58% polymer and 17.85% vancomycin hydrochloride.

3.3 Characterization of Vancomycin containing Polymer/Bioceramic Composites

3.1.1 Scanning Electron Microscopy

Surface topography of the vancomycin containing PLGA/β-TCP and PDLLA/β-TCP composite discs were analyzed by using Nova Nanosem 430 (Fei, Oregon, USA) Scanning Electron Microscope in METU Metallurgical and Materials Engineering Department. The images were taken at 500, 1000 and 2500 magnifications. The composite discs were fixed on supports and coated with gold film to obtain a conducting surface before the analysis. The surface composition of the composite discs was also analyzed with a built-in X-ray energy-dispersive spectrometry (EDS).

3.1.2 Fourier Transform Infrared Spectroscopy

The vancomycin containing composite discs were evaluated by using fourier transformed infrared microscopy (FTIR-ATR) (Bruker Alpha, Bruker, Massachusetts, United States of America). PLGA, PDLLA, β-TCP and vancomycin were also analyzed to determine the similarities and differences between the composite discs and plain materials. The infrared spectrum was collected in the range of 4000–400cm^{-1} with a resolution of 4cm^{-1} and scans of 24.

3.4 *In vitro* Degradation of Vancomycin containing Polymer/Bioceramic Composites

The vancomycin containing composite discs from each group were immersed into simulated body fluid (SBF) for *in vitro* degradation. SBF was prepared as follows:

sterilized polyethylene bottle was filled with 750 ml of ultra pure water. A magnetic stirring bar was placed into the bottle and the water was heated up to 37°C on a magnetic stirrer. Afterwards, 7996 mg of sodium chloride (NaCl, Merck, New Jersey, United States of America), 350 mg of sodium bicarbonate ($NaHCO_3$, Merck, New Jersey, United States of America), 224 mg of potassium chloride (KCl, Horasan Chemistry, Ankara, Turkey), 228 mg of potassium phosphate dibasic trihydrate ($K_2HPO_43H_2O$, Sigma Aldrich, Missouri, United States of America), 305 mg of magnesium chloride hexa hydrate ($MgCl_26H_2O$, Riedel-de Haenn AG, Hanover, Germany), 40 ml 1M hydrogen chloride (HCl, Sigma Aldrich, Missouri, United States of America), 278 mg of calcium chloride ($CaCl_2$, Sigma Aldrich, Missouri, United States of America), 71 mg of sodium sulphate (Na_2SO_4, Sigma Aldrich, Missouri, United States of America) and 6057 mg of tris-(hydromethyl) aminomethane ($(CH_2OH)_3CNH_2$, Sigma Aldrich, Missouri, United States of America donated from Hacettepe University Faculty of Pharmacy) were added, respectively. pH of the solution was set to 7.4 by adding 1 kmol/dm^3 of HCl solution. Later, the volume was completed to 1000 ml by adding ultra pure water (96).

In vitro degradation of the composite discs were analyzed for 1 week, 3 weeks and 6 weeks. For each time point vancomycin containing composite discs from each group (n=3) were weighted and placed into polystyrene bottles filled with 10 ml of SBF. At the predetermined time points, the composite discs were removed from the bottles; excess solution was removed with a filter paper and weighted. The wet composite discs were dried under a laminar flow for 24 h and dry discs were weighted. The mass loss of the composite discs were determined by the following equation where m_i is the initial dry weight of the composite disc and m_f is the final dry weight of the composite disc.

$$mass\ loss\ (\%) = \frac{m_i - m_f}{m_i} \times 100\%$$

For water uptake calculation, percent of absorbed SBF was determined like mass loss equation. This time, initial dry weight of the composite disc was subtracted from wet

weight of the composite disc and divided with initial dry weight of the composite disc. The result was multiplied with hundred to obtain the percentage.

3.5 Bone Like Apatite Formation on the Surface of Vancomycin containing Polymer/Bioceramic Composites

Apatite formation on the surface of the composite discs that were immersed into SBF solution for 1, 3 and 6 weeks were determined with Nova Nanosem 450 (Fei, Oregon, USA) Scanning Electron Microscope. The elemental compositions of the composite discs were analyzed with EDS and the discs FTIR spectra were obtained.

3.6 Vancomycin Release Study for Vancomycin containing Polymer/Bioceramic Composites

Vancomycin containing composite discs from each group (n=6) were immersed into 50 ml phosphate buffered saline (PBS) containing polystyrene tubes. PBS was prepared by dissolving one PBS tablet (Oxoid, Hampshire, United Kingdom) in 100 ml distilled water. The tubes were placed into a hot water bath at 37°C and shaken constantly at 30 rpm. At predetermined time points (1, 2, 4, 8, 12, 24, 48, 120 h and 1, 2, 3, 4, 5, 6 weeks) 1 ml PBS was withdrawn and replaced with equal amount of fresh PBS. The withdrawn solutions were analyzed spectrophotometrically with Nanodrop ND 1000 spectrophotometer (Thermo Scientific, Massachusetts, United States of America) at 280 nm with 1:10 dilution factor. A calibration curve for vancomycin was generated to calculate the amount of released vancomycin in the solution.

The validation of spectrophotometer analysis was done by measuring three different vancomycin concentrations (100 μg/ml, 200 μg/ml and 300 μg/ml) at three different time points for six times.

3.7 Content Uniformity of Vancomycin containing Polymer/Bioceramic Composites

In order to determine the vancomycin stability in the composite discs, the discs were weighted and dissolved in 30 ml of dichloromethane. Later, 15 ml PBS was added and the mixture was vortexed for 10 min followed with 1 h of stirring. The supernatant was separated by centrifugation at 1500 rpm for 5 min. The solution was analyzed spectrophotometrically with Nanodrop ND 1000 spectrophotometer (Thermo Scientific, Massachusetts, United States of America) at 280 nm with 1:100 dilution factor.

3.8 Microbiological Studies of Vancomycin containing Polymer/Bioceramic Composites

3.8.1 Antibiotic Susceptibility Test for Vancomycin containing Polymer/Bioceramic Composites

The microbiological effects of the vancomycin containing composite discs were evaluated with antibiotic susceptibility test. Slime forming and slime non-forming methicillin resistant *Staphylococcus aureus* (MRSA) strains were obtained from Hacettepe University Faculty of Medicine Department of Clinical Microbiology. Bacterial suspensions were pipetted into sterile glass tubes containing 2 ml of trypticase soy broth (Becton Dickinson, New Jersey, United States of America) and the bacterial cultures were set to 0.5 McFarland standard with a benchtop turbidity meter (Grant Instruments, Cambridge, United Kingdom). Sterile tampon swabs (LP Italiana Spa, Milano, Italy) were dipped into bacterial cultures and streaked to sterile 90 mm Mueller Hinton agar plates (Orbak, Çağdaş Health Services, Ankara, Turkey). A single vancomycin containing composite disc from each group (n=3) were placed into the middle of the agar plate and the plate was incubated at 37°C overnight. The bacterial cultures were passaged in new sterile glass tubes containing fresh 2 ml trypticase soy broth by setting the fresh bacterial solution to 0.5 McFarland standard. The zone of inhibitions were measured and recorded. The fresh bacterial cultures were again streaked to fresh sterile agar plates like the day before and the composite discs were removed from the old plates and placed to new agar plates. The entire assay was done under aseptic conditions and lasted for 21 days.

3.8.2 Biofilm Inhibition Study for Vancomycin containing Polymer/Bioceramic Composites

Biofilm inhibition capabilities of vancomycin containing composites discs were evaluated with tissue culture plate method. A vancomycin containing composite disc from each group (n=3) was put into a polystyrene tube containing 10 ml of SBF and placed in a hot water bath at 37°C and shaken constantly at 30 rpm. Every week, 1 ml SBF was withdrawn and replaced with equal amount of fresh SBF until week 6. Beside SBF release mediums, PBS release mediums were also used for the assay. Each time point was carried out in triplicate. Only slime forming MRSA strain was used for this study. 200 µl bacteria was inoculated to fresh 2 ml trypticase soy broth and incubated at 37°C overnight. On the other day, bacteria suspension turbidity was checked with a benchtop turbidity meter and the bacteria suspension with 11.0 turbidity was poured into fresh 48 ml trypticase soy broth. This process was done in duplicate. 200 µl bacterial culture was added into each well of round bottom 96 well plates and 20 µl of drug release mediums collected from release studies were added to the wells. The plates were incubated at 37°C for 48 h. Trypticase soy broth without any bacteria was used as negative control while bacterial culture without any release medium was used as positive control.

After incubation, tissue culture plates were turned upside down and the planktonic bacteria were poured out. The plates were washed three times with tap water (200 µl water for each well). After washing, 125 µl 0.1% crystal violet stain was added to each well and plates were incubated at room temperature for 10 min. The plates were shaken and the excess stain was poured out, again the wells were washed twice with water. The plates were placed onto paper towel and allowed to dry. Each well was filled with 200 µl 95% ethanol and the plates were incubated at room temperature with closed lids for 15 min. The wells were gently mixed with pipetting and 125 µl ethanol-crystal violet mix from each well were placed into a new 96 well plate. The new plates were spectrophotometrically analyzed in ELISA reader (Tecan Sunrise, Mannedorf, Switzerland) at 620 nm.

3.9 Cell Culture Studies of Vancomycin containing Polymer/Bioceramic Composites

Two different vancomycin containing composite discs were evaluated for their proliferation and osteogenic potential. Cell proliferation and alkaline phosphatase activities of the composite discs were done with both human bone marrow originated mesenchymal stem cells (MSC, passage 6) (Poietics PT 2501, Lonza, Basel, Switzerland) and SaOS-2 osteosarcoma cells (passage 17) (Sigma Aldrich, Missouri, United States of America). Both cell cryovials were thawed in 37°C water and the cells were transferred into polypropylene tubes with 2 ml PBS. Empty cryovials were washed with 4 ml PBS and the PBS was added to the polypropylene tube. The PBS amount in the propylene tube was completed to ten milliliters. The tubes were centrifuged at 1500 rpm for 5 min and supernatant was poured. 5 ml PBS was added to each tube and the cell pellet was dispersed. 50 µl cell suspension was mixed with 50 µl tryphan blue (Biological Industries, Israel) in a centrifuge tube and the cells were counted on a Burker lamina.

For cell proliferation assay, total 202500 MSC and 202500 SaOS-2 cells were used. The assay was done in 24 well cell culture plates (Corning Costar, New York, Unites States of America) for three different time points (1, 3 and 7 days) in triplicate. In a 24 well cell culture plate, 12 wells were used for MSC while the other 12 wells were used for SaOS-2 cells. 7500 cells were seeded on each composite discs and control wells. The cells were cultured with MSC or SaOS-2 medium according to cell type. MSC culture medium consisted of 52.8% Dulbecco's Modified Eagle Medium (DMEM) with 1 g/l glucose (Lonza, Basel, Switzerland), 35.2% MCDB-201 medium (Sigma Aldrich, Missouri, United States of America), 10% heat inactivated fetal bovine serum (FBS) (Sigma Aldrich, Missouri, United States of America), 1% penicillin/streptomycin solution (Biochrom AG, Berlin, Germany) and 1% L-glutamine (Biochrom AG, Berlin, Germany) while SaOS-2 culture medium consisted of 89% DMEM with 4.5 g/l glucose (Sigma Aldrich, Missouri, United States of America), 10% heat inactivated FBS and 1% penicillin/streptomycin solution. In every 3-4 days, the mediums were changed. The plates were incubated at 37°C with relative humidity under an atmosphere of 5% CO_2. At predetermined time points, the

culture mediums were aspirated and 500 µl fresh mediums were added with 50 µl of cell proliferation agent WST-1 (Roche, Basel, Switzerland) for each well. The plates were incubated at 37°C with relative humidity under an atmosphere of 5% CO_2 for 4 hours. After incubation, 110 µl WST-1 containing culture medium was pipetted into a flat bottom 96 well plate and the absorbance of the wells were measured in ELISA reader (Tecan Sunrise, Mannedorf, Switzerland) at 450 nm with 620 nm reference wavelength.

The osteogenic potential of the vancomycin containing composite discs were evaluated with alkaline phosphatase activity staining for both MSC and SaOS-2 cells. 7500 cells were seeded on each composite discs and control wells. The cells were cultured with proper medium for 21 days at 37°C with relative humidity under an atmosphere of 5% CO_2 and in every 3-4 days the mediums were refreshed. On day 21, the mediums were discarded and 400 µl Alkaline Phosphate Yellow Liquid substrate system for ELISA (Sigma Aldrich, Missouri, United States of America) was added to each well. The plate was incubated for 30 min, and 100 µl of 3 N sodium hydroxide (NaOH) was added to each well to stop the reaction. 200 µl final product was pipetted to a flat bottom 96 well plate and analyzed with ELISA reader (Tecan Sunrise, Mannedorf, Switzerland) at 405 nm wavelength.

3.10 Real Time Quantitative Polymerase Chain Reaction (RT-qPCR) Assay for Vancomycin containing Polymer/Bioceramic Composites

Human bone marrow originated MSCs (passage 6, total 1500000 cells) were cultured in T75 flasks with MSC medium at 37°C with relative humidity under an atmosphere of 5% CO_2 and in every 3-4 days the mediums were refreshed. When cell were reached to 60-70% confluency, culture mediums in three flasks were discarded and replaced with osteogenic differentiation medium consisted of %10 FBS, 100 nM dexamethasone, 10 mM ß-glycerophosphate (Applichem, Germany) and 0,2 mM L-ascorbic acid (Sigma Aldrich, Missouri, United States of America) in DMEM-LG. Another three flasks mediums were refreshed with MSC medium and these flasks were used as control. Rest of the flasks were used for two different composite discs and extraction mediums were used for this purpose. Briefly, 33 composite discs from

each group were incubated with 30 ml of MSC culture medium. After 14 days of incubation, the cells were trypsinized with 0.25% Trypsin-EDTA (Invitrogen, Gibco, United Kingdom) and suspended in 200 µl PBS.

mRNA was isolated with High Pure RNA Isolation Kit (Roche, Basel, Switzerland). 400 µl lysis/-binding buffer was added to suspended cells and vortexed for 15 s. The sample was pipetted into a filter tube inserted in a collection tube and the entire tube was centrifuged at 8000 x g for 15 s. After centrifugation, the liquid in the collection tube was discarded. On the other hand, 90 µl DNase incubation buffer was mixed with 10 µl DNase I and pipetted to the upper reservoir of the filter tube. The entire tube was incubated at room temperature for 15 min. 500 µl wash buffer I was added to filter tube and the entire tube was centrifuged at 8000 x g for 15 s. The liquid in the collection tube was discarded again and this time 200 µl wash buffer II was added to the filter tube and the entire tube was centrifuged at 13000 x g for 2 min. The filter tube was removed from collection tube and inserted into a sterile microcentrifuge tube. 60 µl elution buffer was added to the filter tube and centrifuged at 8000 x g for 1 min. Eluted mRNA in the microcentrifuge tube was analyzed for its concentration and quality with Alphaspec spechtrophotometer and stored at -80°C for later analysis.

Complementary DNA (cDNA) was synthesized with Transcriptor High Fidelity cDNA Synthesis kit (Roche, Basel, Switzerland). Total RNA was mixed with 2 µl Random Hexamer Primer and PCR-grade water to make 11.4 µl total volume. The tube was incubated at 65°C for 10 min in Geneamp 9700 Classic PCR machine (Applied Biosystems, Thermo Scientific, Massachusetts, United States of America) and immediately cooled on ice. Later, 4 µl transcriptor High Fidelity Reverse Transcriptase Reaction Buffer, 0.5 µl Protector RNase inhibitor, 2 µl Deoxynucleotide mix, 1 µl DTT and finally 1.1 µl Transcriptor High Fidelity Reverse Transcriptase was added to tube to make a 20 µl final volume. The reagents were mixed carefully and the tube was incubated at 29°C for 10 min and then incubated at 48°C for 60 min. Finally, reverse transcriptase was inactivated by heating the tube at 85°C for 5 min. The reaction was stopped by placing the tube on ice and cDNA was stored at -20°C.

Real time quantitative PCR analysis was done by using Lightcycler 480 Probes Master Mix (Roche, Basel, Switzerland). 10 µl Probes Master was mixed with 5 µl PCR grade water. 15 µl PCR mix and 5 µl cDNA were pipetted into each well of custom plate designed for 86 different genes. The list of the genes and their forward and reverse primer sequences were given in Appendix C. Final PCR reaction was done in Lightcycler 480 with 1 cycle of preincubation (95°C, 10 min), 45 cycles of amplification (95°C, 10 s; 60°C, 30 s; 72°C, 1s) and cooling (40°C, 30 s). Lightcycler 480 software was used to calculate the crossing point (Cp) for target and reference genes with Advance Relative Quantification method. All target genes were normalized to housekeeping genes ACTB, GAPDH and G6PD. The results were given as fold change corresponding to mesenchymal stem cells control group according to ΔΔCt calculation.

3.11 Statistical Analysis

All the results were given in average /± standard deviation and analyzed with SPSS 11.0 and StatPlus software. Statistically significant values were defined as $p < 0.05$ based on Analysis of Variance (ANOVA). For the analysis of RT-PCR study, binary logarithm of the ΔΔCt values were obtained and ±2 fold changes were assigned as significant.

CHAPTER 4

RESULTS

4.1 Characterization of Vancomycin containing Polymer/Bioceramic Composites

The surfaces of vancomycin containing PDLLA/β-TCP and PLGA/β-TCP composites were analyzed using Nanosem under 500, 1000 and 2500 magnification. SEM micrographs taken from the surfaces of the composites were smooth but micro cracks were noticed as seen in Figure 9 and Figure 10. No notable difference was observed between PDLLA/β-TCP and PLGA/β-TCP composites.

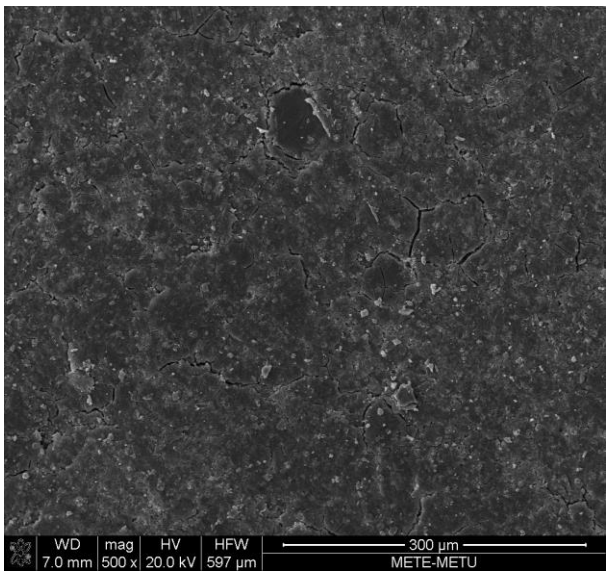

(a)

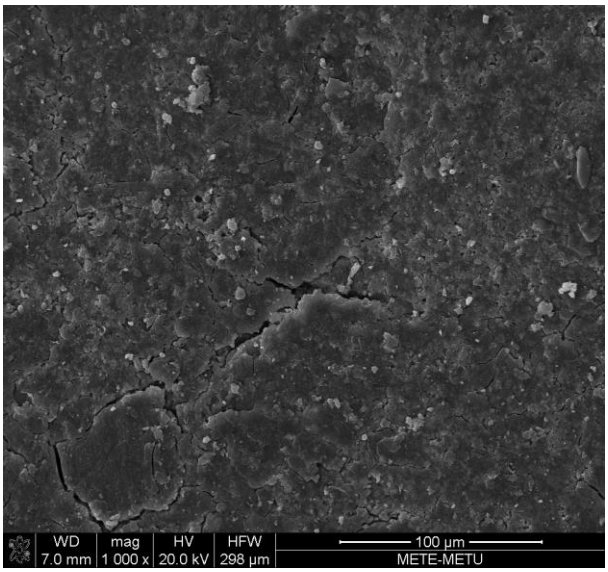

(b)

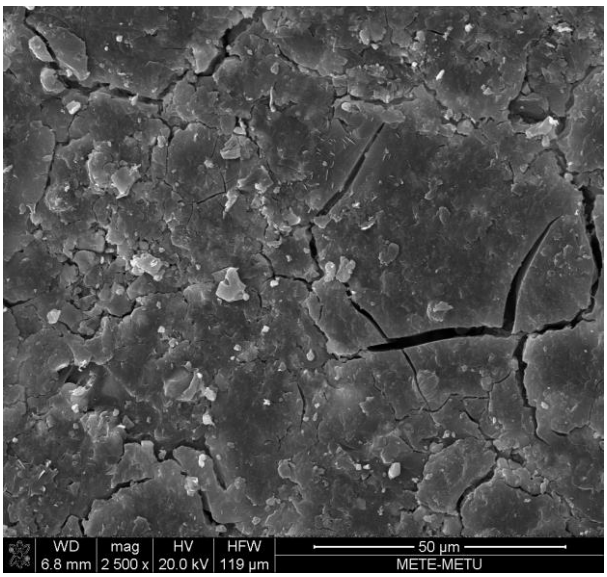

(c)

Figure 9. SEM micrographs of vancomycin containing PDLLA/β-TCP composites at (a) 500X, (b) 1000X and (c) 2500X magnification.

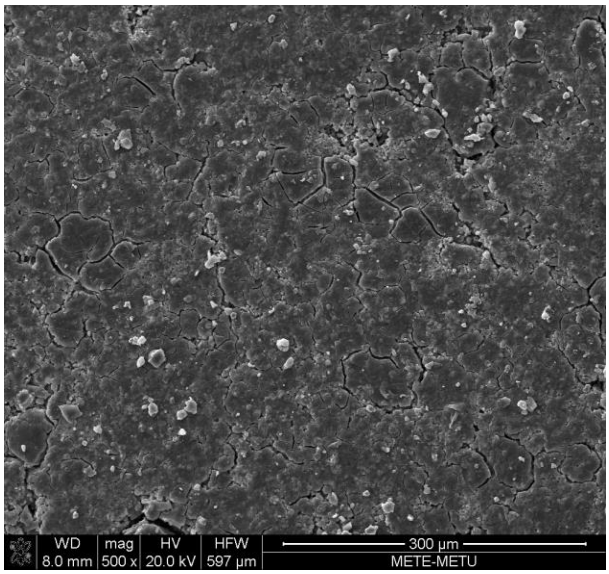
WD
8.0 mm
mag
500 x
HV
20.0 kV
HFW
597 µm
300 µm
METE-METU

(a)

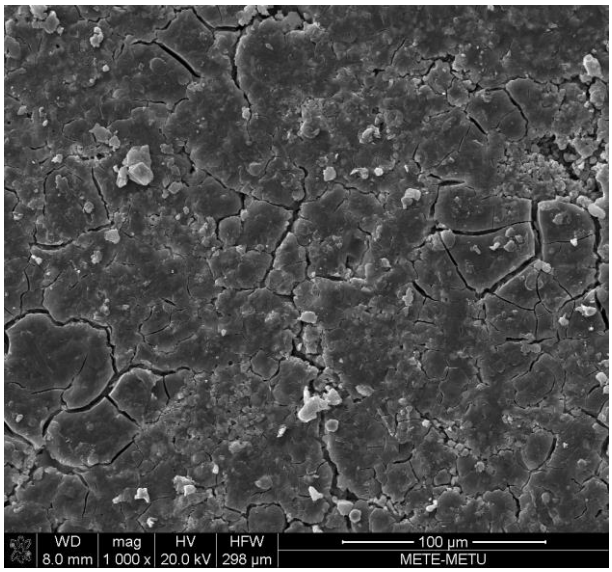
WD
8.0 mm
mag
1 000 x
HV
20.0 kV
HFW
298 µm
100 µm
METE-METU

(b)

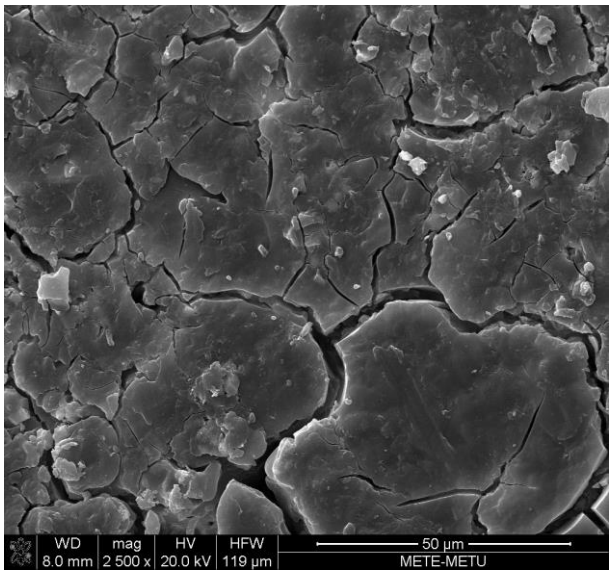

(c)

Figure 10. SEM micrographs of vancomycin containing PLGA/β-TCP composites at (a) 500X, (b) 1000X and (c) 2500X magnification.

Vancomycin containing PDLLA/β-TCP and PLGA/β-TCP composites had similar EDS spectra as seen in Figure 11. In both composites, carbon came from polymer, calcium and phosphorous came from tricalcium phosphate and the source of chloride was vancomycin HCl. EDS analysis revealed that, by neglecting carbon, oxygen, and gold, PDLLA/β-TCP composites composed of 28.62% phosphorus, 14.54% chloride, and 56.84% calcium (wt,%), while PDLLA/β-TCP composites composed of 27.43% phosphorus, 14.16% chloride, and 56.41% calcium, respectively (wt,%). These compositions were alike the intended composition where they composed of 53.57% of tricalcium phosphate and 17.85% of vancomycin hydrochloride.

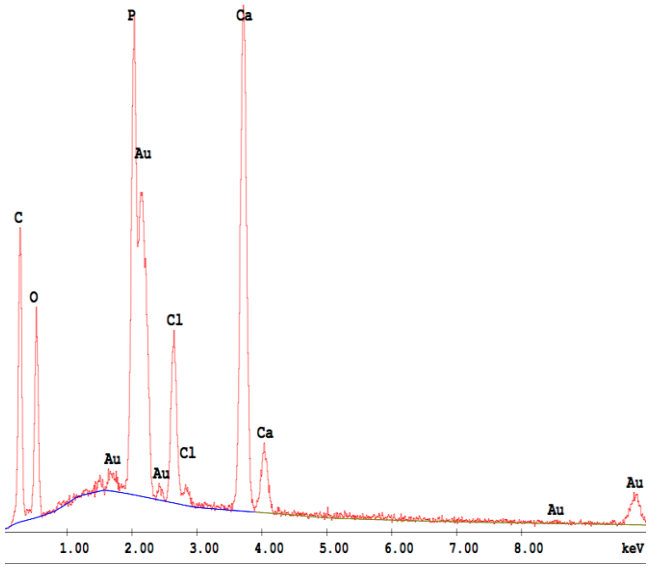

(a)

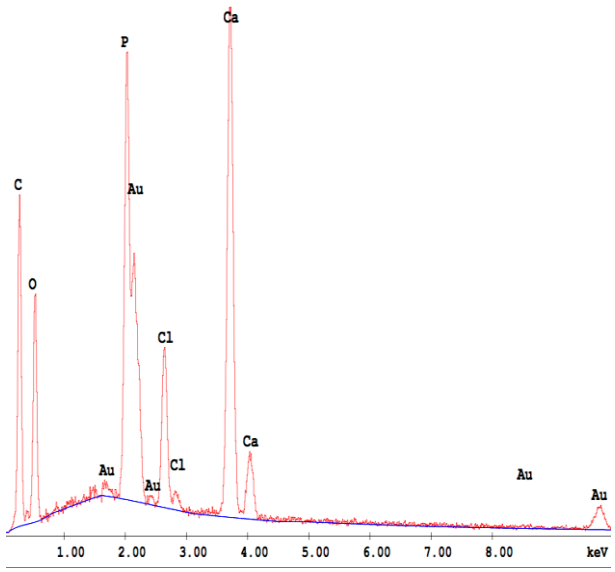

(b)

Figure 11. EDS spectra of (a) vancomycin containing PDLLA/β-TCP and (b) PLGA/β-TCP composites.

The FTIR spectra of both composites were shown in Figure 12. The adsorption bands of vancomycin were found at 3252 cm^{-1}, 1644 cm^{-1}, 1487 cm^{-1}, 1225 cm^{-1}, 1014 cm^{-1} and 426 cm^{-1}. The adsorption band at 3252 cm^{-1} was for O-H stretching, while 1644 cm^{-1} showed C=O stretching. The bands at 1487 cm^{-1}, 1225 cm^{-1} pointed C=C band and C-O-C band, respectively (97). The adsorption bands of β-TCP were found at

1212 cm^{-1} (pyrophosphate CPP group band), 1017 cm^{-1} (C-O stretching), 727 cm^{-1} (P-O stretching) and 542 cm^{-1} (P-O bending) (98). The characteristic peaks of PDLLA and PLGA were found at 1746 cm^{-1} (C=O band), 1183 cm^{-1} (C-O band) 1022 cm^{-1} (C-O band) and 540 cm^{-1} (C-H band) (99). In both vancomycin containing composites, the peaks were found at 1749 cm^{-1} (C=O band), 1017 cm^{-1} (C-O band) and 538 cm^{-1}. The similarities of spectra were pointed in circles, red defined vancomycin, green defined β-TCP, purple defined PDLLA and blue defined PLGA.

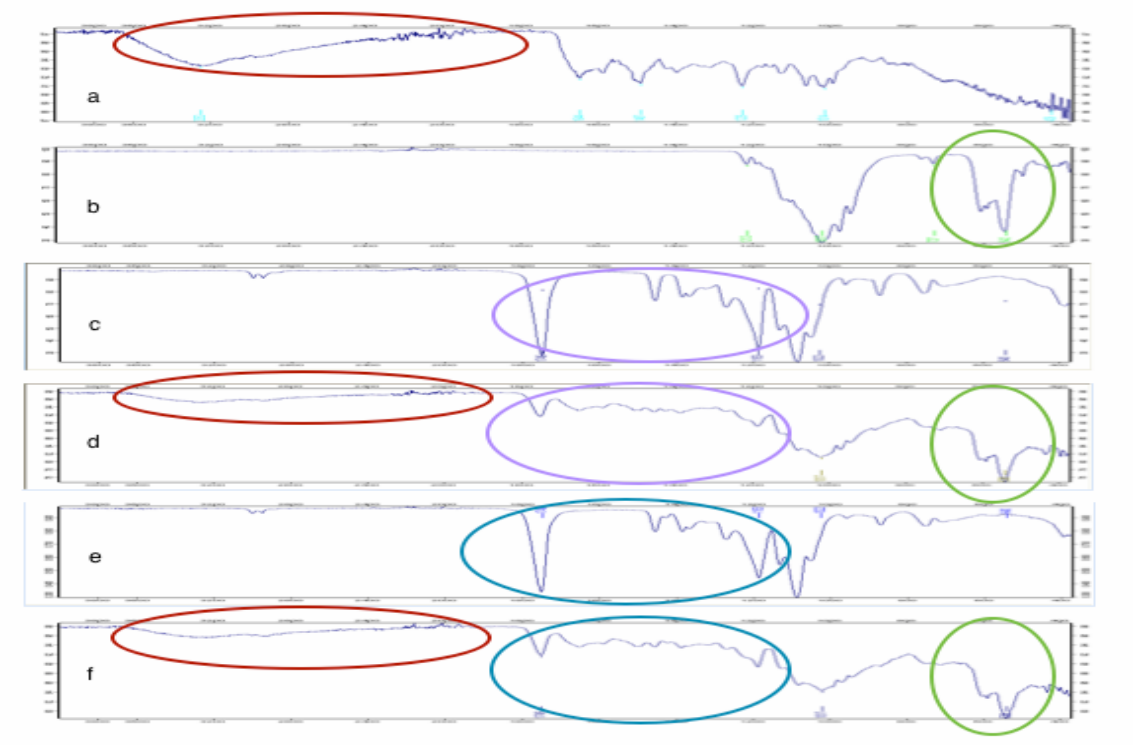

Figure 12. FTIR spectra of (a) vancomycin, (b) β-TCP, (c) PDLLA, (d) vancomycin containing PDLLA/β-TCP composite, (e) PLGA and (f) vancomycin containing PLGA/β-TCP composite.

4.2 *In vitro* Degradation of Vancomycin containing Polymer/Bioceramic Composites

The weight loss percentages of vancomycin containing PDLLA/β-TCP and PLGA/β-TCP composites were given in Figure 13. PDLLA/β-TCP composites lost 31.99±4.8%, 41.01±9.8% and 67.98±1.5% of their mass in week 1, week 3 and week

6, respectively. On the other hand, PLGA/β-TCP groups lost only 10.81±1.1%, 18.33±0.6%, 19.13±0.2% of their mass in week 1, week 3 and week 6, respectively. The loss percentages rose by time and PDLLA/β-TCP composites lost more mass than PLGA/β-TCP composites. The statistical difference between PDLLA/β-TCP and PLGA/β-TCP composites were p: 0.002 for week 1, p: 0.016 for week 3 and p: 0.0001 for week 6. Also for each group, there was a statistical difference between weeks (p: 0.002 for week 1-week 6 and p:0.009 for week 3-6 in PDLLA/β-TCP group and p:0.0005 for week 1-week 3 and p:0.003 for week 1-week 6 in PLGA/β-TCP group).

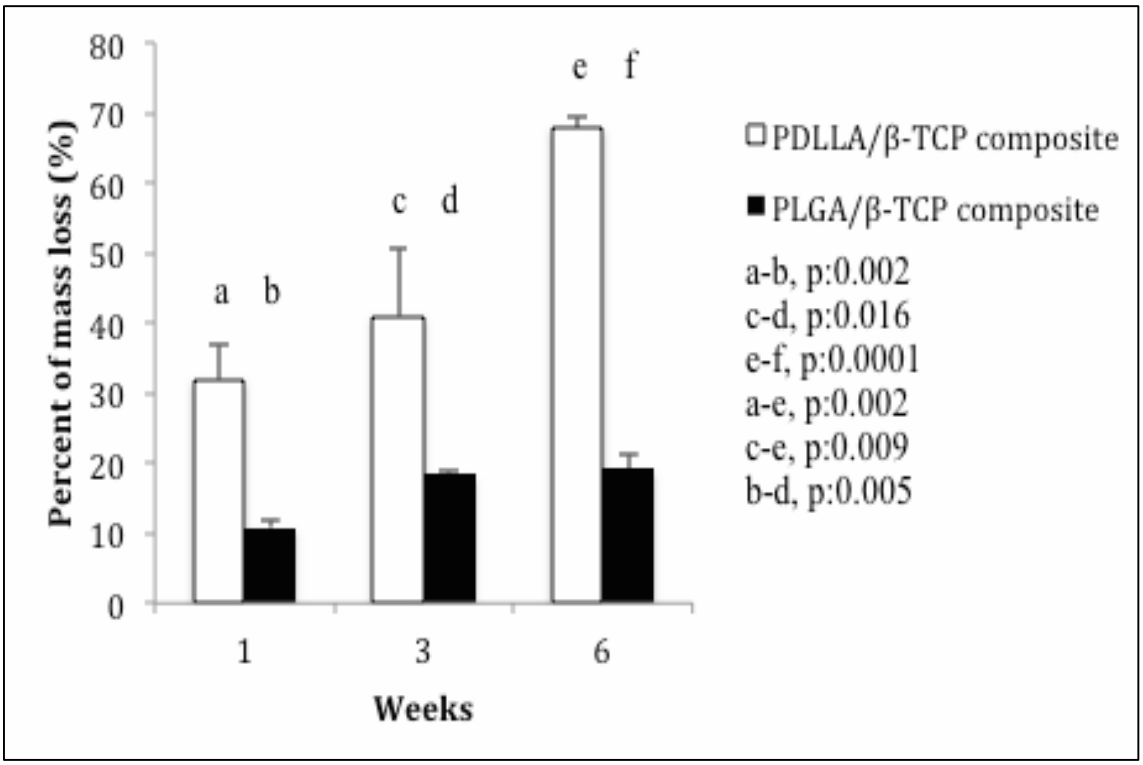

Figure 13. The mass loss percentages of vancomycin containing composites over six weeks.

The water uptake percentages of vancomycin containing PDLLA/β-TCP and PLGA/β-TCP composites were given in Figure 14. PDLLA/β-TCP composites took 45.44±6.6%, 31.15±4.5% and 12.75±1.8% water in week 1, week 3 and week 6, respectively. On the other hand, PLGA/β-TCP groups took 42.02±5.8%, 17.98±1.6%, 16.47±2.9% water in week 1, week 3 and week 6, respectively. The

percentages decreased by time and there was no statistical difference between PDLLA/β-TCP and PLGA/β-TCP groups except week 3 (p:0.008). In PDLLA/β-TCP and PLGA/β-TCP groups, there was a statistical difference between first and third, first and sixth and third and sixth weeks (For PDLLA/β-TCP, the statistical difference between week 1 and 3 was p:0.03, between week 1 and 6 was p:0.001 and between week 3 and 6 was p:0.003. For PLGA/β-TCP, the statistical difference between week 1 and 3, and week 1 and 6 was p: 0.002).

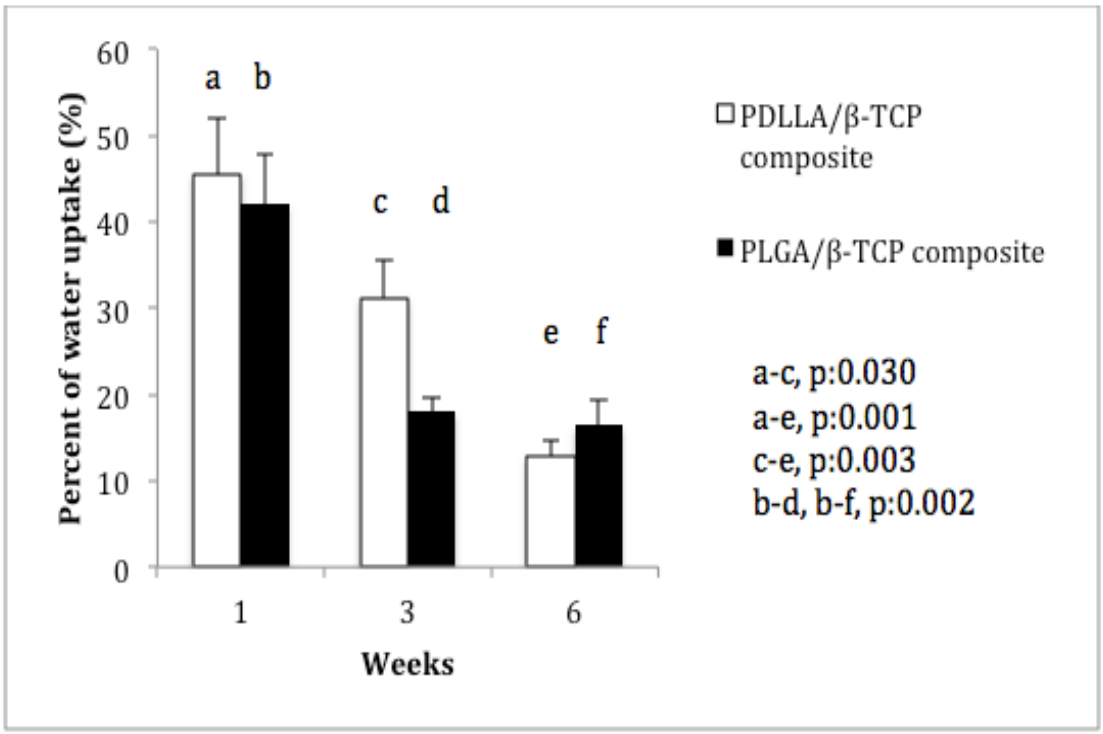

Figure 14. The water uptake percentages of vancomycin containing composites over six weeks.

4.3 Bone Like Apatite Formation on the Surface of Vancomycin containing Polymer/Bioceramic Composites

The apatite formation on the surfaces of vancomycin containing PDLLA/β-TCP and PLGA/β-TCP composites was confirmed with SEM micrographs shown in Figure 15 and Figure 16. With the increase of immersion time, the quantity and size of the precipitates increased. From EDS spectra of the composites, calcium (Ca) and

phosphorous (P) molar ratio for each immersion time was calculated. Ca/P molar ratios for PDLLA/β-TCP composites were 1.57, 1.69 and 1.88 for week 1, week 3 and week 6, respectively. Similarly for PLGA/β-TCP composites, Ca/P molar ratios were found 1.66, 1.73 and 1.77 for week 1, week 3 and week 6, respectively. Only week 3 PDLLA/β-TCP and week 1 PLGA/β-TCP composites had similar Ca/P molar ratios like stoichiometric apatite, which is 1.67 while the others were nonstoichiometric apatite.

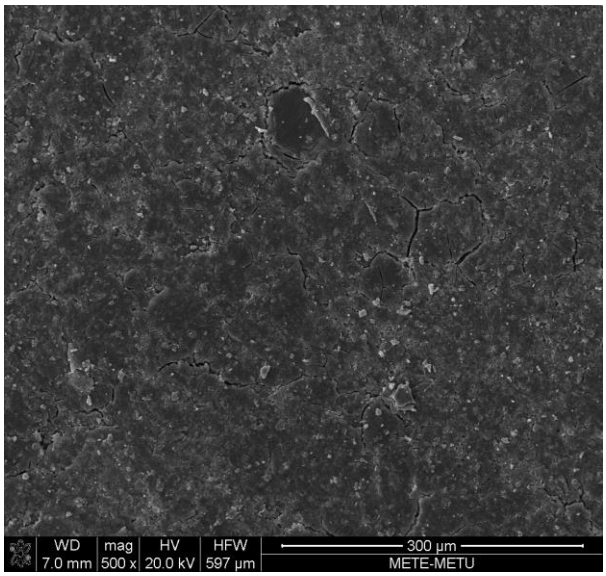

(a)

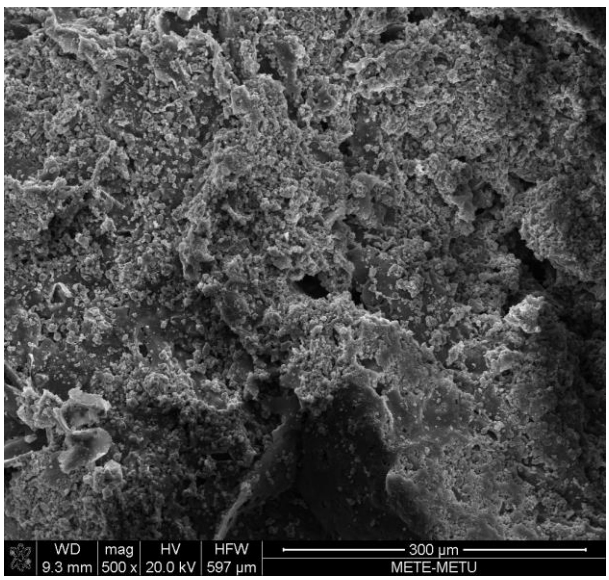

(b)

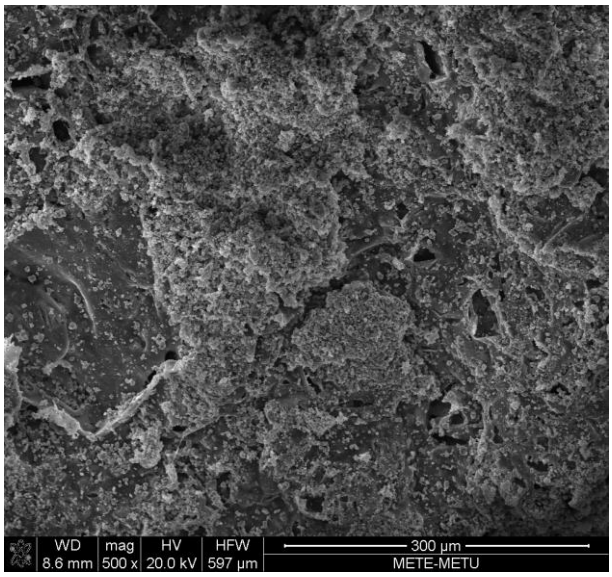

(c)

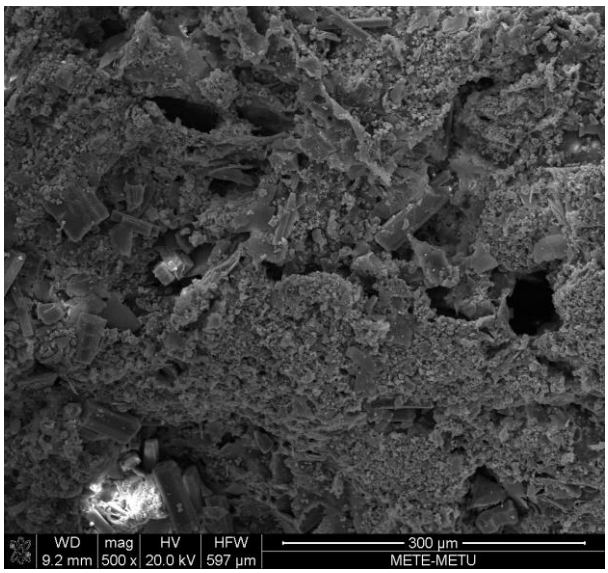

(d)

Figure 15. SEM micrographs of composites PDLLA/β-TCP for apatite formation: (a) was not immersed into SBF, (b) immersed for 1 week, (c) immersed for 3 weeks, (d) immersed for 6 weeks.

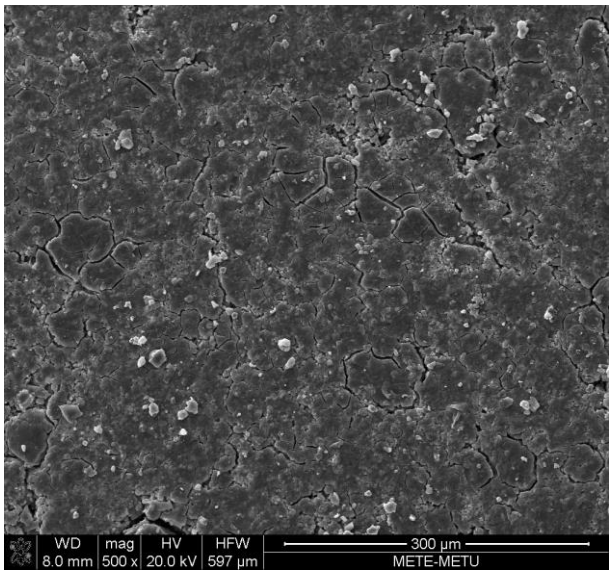
WD
8.0 mm
mag
500 x
HV
20.0 kV
HFW
597 µm
300 µm
METE-METU

(a)

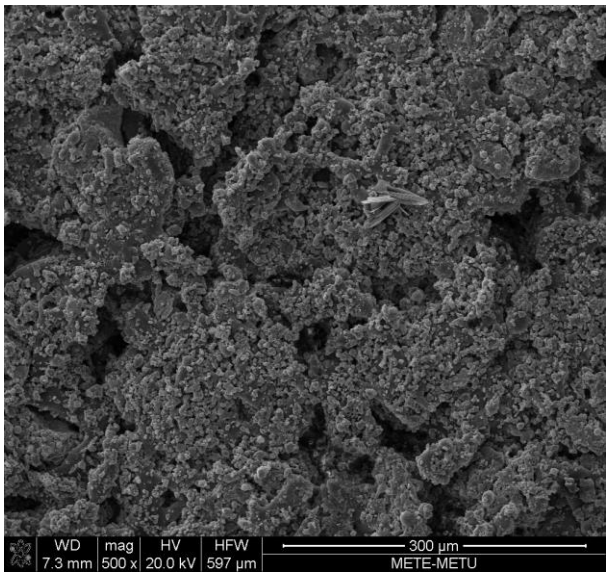
WD
7.3 mm
mag
500 x
HV
20.0 kV
HFW
597 µm
300 µm
METE-METU

(b)

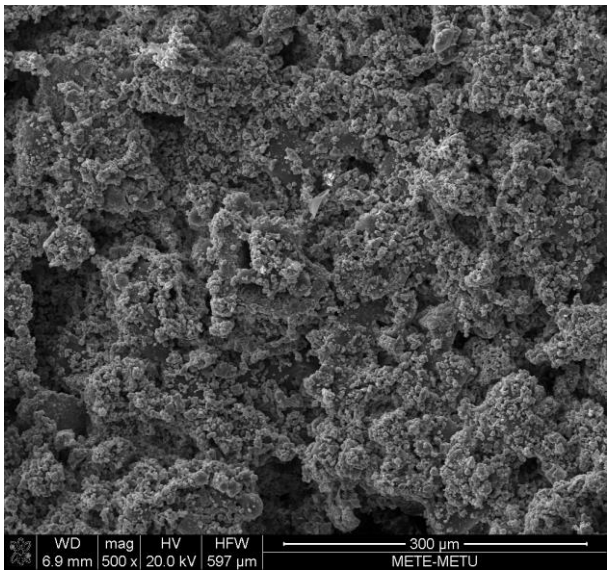

(c)

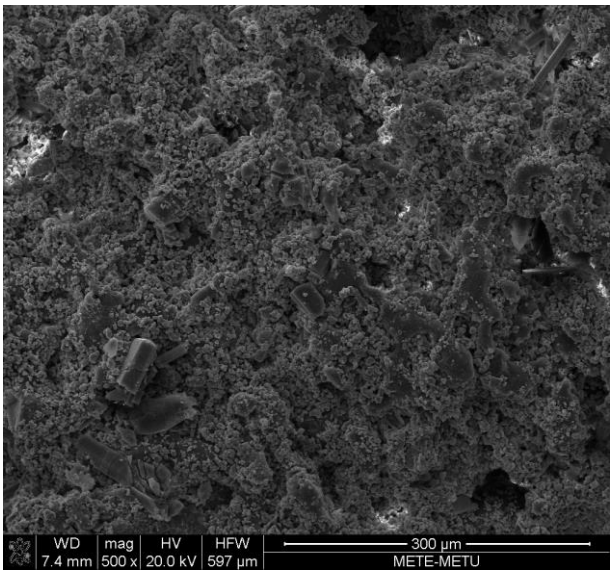

(d)

Figure 16. SEM micrographs of composites PLGA/β-TCP for apatite formation: (a) was not immersed into SBF, (b) immersed for 1 week, (c) immersed for 3 weeks, (d) immersed for 6 weeks.

Also, FTIR spectra of SBF immersed PDLLA/β-TCP and PLGA/β-TCP composites were obtained and compared with the FTIR spectra of composite that was not immersed into SBF. The spectra of both composites were shown in Figure 17 and 18. The characteristic peaks for PDLLA/β-TCP composite after seven days of SBF immersion were found at 1747 cm^{-1}, 1183 cm^{-1}, 1037 cm^{-1} and 540 cm^{-1}. These peaks

were found at 1747 cm^{-1}, 1024 cm^{-1}, 545 cm^{-1}, 453 cm^{-1} and 421 cm^{-1} after three weeks of SBF immersion. After six weeks of SBF immersion, the peaks were found at 3351 cm^{-1}, 1747 cm^{-1}, 1183 cm^{-1}, 1022 cm^{-1} and 539 cm^{-1}. Similarly, the characteristic peaks for PLGA/β-TCP composite after a week of SBF immersion were found at 1747 cm^{-1}, 1038 cm^{-1}, 598 cm^{-1}, 544 cm^{-1} and 405 cm^{-1}. These peaks were found at 1747 cm^{-1}, 1183 cm^{-1}, 1020 cm^{-1} and 540 cm^{-1} after three weeks of SBF immersion. After six weeks of SBF immersion, the peaks were found at 1746 cm^{-1}, 1183 cm^{-1}, 1022 cm^{-1} and 543 cm^{-1}.

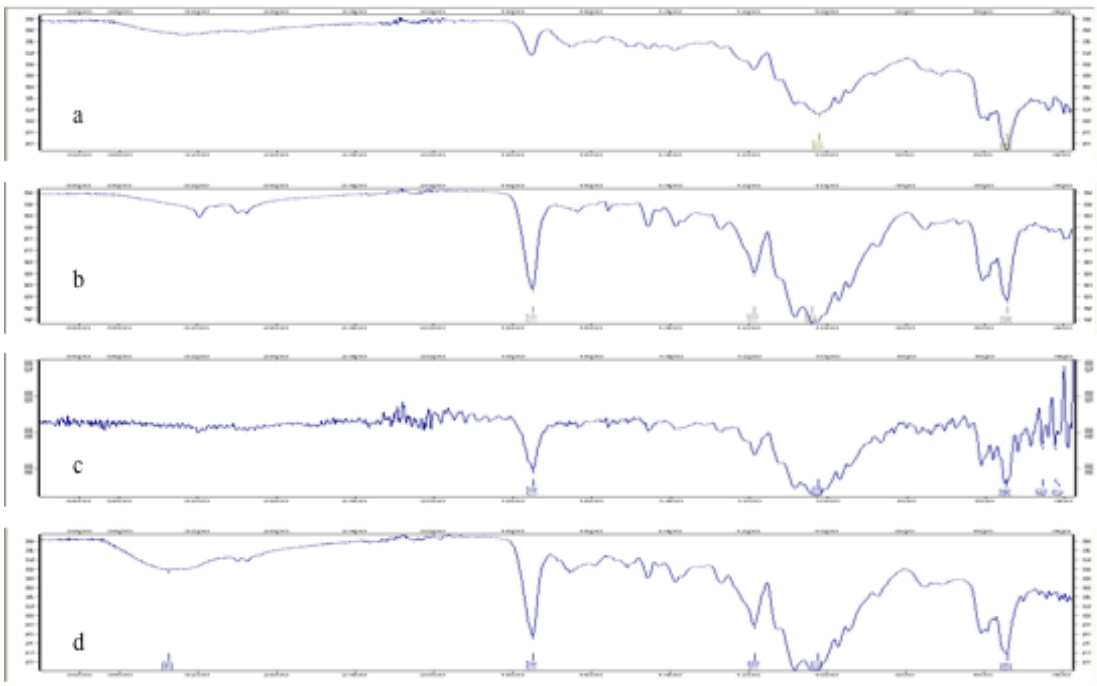

Figure 17. FTIR spectra of (a) PDLLA/β-TCP composite prior to SBF immersion, (b) PDLLA/β-TCP composite immersed in SBF for one week, (c) PDLLA/β-TCP composite immersed in SBF for three weeks, (d) PDLLA/β-TCP composite immersed in SBF for six weeks.

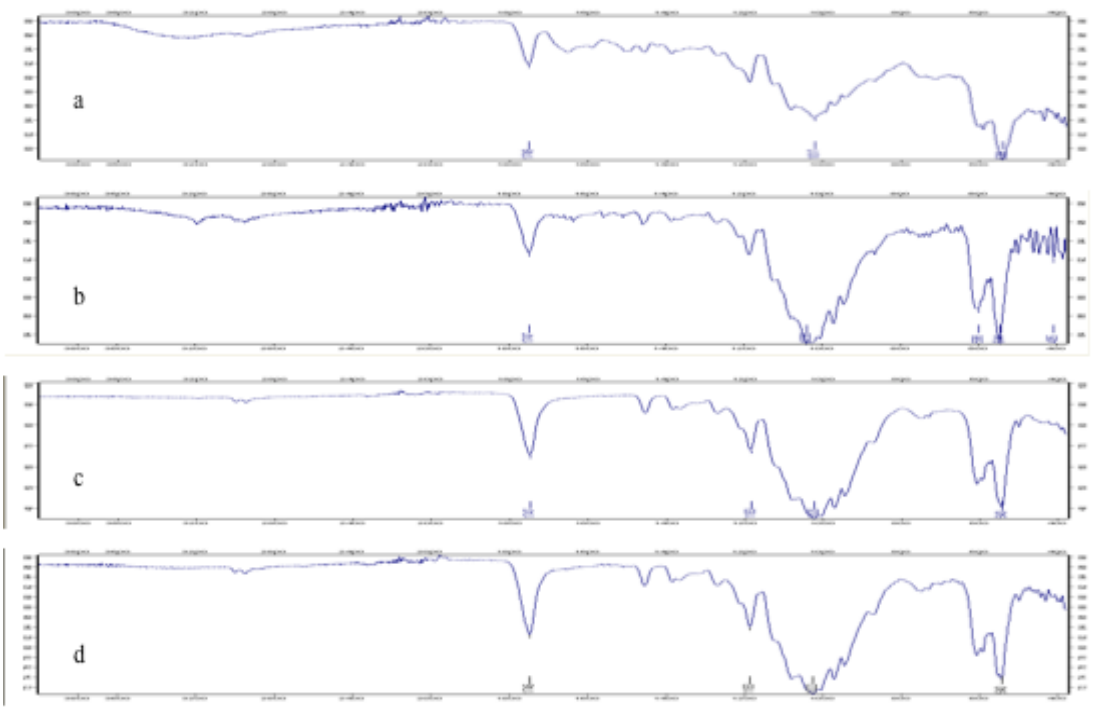

Figure 18. FTIR spectra of (a) PLGA/β-TCP composite prior to SBF immersion, (b) PLGA/β-TCP composite immersed in SBF for one week, (c) PLGA/β-TCP composite immersed in SBF for three weeks, (d) PLGA/β-TCP composite immersed in SBF for six weeks.

4.4 Vancomycin Release Study for Vancomycin containing Polymer/Bioceramic Composites

Both PDLLA/β-TCP and PLGA/β-TCP composites released vancomycin for six weeks (Figure 19) and the calibration curve was given in Appendix A. PDLLA/β-TCP composites released 2278 ± 198 μg vancomycin while PLGA/β-TCP composites released 2102 ± 204 μg in one day. After six weeks, total amount of vancomycin released from composites were found 3115 ± 234 μg for PDLLA/β-TCP and 3443 ± 438 μg for PLGA/β-TCP.

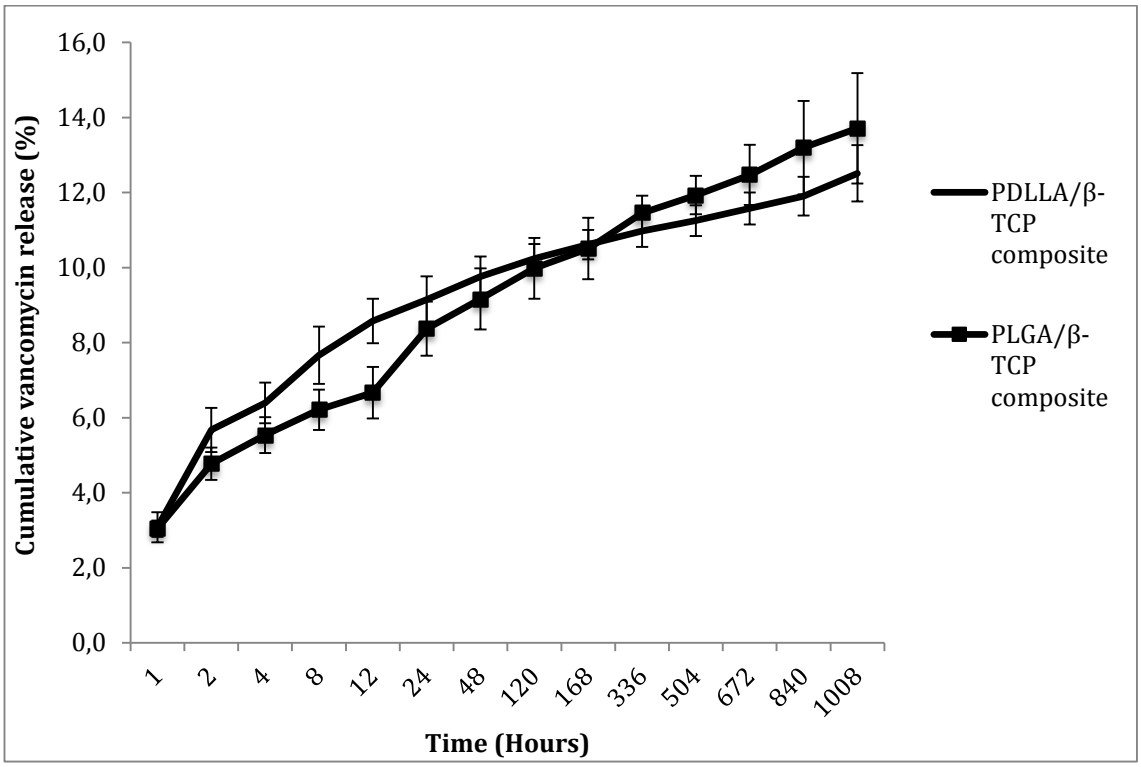

Figure 19. Cumulative released vancomycin percentage of the composites.

The spectrophotometer analysis was validated by measuring three known vancomycin concentrations at three different time points (Table 1). The absorbances were almost same for each concentration with minimal standard deviation.

Table 1. The absorbance values of three different concentrations at three different times (Average±standard deviation).

	100 µg/ml	**200 µg/ml**	**300 µg/ml**
Day 1	0.045±0.003	0.090±0.002	0.133±0.002
Day 2	0.045±0.002	0.088±0.001	0.133±0.002
Day 3	0.044±0.001	0.089±0.002	0.133±0.002

4.5 Content Uniformity of Vancomycin containing Polymer/Bioceramic Composites

The composites from each group (n=10) weighted and dissolved in dichloromethane. The dissolved solution was analyzed with spectrophotometer. The theoretical and measured vancomycin entrapment amounts were given in Table 2.

Table 2. Theoretical and actual vancomycin amounts in the composites.

Composite	Theoretical vancomycin amount	Measured vancomycin amount
PDLLA/β-TCP composite	23.077±1.298 mg (21.346-25.876 mg)	20.680±1.582 mg (18.636-23.179 mg)
PLGA/β-TCP composite	23.091±0.948 mg (21.202-24.023 mg)	19.599±0.931 mg (18.311-20.907 mg)

The results showed that actual vancomycin amounts were between 85% (17578.27 μg for PDLLA/β-TCP composite and 16658,79 μg for PLGA/β-TCP composite) and 115% (23782,36 μg for PDLLA/β-TCP composite and 22538,37 μg for PLGA/β-TCP composite) of the average content.

4.6 Antibiotic Susceptibility Test for Vancomycin containing Polymer/Bioceramic Composites

The inhibition zone diameters of the composites were measured for 21 days and found that both vancomycin containing composites were susceptible to both strains of MRSA (for strain capable of forming biofilm and for strain which did not form any biofilm) for 21 days (Figure 20).

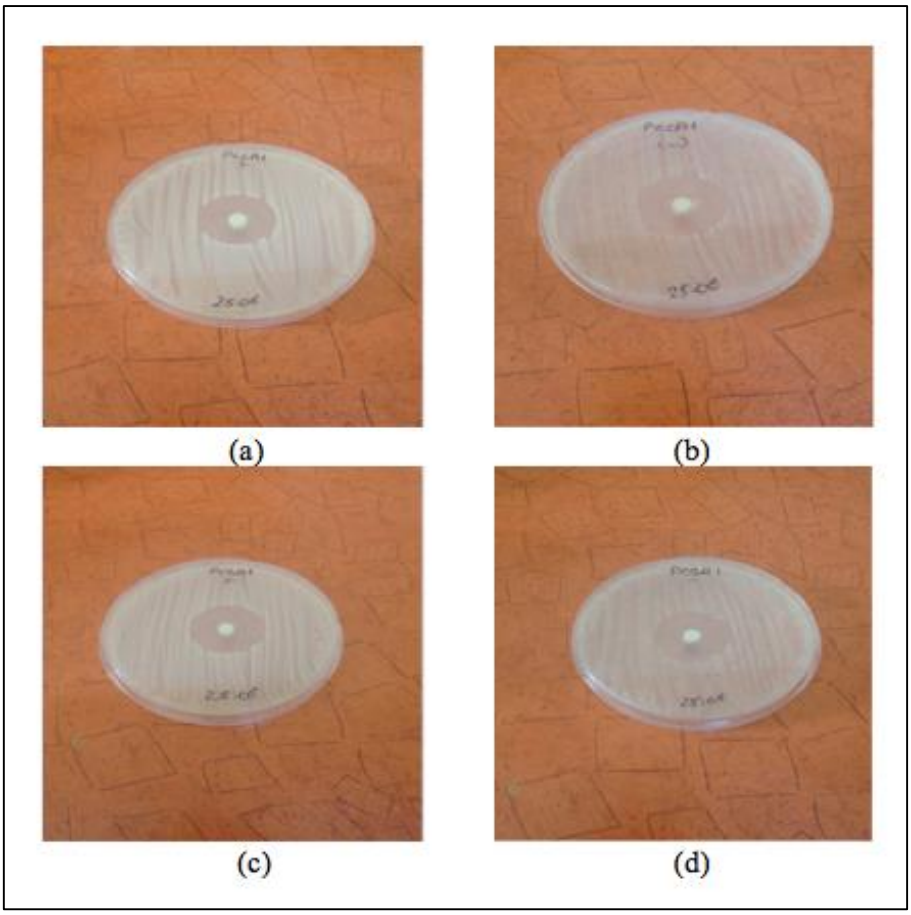

Figure 20. The inhibition zones of composites at day 21. (a) PDLLA/β-TCP composite with biofilm forming MRSA strain, (b) PDLLA/β-TCP composite with MRSA strain, (c) PLGA/β-TCP composite with biofilm forming MRSA strain and (d) PLGA/β-TCP composite with MRSA strain.

There was a statistically significant difference between groups (p:0.006) (Figure 21). In PDLLA/β-TCP composites, there was a statistically significant difference between biofilm forming and non biofilm forming MRSA strains (p:0.039). The p value indicating the statistically significant difference between PDLLA/β-TCP and PLGA/β-TCP composites for biofilm forming MRSA strain was 0.021. According to Clinical and Laboratory Standards Institute (CLSI), the inhibition zone diameter must be equal or greater than 15 mm for the susceptibility of MRSA against vancomycin and the results showed that the inhibition zone diameters were never smaller than 18 mm during the study. Thus, MRSA was susceptible to the vancomycin containing composites during the study period.

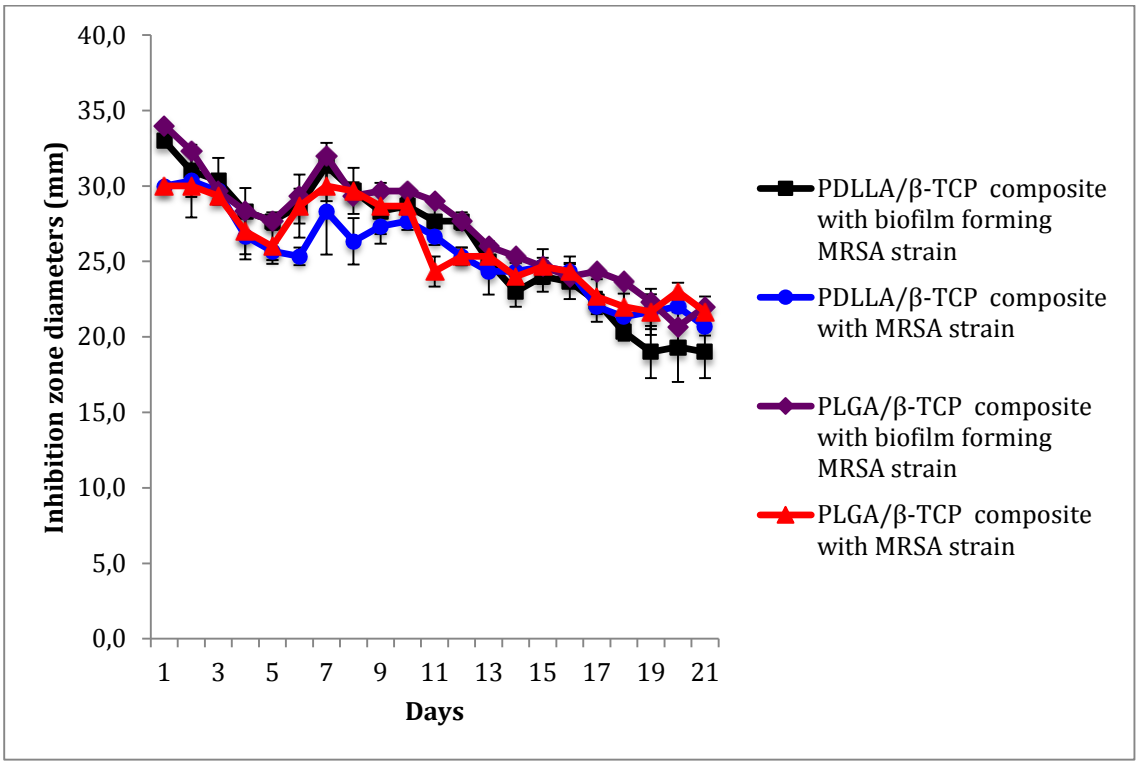

Figure 21. The inhibition zone diameters of the composites for 21 days.

4.7 Biofilm Inhibition Study for Vancomycin containing Polymer/Bioceramic Composites

There were slight differences in absorbance between the bacterial control and composites groups for biofilm inhibition study as seen in Figure 22, and 23. It was found that the released medium added to bacterial suspensions inhibited the formation of biofilm through six weeks. There was no statistically significant difference between the assays done with PBS or SBF, but in both assays, there was a statistically significant difference between composite groups and bacterial control ($p<0.05$).

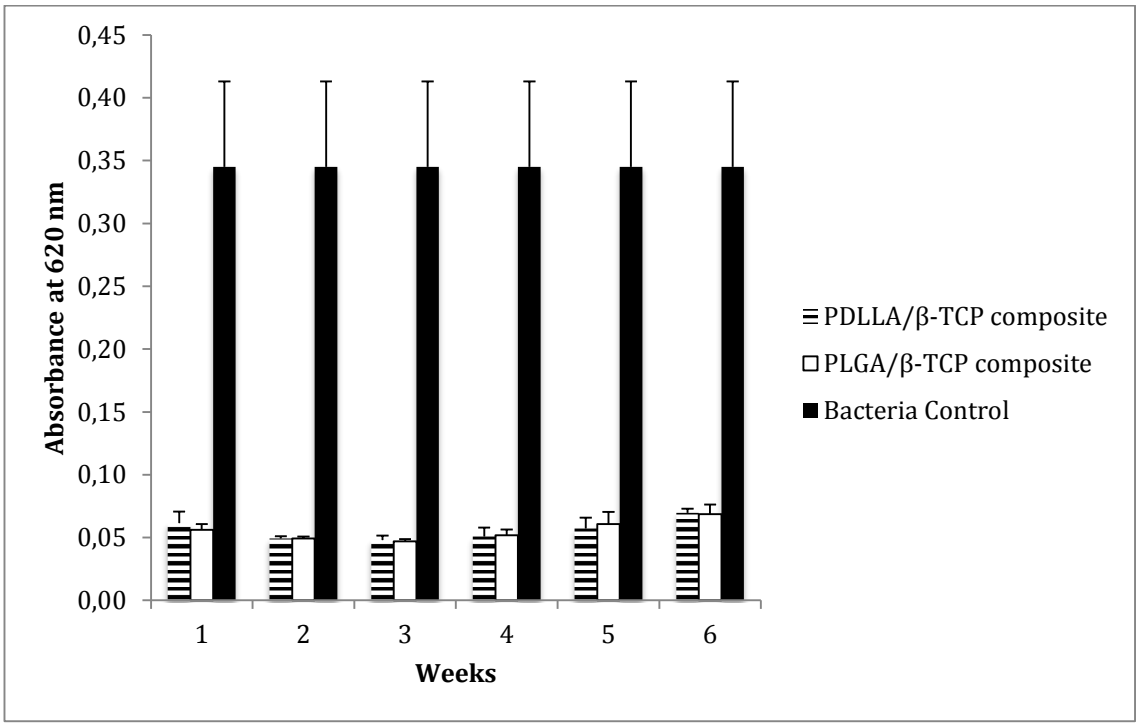

Figure 22. Absorbance of bacterial control, PDLLA/β-TCP and PLGA/β-TCP composites at 620 nm for SBF.

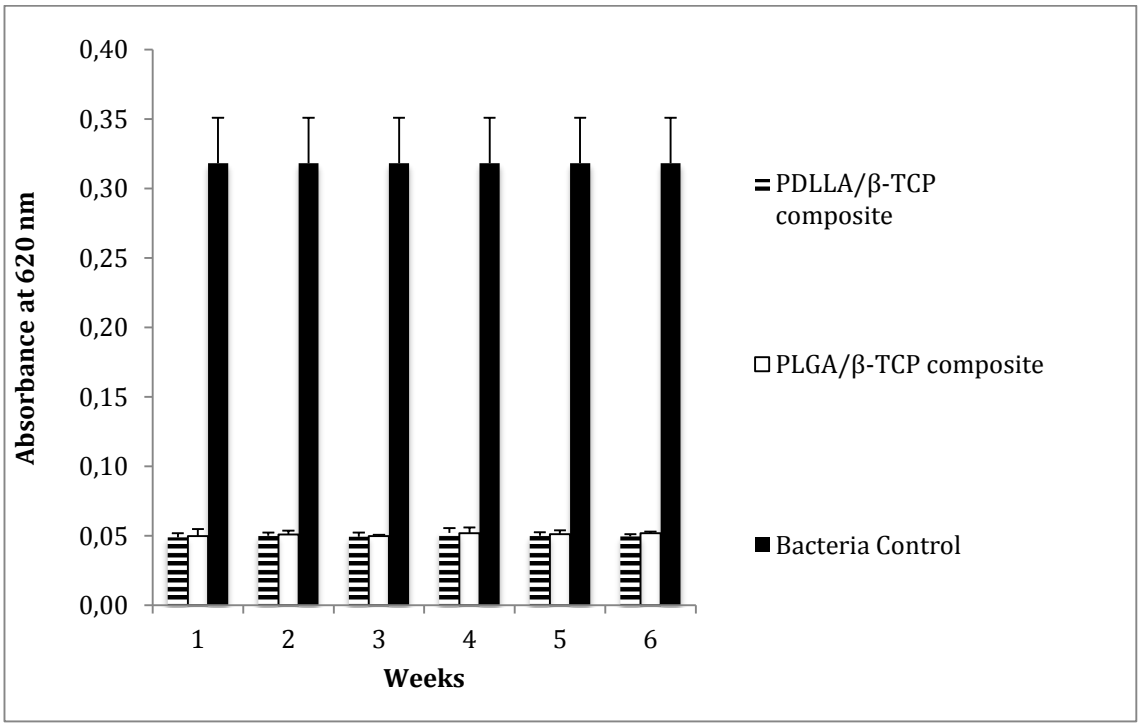

Figure 23. Absorbance of bacterial control, PDLLA/β-TCP and PLGA/β-TCP composites at 620 nm for PBS.

4.8 Cell Culture Studies of Vancomycin containing Polymer/Bioceramic Composites

The proliferation of cells cultured on the surface of the composites was analyzed by WST-1. WST-1 based assays are colorimetric assays used for the quantification of cell proliferation, cell viability and cytotoxicity. The ascending absorbance in the assay indicated cell proliferation. The assay was done by using two different types of cells in order to figure out whether there was a difference in the proliferation of the cells. For both composite groups, the cells cultured on the composites proliferated from day 1 to day 7. However, the proliferation was not as high as the proliferation of cells cultured without any composite (Figure 24). Also mesenchymal stem cells proliferated more rapidly than SaOS-2 cells. The statistical difference in MSCs cultured without any composite was 0.001 and in SaOS-2 cells cultured without any composite was 0.048. For day 1, 3 and 7; there were differences in the PDLLA/β-TCP+MSC group (p:0.004), PDLLA/β-TCP+SaOS-2 group (p:0.014) and PLGA/β-TCP+MSC group (p:0.024).

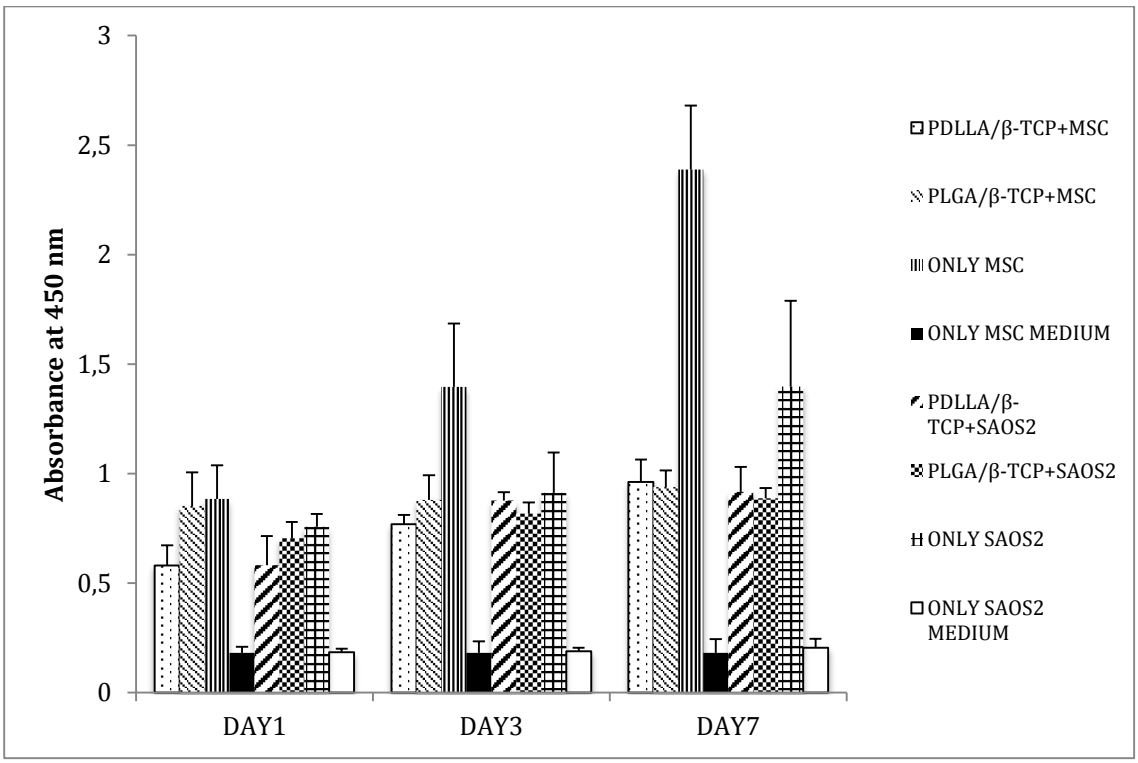

Figure 24. Proliferation of the MSC and SaOS-2 cells in day 1, 3 and 7 according to the absorbance of WST-1 at 450 nm.

The alkaline phosphatase activities of cells cultured with the composites were quantified by using a ready to use buffered alkaline phosphatase substrate containing *p*-nitrophenylphosphate (pNPP). This colorless agent developed a yellow colored solution when reacted with the alkaline phosphatase and gave out an absorbance in order to quantify the activity. The ALP activities of the composites cultured with MSC were higher than the only MSC group but there was no statistical difference between these groups (Figure 25). The ALP activities of the composites cultured with SaOS-2 cells were also higher than the only SaOS-2 cell group, but this time there was a statistical difference between the groups (p:0.003) (PDLLA/β-TCP composite+SaOS-2 cells versus only SaOS-2 cells; p: 0.011, PLGA/β-TCP composite+SaOS-2 cells versus only SaOS-2 cells; p: 0.006).

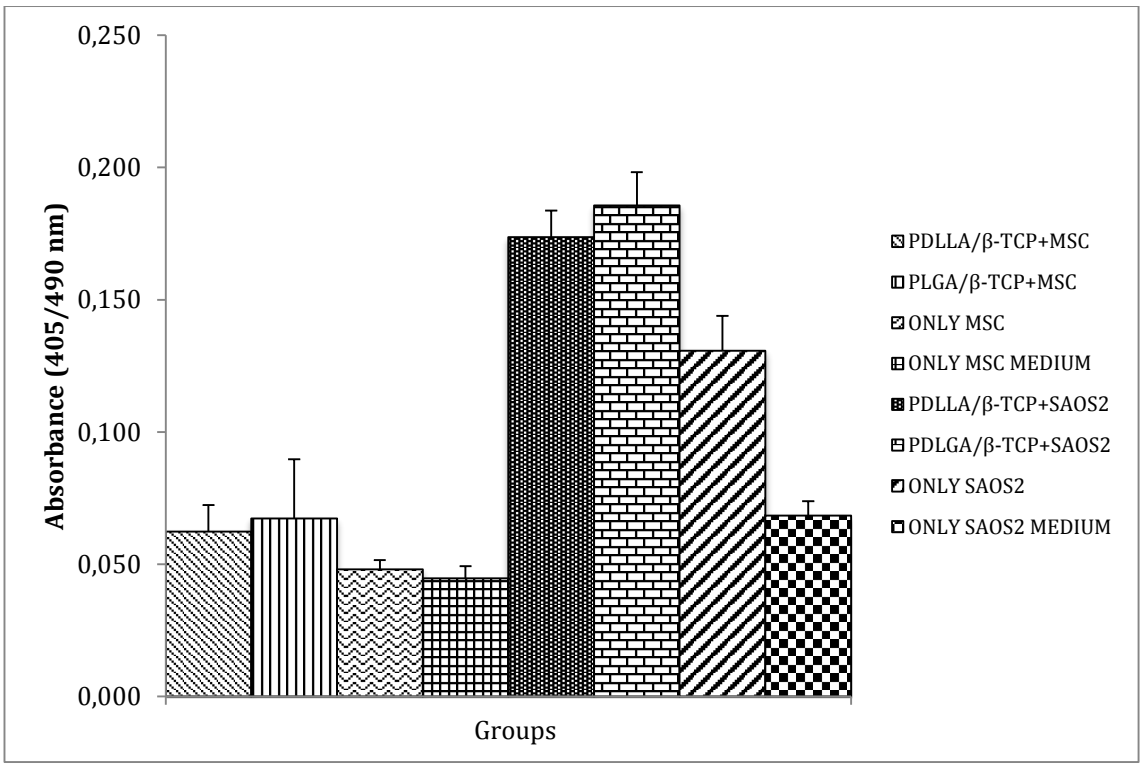

Figure 25. ALP activity of the groups at day 21 according to their absorbances at 405 nm.

4.9 Real Time Quantitative Polymerase Chain Reaction (RT-qPCR) Assay for Vancomycin containing Polymer/Bioceramic Composites

In the RT-qPCR assay, there was no AHSG, BMP5, COL2A1, DMP1, FGF3, MMP9 gene expressions in any groups. Alkaline phosphatase gene, ALPL expressed 10.87±8.85 fold higher in osteogenic medium group while the expression was decreased for PDLLA/β-TCP+MSC (0.39±0.05) and PLGA/β-TCP+MSC (0.77±0.19).

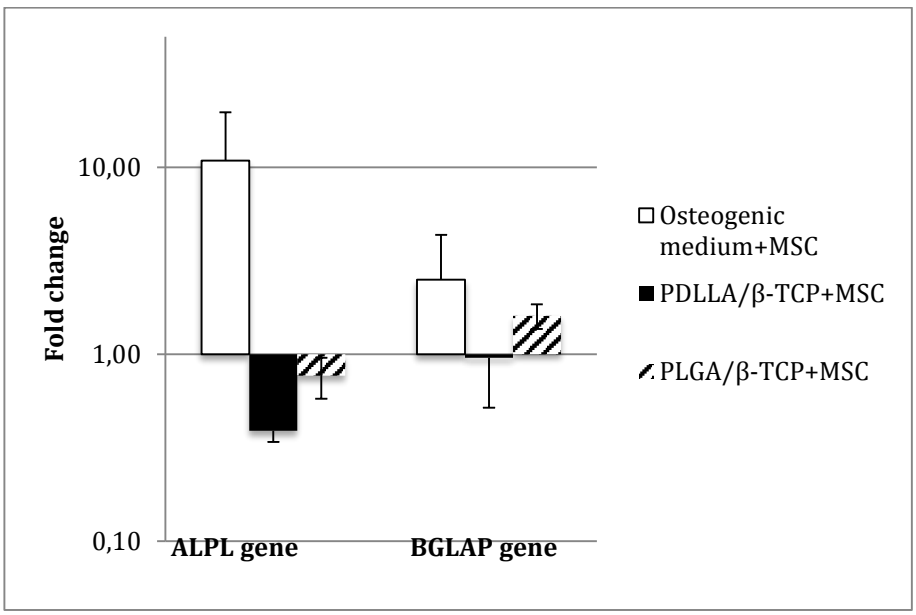

Figure 26. Fold change of ALPL and BGLAP gene expressions between groups.

Bone gamma carboxyglutamic acid containing protein (Bglap) is encoded by BGLAP gene and used as a biochemical marker for bone formation. BGLAP gene expression was 2.52±1.85, 0.96±0.44 and 1.71±0.24 fold higher in osteogenic medium group, PDLLA/β-TCP group and PLGA/β-TCP group, respectively (Figure 26). In the bone morphogenic protein family, the distinct fold changes were observed for BMP-1, BMP-2, BMP-3 and BMP-4 (Figure 27). In osteogenic medium group, BMP-1 gene expression was 4.31±6.02 fold higher while BMP-2 gene expression was 3.43±3.08, BMP-3 gene expression was 0.41±0.29 and BMP-4 gene expression was 1.40±0.27 fold higher. In PDLLA/β-TCP group, BMP-1 gene expression was like control (0.93±0.34) but BMP-2 gene expression was 4.52±0.11 fold higher.

BMP-3 and BMP-4 gene expressions were 0.20±0.05 and 0.45±0.13. In PLGA/β-TCP group, fold change for BMP-1, BMP-2, BMP-3 and BMP-4 genes were 1.43±0.06, 10.28±0.02, 0.46 and 0.51±0.04, respectively.

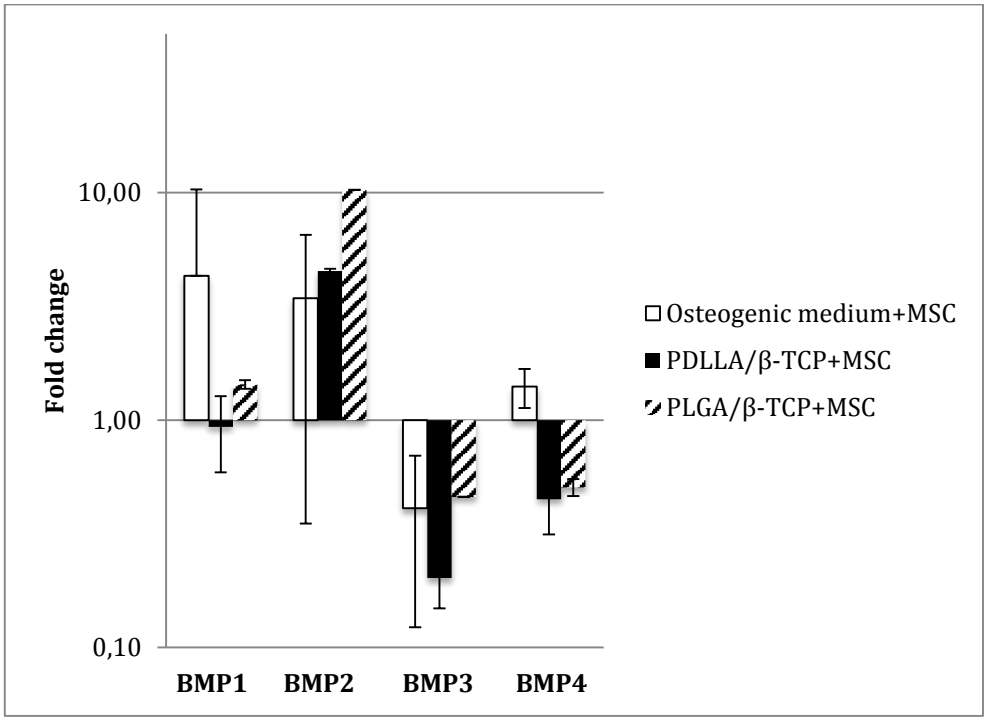

Figure 27. Fold changes of BMP-1, BMP-2, BMP-3 and BMP-4 gene expressions between groups.

For the collagen genes group, the distinct fold changes were observed for COL10A1, and COL3A1 (Figure 28). There was no gene expression for COL2A1 gene in any group.

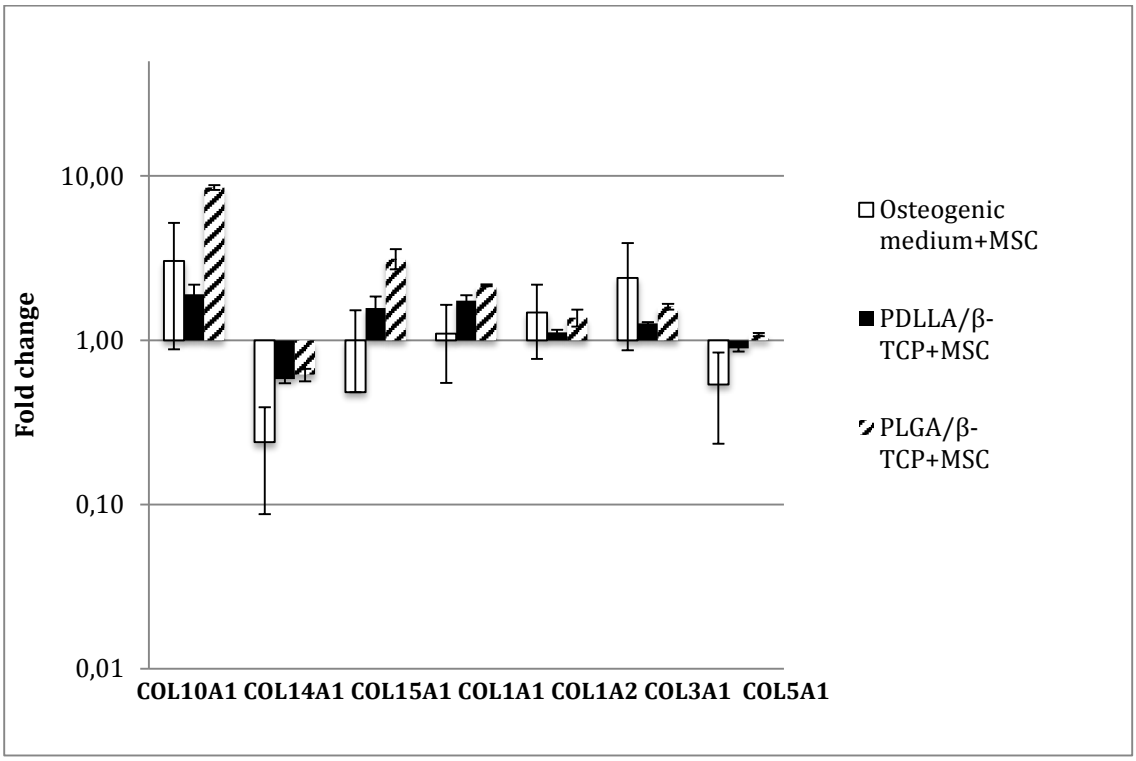

Figure 28. Fold changes of collagen gene expressions between groups.

For fibroblast growth factor (FGF) genes, the expressions were all decreased except FGFR1 gene in all groups (Figure 29).

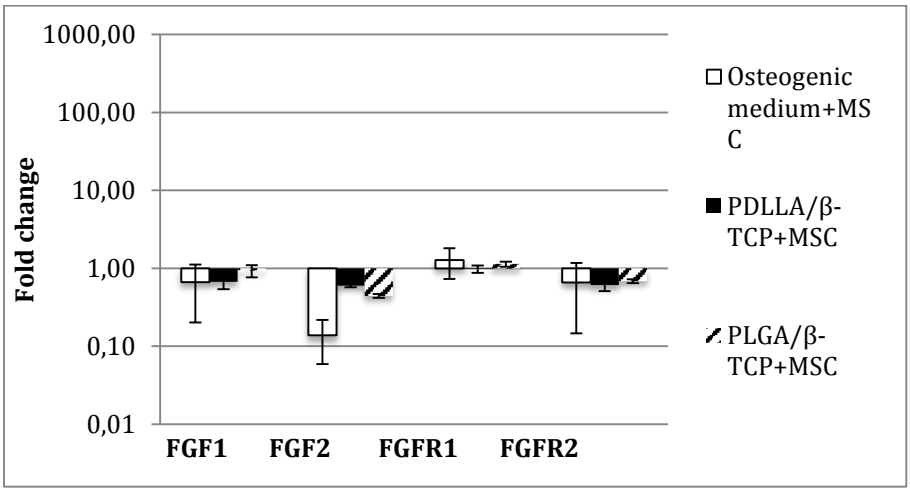

Figure 29. Fold changes of FGF1, FGF2, FGFR1 and FGFR2 gene expressions between groups.

For matrix metallopeptidases (MMP), there was no expression for MMP9 and MMP10 in any group. On the contrary, MMP2 and MMP8 gene expression were increased in all groups according to control (Figure 30).

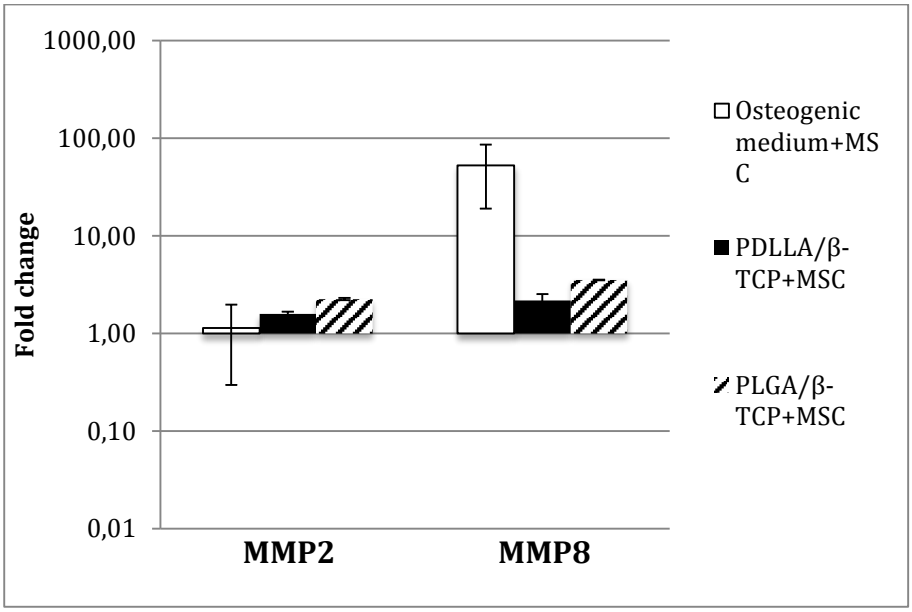

Figure 30. Fold changes of MMP2 and MMP8 gene expressions between groups.

Insulin like growth factors 1 and 2 (IGF1 and IGF2) showed different results in the manner of gene expression. For IGF1, in all groups the gene expression was increased while for IGF2, the gene expression was decreased in composite groups while it was increased for osteogenic medium group (Figure 31).

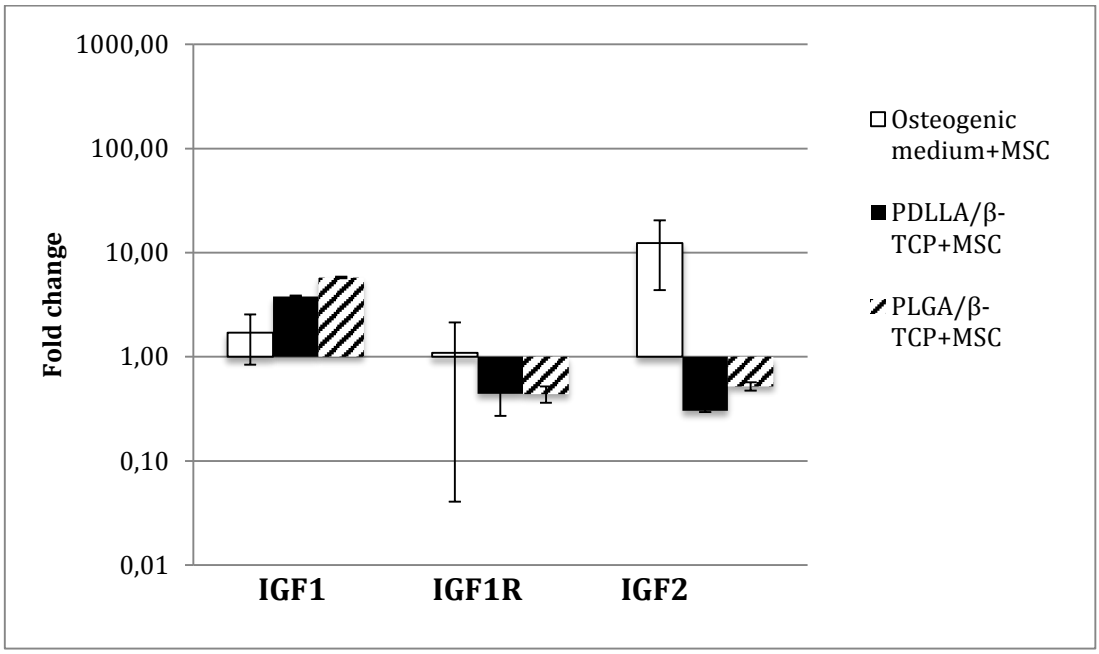

Figure 31. Fold changes of IGF1, IGF1R and IGF2 gene expressions between groups.

The transcription factors related with osteoblast differentiation and skeletal development, runt related transcription factor 2 (RUNX2) and sex determining region Y box 9 (SOX9) were both decreased in composites groups. For osteogenic medium group, RUNX2 expression was increased while it was decreased for SOX9 (Figure 32).

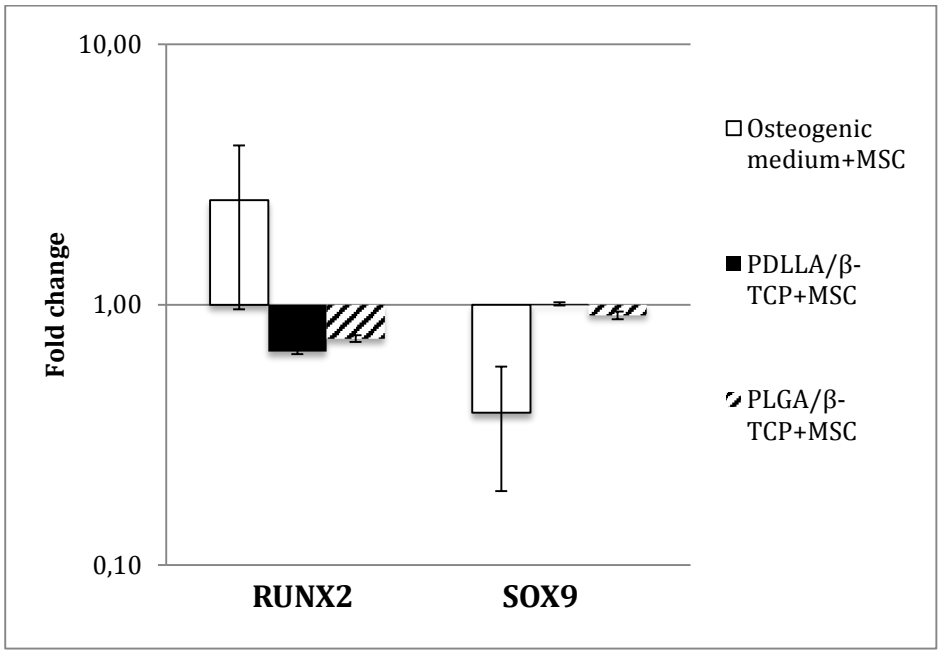

Figure 32. Fold changes of RUNX2 and SOX9 gene expressions between groups.

The SMAD gene expressions were decreased for both composite groups. For osteogenic medium group, all SMAD gene expressions except SMAD 3 were increased (Figure 33).

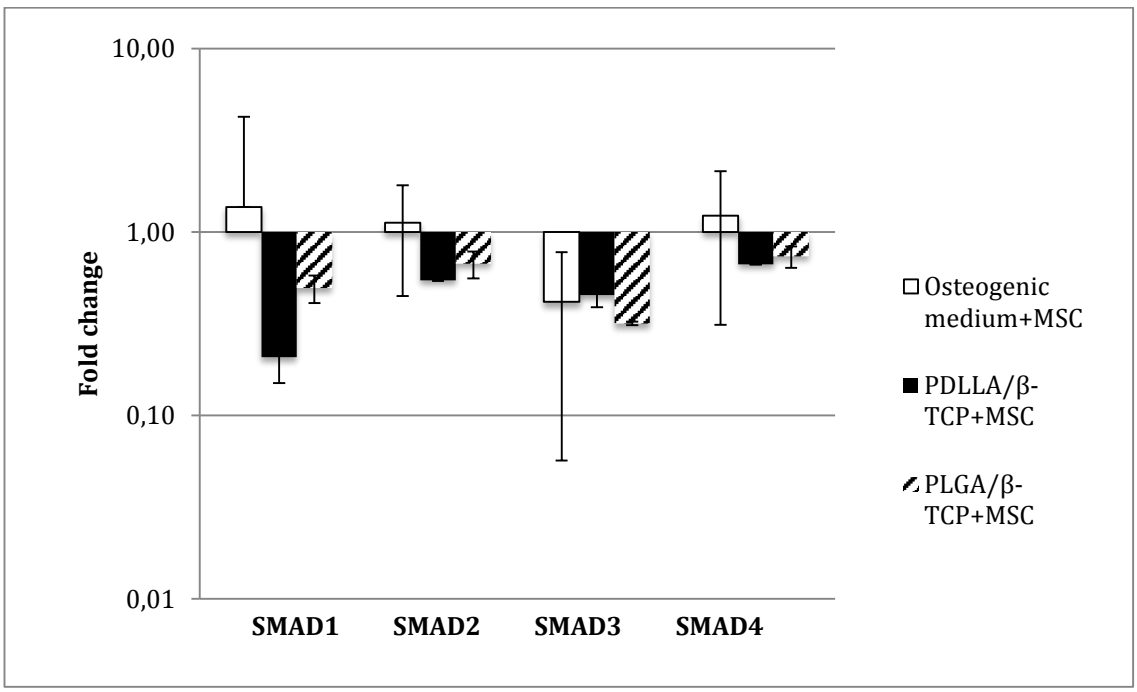

Figure 33. Fold changes of SMAD 1, 2, 3 and 4 gene expressions between groups.

The gene expressions related with transforming growth factor (TGF) and its receptor were given in Figure 34. The expression of genes expressing TGFβ1 and TGFβ3 were increased in all groups; but for the receptor 2 of transforming growth factor beta, the genes expressions were decreased for both composite groups (Figure 34).

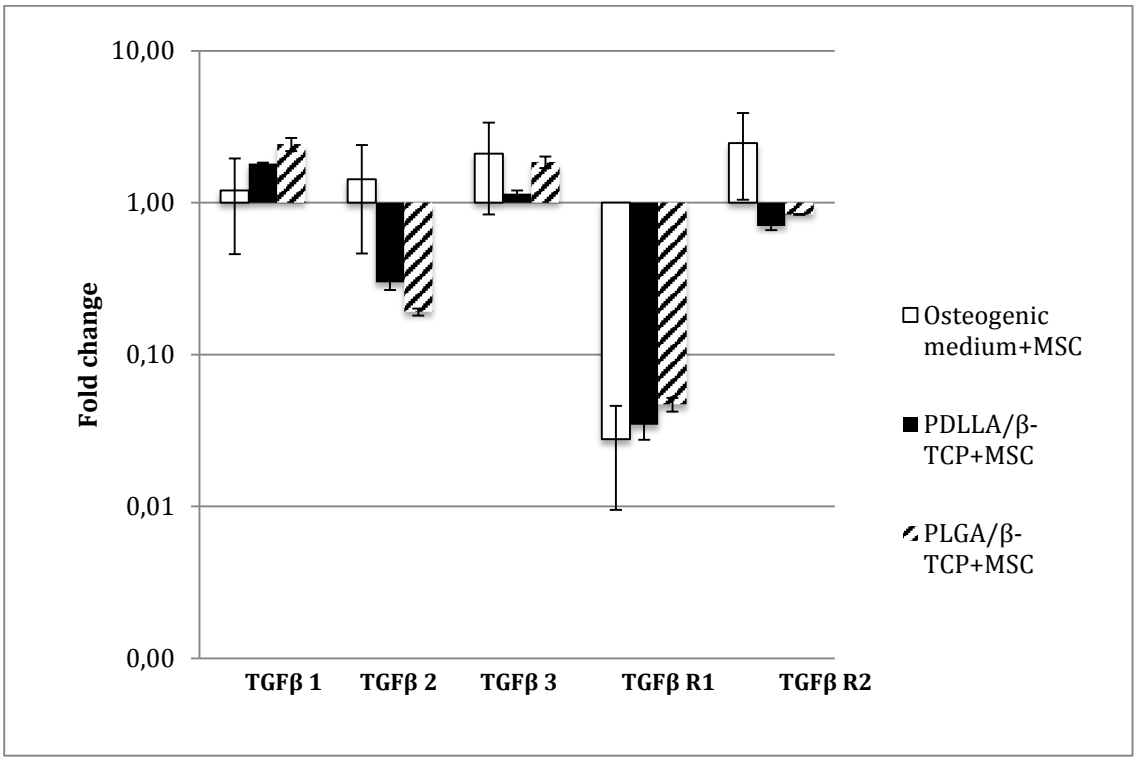

Figure 34. F Fold changes of TGFβ1, TGFβ2, TGFB3, TGFβR1 and TGFβR2 gene expressions between groups.

The expressions of CDH11, CTSK, EGF, EGFR and TWIST1 were given in Figure 35. The expression of CTSK was increased in every group while the expressions of CDH11, EGF and EGFR were all decreased.

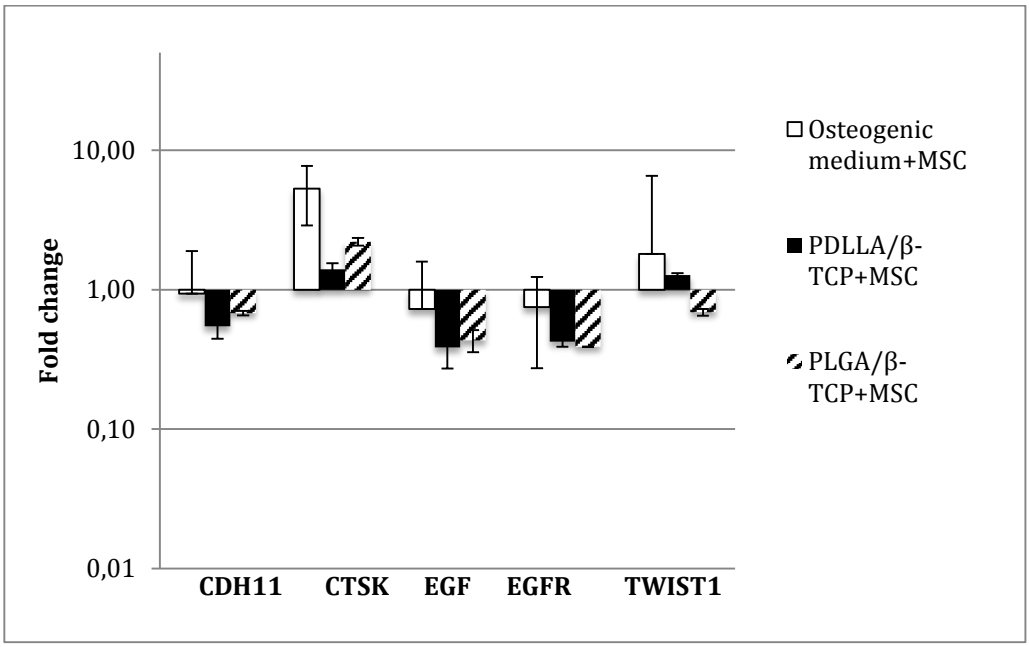

Figure 35. Fold changes of CDH11, CTSK, EGF, EGFR, and TWIST1 gene expressions between groups.

The expressions of ANXA5, ITGB1 and PHEX were all downregulated in composites group according to control (Figure 36). In the expression of twist homolog 1 (TWIST1) gene, osteogenic medium and PDLLA/β-TCP composite group showed elevation in fold change while, PLGA/β-TCP composite group showed a decrease. The expression of phosphate regulating endopeptidase (PHEX) gene was decreased for both composites unlike osteogenic medium group.

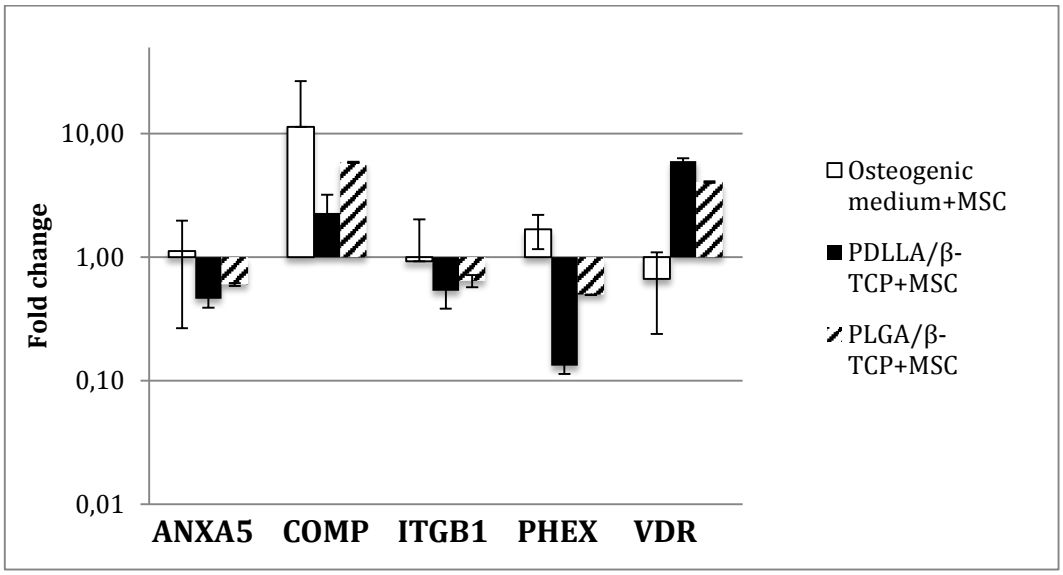

Figure 36. Fold changes of ANXA5, COMP, ITGB1, PHEX and VDR gene expressions between groups.

For determining the genes fold changes significance between the groups, the binary logarithm of the ΔΔCt values were calculated and ±2 fold changes were taken as significant. The significant values were given in grey boxes in Table 3.

Table 3. The upregulation or downregulation of genes in the test groups according to control.

Fold Up- or Down-regulation according to Control			
Gene	Osteogenic Medium + MSC	PDLLA/β-TCP + MSC	PLGA/β-TCP + MSC
ALPL	3,44	-1,36	-0,37
ANXA5	0,17	-1,11	-0,73
BGLAP	1,33	-0,06	0,69
BMP1	2,11	-0,10	0,52
BMP2	1,78	2,18	3,36
BMP3	-1,29	-2,31	-1,12
BMP4	0,49	-1,16	-0,98
CDH11	-0,09	-0,88	-0,56
COL10A1	1,60	0,93	3,09
COL14A1	-2,06	-0,79	-0,70
COL15A1	-1,05	0,65	1,65
COL1A1	0,13	0,80	1,11

Table 3. (continued)

COL1A2	0,56	0,16	0,46
COL3A1	1,26	0,34	0,68
COL5A1	-0,89	-0,17	0,11
COMP	3,51	1,19	2,55
CTSK	2,41	0,49	1,14
EGF	-0,46	-1,37	-1,20
EGFR	-0,41	-1,23	-1,36
FGF1	-0,59	-0,57	-0,10
FGF2	-2,85	-0,74	-1,17
FGFR1	0,35	-0,03	0,19
FGFR2	-0,60	-0,70	-0,54
FLT1	2,38	-1,78	-1,46
IGF1	0,76	1,93	2,53
IGF1R	0,13	-1,18	-1,19
IGF2	3,63	-1,72	-0,94
ITGB1	-0,11	-0,90	-0,63
MMP2	0,19	0,67	1,17
MMP8	5,72	1,12	1,82
PHEX	0,75	-2,91	-1,01
RUNX2	1,34	-0,60	-0,43
SMAD1	0,45	-2,26	-1,01
SMAD2	0,17	-0,87	-0,57
SMAD3	-1,26	-1,14	-1,66
SMAD4	0,30	-0,58	-0,44
SOX9	-1,38	0,01	-0,14
TGFB1	0,27	0,86	1,28
TGFB2	0,51	-1,74	-2,39
TGFB3	1,07	0,20	0,89
TGFBR1	-5,17	-4,85	-4,41
TGFBR2	1,30	-0,51	-0,26
TWIST1	0,85	0,35	-0,54
VDR	-0,59	2,59	2,02

CHAPTER 5

DISCUSSION

Osteomyelitis is a bone infection, generally caused by Staphyloccocus aureus (100). When the infection staged to chronic level, the infection can not be treated with antibiotics alone. Poor blood circulation in the infection area due to the compression of vascular channels and bone necrosis makes osteomyelitis a persistent disease (101). In order to treat osteomyelitis, local drug delivery systems are generated. These systems released the entrapped drug in a controlled manner while being biocompatible.

In this study, vancomycin containing PDLLA/β-TCP and PLGA/ β-TCP composites were fabricated. The composites had smooth surfaces with microcracks. EDS spectras confirmed the content of the composites by giving carbon peaks resembling polymer, phosphorous and calcium peaks resembling bioceramic and chloride resembling the antibiotic, vancomycin HCl. The composites and their materials were analyzed with FTIR and found that composites had similar adsorption bands with their contents.

In the degradation study, PDLLA/β-TCP composites lost 67.98±1.5% of their weight by week six while PLGA/β-TCP composites only lost 19.13±0.2% of their weight. This weight loss was likely due to ionic release of TCP and perhaps to a smaller extent, hydrolytic degradation of polymer. The addition of TCP is hypothesized to accelerate the degradation of the polymer. Since the TCP particles were only physically blended into the polymer, they occupied random spaces in the polymer. After the composite was immersed in solution, the hydrophilic TCP particles tended to fall off and interact with the surrounding medium. The TCP was converted to its more stable soluble phase that is apatite. The falling of TCP also created voids within the polymer, thus exposing their surfaces to hydrolytic attack and weakening the

overall structure of the polymer (102). The molecular weight of PDLLA was between 10-18 kDa, whereas the molecular weight of PLGA was 190-240 kDa. Since the molecular weight of PDLLA was lower than the molecular weight of PLGA, PDLLA/β-TCP composite degraded more rapidly. Also during the fabrication of the composites, there was a pounding step after dissolving all the components in dichloromethane. In this step, PDLLA/β-TCP composites had larger structures than PLGA/β-TCP composite, so during the packing of the composites this may lead the weakness of the composite. The water uptake percent of the composites were decreased by week 6 in both composite types. Baro et. al. characterized the gentamicin bone implants made up of PDLLA, TCP and hydroxyapatite in vitro. According to study, the mass loss and water uptake of the implants were increased by 8 weeks (103). But in this study, same implants were used all through the time. In our study, we used fresh samples for every time point. As a result, our water uptake results were not same with the literature. On the other hand, higher content of hydrophilic TCP in the composites facilitated the absorption and diffusion of SBF and resulted in higher water absorption. This increased water absorption resulted in the higher weight loss (104). The water absorption process is a balance between the dissolution of oligomers in the solution and water uptake of the residual material. Accumulation of the hydrophilic degradation products inside the composites resulted in the increase of water absorption during the whole degradation process. When water absorption reached a certain value, the increase rate began to reduce as a result of the dissolution of the degradation products (83).

The bone like apatite formation on the surface of composites were proved with SEM, EDS and FTIR results. TCP in the composites in this study dissolved in SBF solution, suggesting OH^-, calcium and phosphate ions combined to form an apatite (105). SEM results showed the agglomeration of the apatite particles on the surface of the composites and EDS results gave the Ca/P molar ratio of the apatite. It was found that all the apatite formed on the surface of the composites were non-stoichiometric apatite with Ca/P molar ratio $\neq$ 1.67 (105). But, the Ca/P atomic ratios were 1.57, 1.69 and 1.88, respectively, for the PDLLA/ β-TCP composite immersed for 1, 3 and 6 weeks and 1.66, 1.73 and 1.77 respectively, for the PLGA/ β-TCP

composite immersed for 1, 3 and 6 weeks, which were comparable to the value (1.67) for stoichiometric HA (52). The apatite deposition on the surface of the composite reflected the in vitro bioactivity of the composites (106).

Both PDLLA/β-TCP and PLGA/β-TCP composites released vancomycin for six weeks. PDLLA/β-TCP composite released only 11.21% of its vancomycin while PLGA/β-TCP released 11.64%. These results were quite low when compared with the literature (100). In literature most of the drug delivery system released 80-100% of their drug content during the study. We mentioned before that, our composites did not have a porous structure and the drug can only be released from the microcracks. Therefore, the composites can continue to release their drug content for long times. Also, the composites showed a burst effect in 24 hours. We assumed that this initial burst was related with the diffusion of vancomycin located near to the surface of the composites (107).

Both biofilm forming MRSA strain and MRSA strain without any biofilm formation capability were susceptible to the vancomycin released from both composites. The inhibition zone diameters were measured for 21 days and the diameters changed day by day according to the released vancomycin. The diameters were decreased by day 21 but the bacteria were still susceptible for the composites according to CLSI guidelines (108).

Some strains of MRSA are capable of biofilm forming and this biofilm protects the bacteria from the environmental conditions. Here we conducted a biofilm inhibition study with both composites. We diluted the bacterial solutions by adding 20 µl of the vancomycin release mediums from different times and incubated the plates for 2 days (100). We found that both composites inhibited the biofilm formation for six weeks. This confirms the antibacterial properties of vancomycin containing composites. Biofilm inhibition study was conducted to mimic a condition whereby biofilm formation has been established in osteomyelitis. Both vancomycin containing PDLLA/β-TCP and PLGA/β-TCP composites can eliminate the formation of the biofilm. The result shows these particles are able to release drugs at a concentration sufficient to completely inhibit the formation of a biofilm. Inhibition of biofilm formation in osteomyelitis is beneficial because this is the key to treat the infection

(100).

The biocompatibility of the composites were analyzed by the proliferation assay done with WST-1. WST-1 based assays are colorimetric assays used for the quantification of cell proliferation, cell viability and cytotoxicity based on the cleavage of a tetrazolium salt (WST-1) by mitochondrial dehydrogenases in viable cells. Increased enzyme activity leads to an increase in the amount of formazan dye, which is measured with a spectrophotometer (109). According to results, the cells on the composites proliferated by day 7 for both MSC and SaOS-2 cells. There was no any significant difference between PDLLA/β-TCP and PLGA/β-TCP composites at any time point. But, the proliferation of only cell in cell culture plate was higher than the composite group. Since the surface area of the cell culture plate was larger, cells proliferated more in the wells than the surfaces of the composites.

Alkaline phosphatase (ALP) is an early marker expressed by preosteoblasts and mineralizing osteoblasts (105). We searched the alkaline phosphatase activity of the composites with MSC and SaOS-2 cells for 21 days and found that the composite groups had more ALP activity than only cell groups but there was no significant difference between the groups for MSC. The significant differences in the SaOS-2 cell groups were related with osteoblast-like nature of the SaOS-2 cells. Since these cells had osteoblast-like properties, it was expected that these cells showed higher ALP activity than MSC (110).

On the other hand, according to RT-PCR results, alkaline phosphatase gene expression (ALPL) was decreased for both composite groups. This conflict may be related to the RT-PCR studies were conducted in non-contact mode while the ALP activity study was done in contact mode. Also, ALP activity study was lasted for 21 while RT-PCR studies were lasted for 14 days. The expression of ALPL was low for both composites but the differences in the fold changes were not significant. The cells cultured with osteogenic medium showed higher ALPL expression related with the synergetic effect of the dexamethasone. The gene expression levels of osteo calcin (bone gamma-carboxyglutamic acid-containing protein (BGLAP)) a late secreted protein produced by mature osteoblasts, was also higher in osteogenic

medium group according to composites groups. BMP1 or procollagen C proteinase, a secreted metalloprotease requiring calcium and needed for cartilage and bone formation (111) was upregulated significantly in osteogenic medium group, whereas it was downregulated in both composites groups. RUNX2 is a key regulator of chondroblast and osteoblast differentiation, and of bone development *in vivo* (112). RUNX2 regulates the expression of major extracellular matrix genes (including alkaline phosphatase, osteopontin, osteocalcin, type I collagen, and type X collagen) expressed by chondroblasts and osteoblasts. Expression and activation of RUNX2 is regulated by many bone derived growth factors, including bone morphogenetic proteins (BMPs). BMPs form a unique group of proteins within the TGF-β super family of genes, and play pivotal roles in the regulation of cartilage and bone development. BMP-activated Smads (Smad1, -5, and -8) induce RUNX2 gene expression, and Smads interact physically with the Runx2 protein to induce osteoblast differentiation (113). Here in our study, BMP1 was only upregulated in osteogenic medium group. But for BMP2, there was significant upregulation for both PDLLA/β-TCP and PLGA/β-TCP composites and the upregulation was higher than osteogenic medium group. On the contrary, BMP4 expression was downregulated both composites group. Nevertheless, this upregulation was not induced the upregulation of the SMADs 1, 2, 3 and 4 in composites groups and as a result there was no RUNX2 upregulation. By the way, neither the upregulation of RUNX2 in the osteogenic medium group, nor the downregulation in the composites groups had any significant difference. TGF-β1, another factor involved in osteoblast proliferation and differentiation was also upregulated in composites groups but this increase did not lead the upregulation of the SMAD genes. TGF-β2, one of TGF-β isoforms within bone matrix, modulates the differentiation of osteoblasts and the proliferation of osteoprogenitor cells (114). Here, only the cells cultured with osteogenic differentiation medium showed the upregulation of TGF-β2, so that the cells in composite groups could not differentiate into osteoblasts. Differentiation of human mesenchymal stem cells into bone forming cells is stimulated by endothelial growth factor, EGF (115). Again, the expression of both EGF and its receptor EGFR were downregulated for both composites groups.

CHAPTER 6

CONCLUSION

As a conclusion, PDLLA/β-TCP and PLGA/β-TCP composites were developed and characterized. Vancomycin containing PDLLA/β-TCP and vancomycin containing PLGA/β-TCP composites released 3.1 ± 0.2 mg and 3.4 ± 0.4 mg vancomycin for six weeks, respectively and had antibacterial activity against MRSA while also having biofilm inhibition ability. Vancomycin containing PDLLA/β-TCP and vancomycin containing PLGA/β-TCP composites were biocompatible with Mesenchymal Stem Cells and SaOS-2 osteosarcoma cells and the apatite formation on the surface of the composites indicating the bioactivity of the material. In contact mode, the composites showed ALP activity at 21 days with both MSC and SaOS-2 cells.

Beside the biocompatibility and antibacterial properties of the composites, the composites did not show any osteogenic differentiation, and bioconduction activity in non contact mode according to RT-PCR studies. The vancomycin containing PDLLA/β-TCP and vancomycin containing PLGA/β-TCP composites were not induced the differentiation of mesenchymal stem cells by not expressing some of the osteogenesis related signalling molecules. This may due to the absence of an osteogenic medium, since mesenchymak stem cells cannot differentiate into osteoblast just with the help of the composite. Also, the non contact mode study design may effect the gene expression results, since in the contact mode the gene expression can be elevated.

To conclude, future studies can be conducted both *in vitro* and *in vivo* in order to find out the osteogenic capability of the composites in contact mode.

REFERENCES

1. Brooks BD, Sinclair KD, Davidoff SN, Lawson S, Williams AG, Coats B, et al. Molded polymer-coated composite bone void filler improves tobramycin controlled release kinetics. J Biomed Mater Res - Part B Appl Biomater. 2014;102:1074–83.

2. Ahola N, Männistö N, Veiranto M, Karp M, Rich J, Efimov A, et al. An in vitro study of composites of poly(L-lactide-co-ε-caprolactone), β-tricalcium phosphate and ciprofloxacin intended for local treatment of osteomyelitis. Biomatter, Landes Biosci. 2013;3(2):1–13.

3. Lyndon J a., Boyd BJ, Birbilis N. Metallic implant drug/device combinations for controlled drug release in orthopaedic applications. J Control Release. 2014;179(1):63–75.

4. Nandi SK, Mukherjee P, Roy S, Kundu B, De DK, Basu D. Local antibiotic delivery systems for the treatment of osteomyelitis - A review. Mater Sci Eng C 2009;29(8):2478–85.

5. Jagur-Grodzinski J. Polymers for tissue engineering, medical devices, and regenerative medicine. Concise general review of recent studies. Polymers for Advanced Technologies. 2006. p. 395–418.

6. Ravichandran R, Venugopal JR, Sundarrajan S, Mukherjee S, Ramakrishna S. Precipitation of nanohydroxyapatite on PLLA/PBLG/Collagen nanofibrous structures for the differentiation of adipose derived stem cells to osteogenic lineage. Biomaterials. 2012;33(3):846–55.

7. Seidenstuecker M, Mrestani Y, Neubert RHH, Bernstein A, Mayr HO. Release Kinetics and Antibacterial Efficacy of Microporous b-TCP Coatings. J Nanomater. 2013;2013:1–8.

8. Ahola N, Veiranto M, Männistö N, Karp M, Rich J, Efimov A, et al. Processing and sustained in vitro release of rifampicin containing composites to enhance the treatment of osteomyelitis. Biomatter. 2012;2(December):213–25.

9. Ben-Nissan B. Natural bioceramics: From coral to bone and beyond. Curr Opin Solid State Mater Sci. 2003;7(4-5):283–8.

10. https://en.wikipedia.org/wiki/Bone. Last access date:20.09.2015.

11. Porter JR, Ruckh TT, Popat KC. Bone tissue engineering: A review in bone biomimetics and drug delivery strategies. Biotechnol Prog. 2009;25(6):1539–60.

12. https://en.wikipedia.org/wiki/Osteon. Last access date: 20.09.2015.

13. Capulli M, Paone R, Rucci N. Osteoblast and osteocyte: Games without frontiers. Arch Biochem Biophys. 2014;561:3–12.

14. Shekaran A, García AJ. Extracellular matrix-mimetic adhesive biomaterials for bone repair. J Biomed Mater Res - Part A. 2011;96 A(1):261–72.

15. Deschaseaux F, Sensébé L, Heymann D. Mechanisms of bone repair and regeneration. Trends Mol Med. 2009;15(9):417–29.

16. Chen Y, Alman B a. Wnt pathway, an essential role in bone regeneration. J Cell Biochem. 2009;106(3):353–62.

17. Dimitriou R, Tsiridis E, Giannoudis P V. Current concepts of molecular aspects of bone healing. Injury. 2005;36(12):1392–404.

18. Tsiridis E, Upadhyay N, Giannoudis P. Molecular aspects of fracture healing:Which are the important molecules? Injury. 2007;38(SUPPL. 1).

19. Carreira AC, Alves GG, Zambuzzi WF, Sogayar MC, Granjeiro JM. Bone Morphogenetic Proteins: Structure, biological function and therapeutic applications. Arch Biochem Biophys. 2014;561:64–73.

20. Deckers MM, van Bezooijen RL, van der Horst G, Hoogendam J, van Der Bent C, Papapoulos SE, et al. Bone morphogenetic proteins stimulate angiogenesis through osteoblast-derived vascular endothelial growth factor A. Endocrinology. 2002;143(4):1545–53.

21. Prisell PT, Edwall D, Lindblad JB, Levinovitz A, Norstedt G. Expression of insulin-like growth factors during bone induction in rat. Calcif Tissue Int. 1993;53(3):201–5.

22. Phillips A. Overview of the fracture healing cascade. Injury. 2005;36 Suppl 3:S5–7.

23. Arvidson K, Abdallah BM, Applegate L a., Baldini N, Cenni E, Gomez-Barrena E, et al. Bone regeneration and stem cells. J Cell Mol Med. 2011;15(4):718–46.

24. Anderson JM, Rodriguez A, Chang DT. Foreign body reaction to biomaterials. Semin Immunol. 2008;20(2):86–100.

25. Komori T. Regulation of bone development and extracellular matrix protein genes by RUNX2. Cell Tissue Res. 2010;339(1):189–95.

26. Tocci A, Forte L. Mesenchymal stem cell: use and perspectives. Hematol J. 2003;4:92–6.

27. Liao H-T. Osteogenic potential: Comparison between bone marrow and adipose-derived mesenchymal stem cells. World J Stem Cells. 2014;6(3):288.

28. Scuteri A, Donzelli E, Foudah D, Caldara C, Redondo J, D'Amico G, et al. Mesengenic Differentiation: Comparison of Human and Rat Bone Marrow Mesenchymal Stem Cells. Int J Stem Cells. 2014;7(2):127–34.

29. Bielby R, Jones E, McGonagle D. The role of mesenchymal stem cells in maintenance and repair of bone. Injury. 2007;38(SUPPL. 1).

30. Griffin M, Iqbal S a, Bayat a. Exploring the application of mesenchymal stem cells in bone repair and regeneration. J Bone Joint Surg Br. 2011;93(4):427–34.

31. Knight MN, Hankenson KD. Mesenchymal Stem Cells in Bone Regeneration. Adv wound care. 2013;2(6):306–16.

32. Nombela-Arrieta C, Ritz J, Silberstein LE. The elusive nature and function of mesenchymal stem cells. Nat Rev Mol Cell Biol. 2011;12(2):126–31.

33. Sia IG, Berbari EF. Infection and musculoskeletal conditions: Osteomyelitis. Best Pract Res Clin Rheumatol. 2006;20(6):1065–81.

34. Lew DP, Waldvogel FA. Osteomyelitis. Lancet. 2004;364:369–79.

35. Brady R a., Leid JG, Calhoun JH, Costerton JW, Shirtliff ME. Osteomyelitis and the role of biofilms in chronic infection. FEMS Immunol Med Microbiol. 2008;52:13–22.

36. Zimmerli W. Prosthetic-joint-associated infections. Best Pract Res Clin Rheumatol. 2006;20(6):1045–63.

37. Carek PJ, Dickerson LM, Sack JL. Diagnosis and management of osteomyelitis. Am Fam Physician. 2001;63(12):2413–21.

38. Ueng SWN, Yuan L-J, Lin S-S, Liu S-J, Chan E-C, Chen K-T, et al. In Vitro and In Vivo Analysis of a Biodegradable Poly(lactide-co-glycolide) Copolymer Capsule and Collagen Composite System for Antibiotics and Bone Cells Delivery. J Trauma. 2011;70(6):1503–9.

39. www.slideshare.nt/faranelahi/osteomyelitis-36366026. Last access date: 20.09.2015.

40. Harris LG, Richards RG. Staphylococci and implant surfaces: a review. Injury. 2006;37.

41. Donlan RM. New approaches for the characterization of prosthetic joint biofilms. Clin Orthop Relat Res. 2005;(437):12–9.

42. Gross M, Cramton SE, Götz F, Peschel A. Key role of teichoic acid net charge in Staphylococcus aureus colonization of artificial surfaces. Infect Immun. 2001;69(5):3423–6.

43. Cramton SE, Gerke C, Schnell NF, Nichols WW, Götz F. The intercellular adhesion (ica) locus is present in Staphylococcus aureus and is required for biofilm formation. Infect Immun. 1999;67(10):5427–33.

44. Balaban N, Stoodley P, Fux C a, Wilson S, Costerton JW, Dell'Acqua G. Prevention of staphylococcal biofilm-associated infections by the quorum sensing inhibitor RIP. Clin Orthop Relat Res. 2005;01(437):48–54.

45. Hassan A, Usman J, Kaleem F, Omair M, Khalid A, Iqbal M. Evaluation of different detection methods of biofilm formation in the clinical isolates. Braz J Infect Dis. 2011;15:305–11.

46. Sauer K, Camper AK, Ehrlich GD, Costerton JW, Davies DG. Pseudomonas aeruginosa displays multiple phenotypes during development as a biofilm. J Bacteriol. 2002;184(4):1140–54.

47. www.microbewiki.kenton.edu/index.php/Biofilms_and_Human_Implants. Last access date:20.09.2015.

48. Peeters E, Nelis HJ, Coenye T. Comparison of multiple methods for quantification of microbial biofilms grown in microtiter plates. J Microbiol Methods. 2008;72:157–65.

49. Yang F, Cui W, Xiong Z, Liu L, Bei J, Wang S. Poly(l,l-lactide-co-glycolide)/tricalcium phosphate composite scaffold and its various changes during degradation in vitro. Polym Degrad Stab. 2006;91:3065–73.

50. Bryers JD. Medical biofilms. Biotechnology and Bioengineering. 2008. p. 1–18.

51. Pacheco H, Vedantham K, Aniket, Young A, Marriott I, El-Ghannam A. Tissue engineering scaffold for sequential release of vancomycin and rhBMP2 to treat bone infections. J Biomed Mater Res Part A. 2014;102A:4213–23.

52. Cui X, Zhao C, Gu Y, Li L, Wang H, Huang W, et al. A novel injectable borate bioactive glass cement for local delivery of vancomycin to cure osteomyelitis and regenerate bone. J Mater Sci Mater Med. 2014;25(3):733–45.

53. Yao Q, Nooeaid P, Roether J a., Dong Y, Zhang Q, Boccaccini AR. Bioglass®-based scaffolds incorporating polycaprolactone and chitosan coatings for controlled vancomycin delivery. Ceram Int. 2013;39(7):7517–22.

54. Toma MB, Smith KM, Martin C a, Rapp RP. Pharmacokinetic considerations in the treatment of methicillin-resistant Staphylococcus aureus osteomyelitis. Orthopedics. 2006;29(6):497–501.

55. Zhou H, Lawrence JG, Bhaduri SB. Fabrication aspects of PLA-CaP/PLGA-CaP composites for orthopedic applications: A review. Acta Biomater. 2012;8(6):1999–2016.

56. Swanson TE, Cheng X, Friedrich C. Development of chitosan-vancomycin antimicrobial coatings on titanium implants. J Biomed Mater Res - Part A. 2011;97 A:167–76.

57. Soriano A, Marco F, Martínez J a, Pisos E, Almela M, Dimova VP, et al. Influence of vancomycin minimum inhibitory concentration on the treatment of methicillin-resistant Staphylococcus aureus bacteremia. Clin Infect Dis. 2008;46:193–200.

58. Uhrich KE, Cannizzaro SM, Langer RS, Shakesheff KM. Polymeric systems for controlled drug release. Chem Rev. 1999;99:3181–98.

59. Bajpai a. K, Shukla SK, Bhanu S, Kankane S. Responsive polymers in controlled drug delivery. Prog Polym Sci. 2008;33:1088–118.

60. Liechty WB, Kryscio DR, Slaughter B V., Peppas NA. Polymers for Drug Delivery Systems. Annual Review of Chemical and Biomolecular Engineering. 2010. p. 149–73.

61. Langer R, Peppas N a. Advances in Biomaterials, Drug Delivery, and Bionanotechnology. AIChE J. 2003;49(12):2990–3006.

62. Cabañas M V., Peña J, Román J, Vallet-Regí M. Tailoring vancomycin release from β-TCP/agarose scaffolds. Eur J Pharm Sci. 2009;37:249–56.

63. Ueng SWN, Lee MS, Lin SS, Chan EC, Liu SJ. Development of a biodegradable alginate carrier system for antibiotics and bone cells. J Orthop Res. 2007;25(January):62–72.

64. Luo Y, Kirker KR, Prestwich GD. Cross-linked hyaluronic acid hydrogel films: New biomaterials for drug delivery. J Control Release. 2000;69(1):169–84.

65. Yang CC, Lin CC, Liao JW, Yen SK. Vancomycin-chitosan composite deposited on post porous hydroxyapatite coated Ti6Al4V implant for drug controlled release. Mater Sci Eng C. 2013;33(4):2203–12.

66. Naraharisetti PK, Ning Lew MD, Fu YC, Lee DJ, Wang CH. Gentamicin-loaded discs and microspheres and their modifications: Characterization and in vitro release. J Control Release. 2005;102:345–59.

67. Xing J, Hou T, Luobu B, Luo F, Chen Q, Li Z, et al. Anti-Infection Tissue Engineering Construct Treating Osteomyelitis in Rabbit Tibia. Tissue Eng Part A. 2012;19:120926061554009.

68. Zugravu M V, Smith R a, Reves BT, Jennings J a, Cooper JO, Haggard WO, et al. Physical properties and in vitro evaluation of collagen-chitosan-calcium phosphate microparticle-based scaffolds for bone tissue regeneration. J Biomater Appl. 2013;28(4):566–79.

69. Yagmurlu MF, Korkusuz F, Gürsel I, Korkusuz P, Örs Ü, Hasirci V. Sulbactam-cefoperazone polyhydroxybutyrate-co-hydroxyvalerate (PHBV) local antibiotic delivery system: In vivo effectiveness and biocompatibility in the treatment of implant-related experimental osteomyelitis. J Biomed Mater Res. 1999;46:494–503.

70. Kim HW, Knowles JC, Kim HE. Hydroxyapatite/poly(e-caprolactone) composite coatings on hydroxyapatite porous bone scaffold for drug delivery. Biomaterials. 2004;25:1279–87.

71. Laurencin CT, Gerhart T, Witschger P, Satcher R, Domb A, Rosenberg a. E, et al. Bioerodible polyanhydrides for antibiotic drug delivery: In vivo osteomyelitis treatment in a rat model system. J Orthop Res. 1993;11:256–62.

72. Yang YY, Chung TS, Ping Ng N. Morphology, drug distribution, and in vitro release profiles of biodegradable polymeric microspheres containing protein fabricated by double-emulsion solvent extraction/evaporation method. Biomaterials. 2001;22:231–41.

73. Sayin B, Caliş S, Atilla B, Marangoz S, Hincal a A. Implantation of vancomycin microspheres in blend with human/rabbit bone grafts to infected bone defects. J Microencapsul. 2006;23(772814176):553–66.

74. Neut D, van de Belt H, Stokroos I, van Horn JR, van der Mei HC, Busscher HJ. Biomaterial-associated infection of gentamicin-loaded PMMA beads in orthopaedic revision surgery. J Antimicrob Chemother. 2001;47:885–91.

75. Khang G, Choi HS, Rhee JM, Yoon SC, Cho JC, Lee HB. Controlled Release of Gentamicin Sulfate from Poly (3-hydroxybutyrate-co-3-hydroxyvalerate) Wafers for the Tretment of Osteomyelitis. Korea Polym J. 2000;8(6):253–60.

76. Beenken KE, Smith JK, Skinner R a, McLaren SG, Bellamy W, Gruenwald MJ, et al. Chitosan coating to enhance the therapeutic efficacy of calcium sulfate-based antibiotic therapy in the treatment of chronic osteomyelitis. J Biomater Appl. 2014;29(4):514–23.

77. Coraca-Huber DC, Duek EADR, Etchebehere M, Magna LA, Amstalden EMI. The use of vancomycin-loaded poly-l-lactic acid and poly-ethylene oxide microspheres for bone repair: an in vivo study. Clinics. 2012;67(7):793–8.

78. Rezwan K, Chen QZ, Blaker JJ, Boccaccini AR. Biodegradable and bioactive porous polymer/inorganic composite scaffolds for bone tissue engineering. Biomaterials. 2006;27:3413–31.

79. Zhang LF, Sun R, Xu L, Du J, Xiong ZC, Chen HC, et al. Hydrophilic poly (ethylene glycol) coating on PDLLA/BCP bone scaffold for drug delivery and cell culture. Mater Sci Eng C. 2008;28:141–9.

80. Heidemann W, Jeschkeit S, Ruffieux K, Fischer JH, Wagner M, Krüger G, et al. Degradation of poly(D,L)lactide implants with or without addition of calciumphosphates in vivo. Biomaterials. 2001;22(17):2371–81.

81. McLaren JS, White LJ, Cox HC, Ashraf W, Rahman C V., Blunn GW, et al. A biodegradable antibiotic-impregnated scaffold to prevent osteomyelitis in a contaminated in vivo bone defect model. Eur Cells Mater. 2014;27:332–49.

82. Makadia HK, Siegel SJ. Poly Lactic-co-Glycolic Acid (PLGA) as biodegradable controlled drug delivery carrier. Polymers (Basel). 2011;3:1377–97.

83. Yang Y, Zhao Y, Tang G, Li H, Yuan X, Fan Y. In vitro degradation of porous poly(l-lactide-co-glycolide)/β-tricalcium phosphate (PLGA/β-TCP) scaffolds under dynamic and static conditions. Polym Degrad Stab. 2008;93:1838–45.

84. Tamariz E, Rios-ramírez A. Biodegradation of Medical Purpose Polymeric Materials and Their Impact on Biocompatibility. Biodegrad - Life Sci 2. 2013;3–30.

85. Ulery BD, Nair LS, Laurencin CT. Biomedical applications of biodegradable polymers. Journal of Polymer Science, Part B: Polymer Physics. 2011. p. 832–64.

86. Commandeur S, Van Beusekom HMM, Van Der Giessen WJ. Polymers, drug release, and drug-eluting stents. Journal of Interventional Cardiology. 2006. p. 500–6.

87. El-Husseiny M, Patel S, MacFarlane RJ, Haddad FS. Biodegradable antibiotic delivery systems. J Bone Joint Surg Br. 2011;93(2):151–7.

88. Arcos D, Vallet-Regí M. Bioceramics for drug delivery. Acta Mater. 2013;61(3):890–911.

89. Lian XJ, Wang XM, Cui FZ. In Vitro Antibacterial Properties of Vancomycin-Loaded Nano-Hydroxyapatite/Collagen/Calcium Sulfate Hemihydrates (VCM/nHAC/CSH) Bone Substitute. Mater Sci Forum. 2013;745-746:6–12.

90. Wu T, Zhang Q, Ren W, Yi X, Zhou Z, Peng X, et al. Controlled release of gentamicin from gelatin/genipin reinforced beta-tricalcium phosphate scaffold for the treatment of osteomyelitis. J Mater Chem B. 2013;1:3304.

91. Dion A, Langman M, Hall G, Filiaggi M. Vancomycin release behaviour from amorphous calcium polyphosphate matrices intended for osteomyelitis treatment. Biomaterials. 2005;26:7276–85.

92. Thomas M V., Puleo D a. Calcium sulfate: Properties and clinical applications. J Biomed Mater Res - Part B Appl Biomater. 2009;88:597–610.

93. Rottensteiner U, Sarker B, Heusinger D, Dafinova D, Rath SN, Beier JP, et al. In vitro and in vivo biocompatibility of alginate dialdehyde/gelatin hydrogels with and without nanoscaled bioactive glass for bone tissue engineering applications. Materials. 2014;7(February):1957–74.

94. Bose S, Tarafder S, Edgington J, Bandyopadhyay A. Calcium phosphate ceramics in drug delivery. JOM. 2011. p. 93–8.

95. Kundu B, Nandi SK, Roy S, Dandapat N, Soundrapandian C, Datta S, et al. Systematic approach to treat chronic osteomyelitis through ceftriaxone-sulbactam impregnated porous ??-tri calcium phosphate localized delivery system. Ceram Int. 2012;38(2):1533–48.

96. Kokubo T, Kushitani H, Sakka S, Kitsugi T, Yamamum T. Solutions able to reproduce in vivo surface-structure changes in bioactive glass-ceramic A-W. J Biomed Mater Res. 1990;24:721–34.

97. Zarif MS, Afidah a. R, Abdullah JM, Shariza a. R. Physicochemical characterization of vancomycin and its complexes with ??-cyclodextrin. Biomed Res. 2012;23(4):513–20.

98. Prem Ananth K, Shanmugam S, Jose SP, Nathanael a. J, Oh TH, Mangalaraj D, et al. Structural and chemical analysis of silica-doped β-TCP ceramic coatings on surgical grade 316L SS for possible biomedical application. J Asian Ceram Soc. 2015;4–11.

99. Park JW, Lee DJ, Yoo ES, Im SS, Kim SH, Kim YH. Biodegradable polymer blends of poly(L-lactic acid) and starch. Polym Eng Sci. 1999 Dec;7(7):93–101.

100. Bastari K, Arshath M, Ng ZHM, Chia JH, Yow ZXD, Sana B, et al. A controlled release of antibiotics from calcium phosphate-coated poly(lactic-co-glycolic acid) particles and their in vitro efficacy against Staphylococcus aureus biofilm. J Mater Sci Mater Med. 2014;25:747–57.

101. Di Silvio L, Bonfield W. Biodegradable drug delivery system for the treatment of bone infection and repair. J Mater Sci Mater Med. 1999;10:653–8.

102. Lei Y, Rai B, Ho KH, Teoh SH. In vitro degradation of novel bioactive polycaprolactone-20% tricalcium phosphate composite scaffolds for bone engineering. Mater Sci Eng C. 2007;27(2):293–8.

103. Baro M, Sánchez E, Delgado a., Perera a., Évora C. In vitro-in vivo characterization of gentamicin bone implants. J Control Release. 2002;83:353–64.

104. Kang Y, Xu X, Yin G, Chen A, Liao L, Yao Y, et al. A comparative study of the in vitro degradation of poly(l-lactic acid)/B-tricalcium phosphate scaffold in static and dynamic simulated body fluid. Eur Polym J. 2007;43:1768–78.

105. Patlolla A, Arinzeh TL. Evaluating apatite formation and osteogenic activity of electrospun composites for bone tissue engineering. Biotechnol Bioeng. 2014;111(5):1000–17.

106. Thanyaphoo S, Kaewsrichan J. Synthesis and Evaluation of Novel Glass Ceramics as Drug Delivery Systems in Osteomyelitis. J Pharm Sci. 2012;101(8):2870–82.

107. Makarov C, Berdicevsky I, Raz-Pasteur A, Gotman I. In vitro antimicrobial activity of vancomycin-eluting bioresorbable b-TCP-polylactic acid nanocomposite material for load-bearing bone repair. J Mater Sci Mater Med. 2013;24:679–87.

108. Institute C and LS. Performance Standards for Antimicrobial Susceptibility Testing ; Twenty-Second Informational Supplement. Clinical Laboratory Standards Institute. 2012. 1-188 p.

109. Lu H, Kawazoe N, Tateishi T, Chen G, Jin X, Chang J. In vitro proliferation and osteogenic differentiation of human bone marrow-derived mesenchymal stem cells cultured with hardystonite (Ca2ZnSi 2O7) and {beta}-TCP ceramics. J Biomater Appl. 2010;25:39–56.

110. Schröder HC, Boreiko O, Krasko A, Reiber A, Schwertner H, Müller WEG. Mineralization of SaOS-2 cells on enzymatically (silicatein) modified bioactive osteoblast-stimulating surfaces. J Biomed Mater Res - Part B Appl Biomater. 2005;75:387–92.

111. Mendonça G, Mendonça DBS, Simões LGP, Araújo AL, Leite ER, Duarte WR, et al. The effects of implant surface nanoscale features on osteoblast-specific gene expression. Biomaterials. 2009;30(25):4053–62.

112. Matsubara T, Kida K, Yamaguchi A, Hata K, Ichida F, Meguro H, et al. BMP2 regulates osterix through Msx2 and Runx2 during osteoblast differentiation. J Biol Chem. 2008;283(43):29119–25.

113. Jeon EJ, Lee KY, Choi NS, Lee MH, Kim HN, Jin YH, et al. Bone morphogenetic protein-2 stimulates Runx2 acetylation. J Biol Chem. 2006;281(24):16502–11.

114. Honsawek S, Dhitiseith D, Phupong V. Gene expression characteristics of osteoblast differentiation in human umbilical cord mesenchymal stem cells induced by demineralized bone matrix. 2007;1(4):383–91.

115. Adachi S, Hashimoto Y, Nakamura M. Effect of S100A4 siRNA on Genes Related to Osteogenic Differentiation in Human Mesenchymal Stem Cells. J Oral Tissue Engin. 2009;6(3):140–51.

APPENDIX A

CALIBRATION CURVE FOR VANCOMYCIN

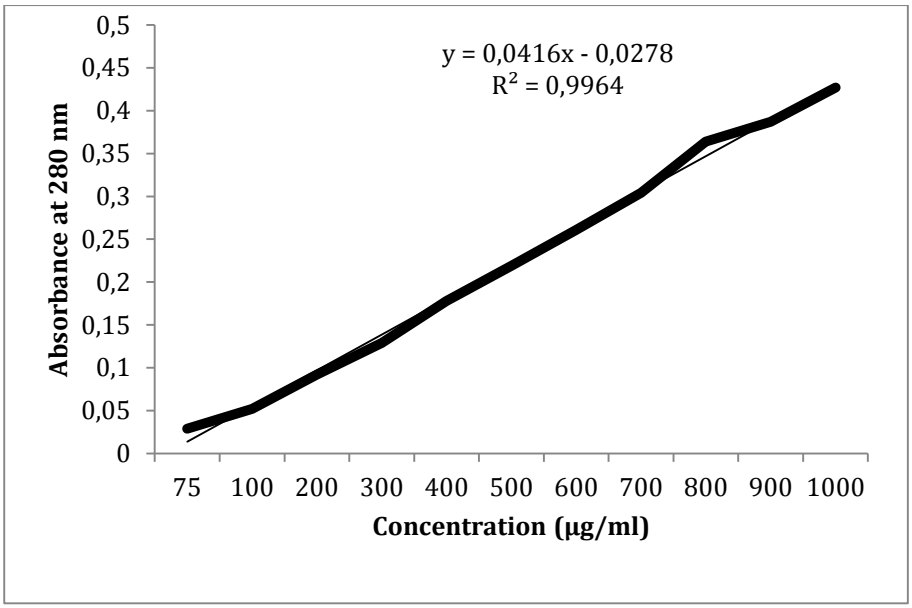

Figure 37. Calibration curve of vancomycin

APPENDIX B

GENE LIST FOR RT-PCR CUSTOM PLATES

Table 4. Gene List for RT-PCR custom plates

Gene Name	Gene Description	Forward Primer Sequence	Reverse Primer Sequence
AHSG	alpha-2-HS-glycoprotein	TGCTAAAGAGGCCACAGAGG	TGTTGCCTTACAAAAGCCATATT
ALPL	alkaline phosphatase, liver/bone/ kidney	AGAACCCCAAAGGCTTCTTC	CTTGGCTTTTCCTTCATGGT
ANXA5	annexin A5	TCTTCGGAAGGCTATGAAAGG	GGGATGTCAACAGAGTCAGGA
BGLAP	bone gamma-carboxyglutamate (gla) protein	CCAGCCCTATGGATGTGG	TTTTCAGATTCCTCTTCTGGAGTT
BMP1	bone morphogenetic protein 1	TATGTGGAGGTCCGAGATGG	GAGTTTGGACCCGCAGAA
BMP2	bone morphogenetic protein 2	GACTGCGGTCTCCTAAAGGTC	GGAAGCAGCAACGCTAGAAG
BMP3	bone morphogenetic protein 3	CCCAAGTCCTTTGATGCCTA	TCTGGATGGTAGCATGATTTGA
BMP4	bone morphogenetic protein 4	GAGGAAGGAAGATGCGAGAA	GCACTACGGAATGGCTCCT
BMP5	bone morphogenetic protein 5	GCAATAAATCCAGCTCTCATCA	TGTTTTTGCTCACTTGTGTTATAATCT
BMP6	bone morphogenetic protein 6	ACATGGTCATGAGCTTTGTGA	ACTCTTTGTGGTGTCGCTGA
CALCR	calcitonin receptor	CGCTTGCGGTGGTATTATCT	GGTAATAGCATGGATAGTGGTTGG
CDH11	cadherin 11, type 2,	CATCGTCATTCTCCTGGTCA	TCAAAGACAATGAGTGGTTCTTTC

Table 4. (continued)

COL10A1	collagen, type X, alpha 1	CAGTTCTTCATTCCCTACACCA	AGGACTTCCGTAGCCTGGTT
COL14A1	collagen, type XIV, alpha 1	GACCCCTCATCATGTTCTGC	ATGGCTTCCAGCTCATCTTG
COL15A1	collagen, type XV, alpha 1	TGATGGTCGAGACATAATGACA	GGAGCCATGCCAAATGAC
COL1A1	collagen, type I, alpha 1	AGGTGAAGCAGGCAAACCT	CTCGCCAGGGAAACCTCT
COL1A2	collagen, type I, alpha 2	TCTGGAGAGGCTGGTACTGC	GAGCACCAAGAAGACCCTGA
COL2A1	collagen, type II, alpha 1	TTTCAAGGCAATCCTGGTG	TCCAGGTTTTCCAGCTTCAC
COL3A1	collagen, type III, alpha 1	ACTGGAGCACGGGGTCTT	TCCTGGTTTCCCACTTTCAC
COL5A1	collagen, type V, alpha 1	TCTTGGCCCAAAGAAAACC	GGCGTCCACATAGGAGAGC
COMP	cartilage oligomeric matrix protein	GGGTCCCCAATGAAAAGG	CCTTTTGGTCGTCGTTCTTC
CTSK	cathepsin K	CGAAGCCAGACAACAGATTTC	AGAGCAAAGCTCACCACAGG
DMP1	dentin matrix acidic phosphoprotein 1	TTCCTTTGGGGATTATCCTGT	TGCCTGAGCCAAATGACC
EGF	epidermal growth factor	CCTCAGATGGGAAAACGTG	GTTCTTTAGATCAACTTCACCACCT
EGFR	epidermal growth factor receptor	CAGCCACCCATATGTACCATC	AACTTTGGGCGACTATCTGC
FGF1	fibroblast growth factor 1 (acidic)	AATCAGCCAAAGAGCCTGTC	CAAAACAGAGCAGGGAACTACC
FGF2	fibroblast growth factor 2 (basic)	CCCGACGGCCGAGTTGAC	CACATTTAGAAGCCAGTAATCT
FGF3	fibroblast growth factor 3	GCGTCTGGGTTCTCAGCTAT	CTTGGGCCCTCTTCAGTTC
FGFR1	fibroblast growth factor receptor 1	AAGATTGGCCCAGACAACC	GCACCTCCATCTCTTTGTCG
FGFR2	fibroblast growth factor receptor 2	GACCCAAAATGGGAGTTTCC	GACCACTTGCCCAAAGCA

Table 4. (continued)

IGF1	insulin-like growth factor 1	TGCTTTTGTGATTTCTTGAAGG	GCAGAGCTGGTGAAGGTGA
IGF1R	insulin-like growth factor 1 receptor	TCAGCGCTGCTGATGTGT	GGCTCATGGTGATCTTCTCC
IGF2	insulin-like growth factor 2	GCTGGCAGAGGAGTGTCC	GGGATTCCCATTGGTGTCT
ITGB1	integrin, beta 1 (fibronectin receptor, antigen CD29 includes MDF2, MSK12)	CTTGGAACAGATCTGATGAATGA	TCCACAAATGAGCCAAATCC
MMP10	matrix metallopeptidase 10	CAAAAGAGGAGGACTCCAACA	TTCACATCCTTTTCGAGGTTG
MMP2	matrix metallopeptidase 2	TATTTGATGGCATCGCTCAG	ACAGTCCGCCAAATGAACC
MMP8	matrix metallopeptidase 8	GGGAACGCACTAACTTGACC	TTCAAAGGCATCCTTGATAGC
MMP9	matrix metallopeptidase 9	ATCCGGCACCTCTATGGTC	CAGACCGTCGGGGGAG
PHEX	phosphate regulating endopeptidase homolog, X-linked	AGTGCATCCACCAACCAGAT	TTCCCCAAAAGAAAGGCTTC
RUNX2	runt-related transcription factor 2	GCCTAGGCGCATTTCAGAT	CTGAGAGTGGAAGGCCAGAG
SMAD1	SMAD family member 1	TGTGTACTATACGTATGAGCTTTGTGA	TAACATCCTGGCGGTGGTA
SMAD2	SMAD family member 2	AAAGGGTGGGGAGCAGAATA	GAAGTTCAATCCAGCAAGGAGT
SMAD3	SMAD family member 3	GCATGAGCTTCGTCAAAGG	AATCCAGCAGGGGGTACTG
SMAD4	SMAD family member 4	TGGCCCAGGATCAGTAGGT	CATCAACACCAATTCCAGCA
SOX9	SRY (sex determining region Y)-box 9	TACCCGCACTTGCACAAC	TCTCGCTCTCGTTCAGAAGTC

Table 4. (continued)

TGFB1	transforming growth factor, beta 1	ACTACTACGCCA AGGAGGTCAC	TGCTTGAACTTG TCATAGATTTCG
TGFB2	transforming growth factor, beta 2	GAAGAACTAGAA GCAAGATTTGCA G	TGATCACCACTG GTATATGTGGA
TGFB3	transforming growth factor, beta 3	GCTTTGGACACC AATTACTGC	CCCAGATCCTGT CGGAAGT
TGFB R1	transforming growth factor, beta receptor 1	AAATTGCTCGAC GATGTTCC	CATAATAAGGCA GTTGGTAATCTT CA
TGFB R2	transforming growth factor, beta receptor II	GACCAGAAATTC CCAGCTTCT	CAACGTCTCACA CACCATCTG
TNF	Tumor necrosis factor Precursor (TNF-alpha)	CGGTGCTTGTTC CTCAGC	GCCAGAGGGCTG ATTAGAGA
TWIST 1	twist homolog 1 (Drosophila)	AGCTACGCCTTC TCGGTCT	TCCTTCTCTGGA AACAATGACA
VDR	vitamin D (1,25-dihydroxyvitami n D3) receptor	CTTCTCTGGGGA CTCCTCCT	TGGACGAGTCCA TCATGTCT
HPRT1	hypoxanthine phosphoribosylt ransferase 1	TGACCTTGATTT ATTTTGCATACC	CGAGCAAGACGT TCAGTCCT
GDF10	growth differentiation factor 10	TGAATGGATAAT CTCACCGAAA	GTTGGATGGACG AACGATCT
ACTB	actin, beta	GGCCAGGTCATC ACCATT	GGATGCCACAGG ACTCCAT
GAPD H	glyceraldehyde-3-phosphate dehydrogenase	CTCTGCTCCTCCT GTTCGAC	ACGACCAAATCC GTTGACTC
G6PD	glucose-6-phosphate dehydrogenase	TCCATCAGTCGG ATACACACA	CACCAGATGGTG GGGTAGAT
Control	polymerase (RNA) II (DNA directed) polypeptide A, 220kDa	CCTGAGTCCGGA TGAACTG	GCCTCCCTCAGT CGTCTCT
Control	polymerase (RNA) II (DNA directed)	GCAAATTCACCA AGAGAGACG	CACGTCGACAGG AACATCAG

Table 4. (continued)

Control	polymerase (RNA) II (DNA directed) polypeptide A, 220kDa	TCCGTATTCGCA TCATGAAC	TCATCCATCTTGT CCACCAC
Control	transferrin receptor (p90, CD71)	TGGGTTTTTGTTA CCTTTATGGTT	GGAGGTAACATG CAAATAATGTGA
Control	transferrin receptor (p90, CD71)	TGGGTTTTTGTTA CCTTTATGGTT	GGAGGTAACATG CAAATAATGTGA

VITA

BERNA KANKILIÇ

Address: Erler Mahallesi Türk Kızılayı Caddesi Toki Deniz Lojmanları Apt No:41 F Blok Daire No:14 Etimesgut/Ankara
Home: (0312)5538241 **Cell Phone:** (0535)8462398
E-mail:uysalberna@yahoo.com

PERSONAL INFORMATION

Citizenship: Turkish Republic
Birthplace and Date: Ankara, 30.10.1985
Marital Status: Married, 1 child

EDUCATION

1999-2002: TED Ankara College High School
2002-2006: Başkent University Faculty of Engineering, Department of Biomedical Engineering
2006- 2009: Middle East Technical University, Graduate School of Natural and Applied Sciences Biotechnology Graduate Programme
2009- ....: Middle East Technical University Graduate School of Natural and Applied Sciences Biotechnology Doctorate Programme

INTERNSHIP

2004-Gazi University Hospital Biomedical Calibration and Research Center (BİYOKAM), Ankara
2005-Philips Health Systems, Ankara

WORK EXPERIENCE

June 2013-present: R&D Engineer- FAME-MED MEDICAL. Hacettepe Technopolis 4. R&D Building Floor:2 Office No:52 Çankaya Ankara/Türkiye

ATTENDED SEMINARS, EXHIBITIONS and WORKSHOPS

2004-BIOMED 2004, Hacettepe University, Ankara

2005-EXPOMED, TÜYAP, İstanbul

2006-Ankara Engineering Students Community Young Engineer Development Days, TOBB Economy and Technology University, Ankara

2006-Cutting Edge Science in Medical Informatics and Medicine, Middle East Technical University, Ankara

2007-Workshop on Alternative Methods to Animal Tests, Hacettepe University, Ankara

2008-Clinical Orthopaedics and Related Research Writing Workshop, İstanbul

2008-BİYOMUT 2008, Middle East Technical University, Ankara

2009- Biomaterial- Tissue Compatibility in Tissue Engineering Applications, Hacettepe University, Ankara

2009-International Symposium on Biotechnology: Developments and Trends, Middle East Technical University, Ankara

2009- XXI. National Turkish Orthopaedics and Traumatology Congress, Sheraton Hotel, Çeşme, İzmir

2010- TOTBİD and TOTEK Orthopaedic and Traumatology Basic Sciences Research Workshop, TSK Rehabilitation Center, Ankara

2011-TÜBA II. Stem Cell Workshop and VI. Stem Cell Symposium, Ankara University, Ankara

2011- BIOMED 2011, Dedeman Hotel, Ankara

2014- Advanced Technologies on Health Sciences, Hacettepe University, Ankara

PROCEEDINGS IN INTERNATIONAL AND NATIONAL CONGRESSES

1- Uysal B, Bayramlı E, Korkusuz P, Dağdeviren S, Gümüşel B, Korkusuz F; "*Vancomycin-containing Plla Delivery System For The Treatment of Implant Related Chronic Osteomyelitis:An In Vivo Study*", International Symposium on Biotechnology: Developments and Trends, Middle East Technical University, Ankara

2- Uysal B, Bayramlı E, Korkusuz P. Dağdeviren S, Gümüşel B, Korkusuz F; "*Vankomisin İçeren Plla Taşıyıcı Sisteminin İmplant İlişkili Kronik Osteomiyelit Tedavisinde Kullanımı :in-vivo Çalışma*", XXI. National Turkish Orthopaedics and Traumatology Congress, Sheraton Hotel, Çeşme, İzmir

3- Kankılıç B, Bayramlı E, Bilgiç E, Korkusuz P, Kılıç E, Dağdeviren S, Korkusuz F. Vankomisin içeren PLLA/β-TCP implantla ilişkili osteomiyeliti iyileştirmektedir. 20. National Electron Microscopy Congress, Kemer, Antalya

4-Korkusuz F, Dağdeviren S, Uysal B, Korkusuz P, Zeybek D, Akpulat U, Yıldız Y, Kocaefe Ç. Gene expression and immunohistochemical changes in skeletal muscles after ovariectomy and TNF-alpha antagonist admnistration in aged rats. 63rd Annual Meeting of the Association of Bone and Joint Surgeons, June 8-12, 2011, Dublin, Ireland (Proceedings book: pp 54-56).

5.Korkusuz F, Kankilic B, Kopru CZ. Material Characterization, Anti-microbiological Action and Biofilm Inhibition Potential of Vancomycin Containing VK1000, 25th European Conference on Biomaterials,September 8-12, Madrid, İspanya (Proceedings book: pp 169)

6. Korkusuz F, Kankilic B, Korkusuz P, Dagdeviren S, Bayramli E, Kilic E, Bilgic E. The Biocompatibility of Vancomycin Containing PLLA/β -TCP Composite and Its Role in Implant Related Osteomyelitis, Musculoskeletal Infection Society 23rd Open Scientific Meeting, August 2-3, 2013, Philadelphia, USA

7. Korkusuz F , Kankilic B, Korkusuz P, Kopru CZ. In Vitro Assessment of Novel Vancomycin containing VK100 for Cell Culture Studies, Vancomycin Release Studies and Anti-microbiological Action, EORS 2014, July 2-4, 2014, Nantes, France (Proceedings book: pp 48)

INTERNATIONAL PUBLICATIONS

1- Dagdeviren S, Kandilci HB, Uysal B, Zeybek ND, Korkusuz P, Gümüsel B, Korkusuz F. Tumor necrosis factor-alpha antagonist administration recovers skeletal muscle dysfunction in ovariectomized rats. J Orthop Res 2010; 29(2), 275-80.

2- Kankilic B, Bayramli E, Kilic E, Dağdeviren S, Korkusuz F. Vancomycin Containing PLLA/β-TCP Controls MRSA In Vitro. Clin Orthop Relat Res 2011;469: 3222-3228.

3- Kankilic B, Bilgic E, Korkusuz P, Korkusuz F. Vancomycin containing PLLA/β-TCP controls experimental osteomyelitis *in vivo*. J Orthop Surg Res. 2014; 9: 114.

4- Kankilic B, Köse S, Korkusuz P, Timuçin M, Korkusuz F. Mesenchymal Stem Cells And Nano-Bioceramics For Bone Regeneration. Current Stem Cell Research & Therapy 2015 (in press)

FOREIGN LANGUAGES

English: Advanced
German: Beginner